ABSTRACT

Enzymatic and Non-enzymatic Reactions of Flavonol and Flavonolate Ruthenium Complex with Small Molecules: HNO and O_2

Xiaozhen Han, Ph.D.

Mentor: Patrick J. Farmer, Ph.D.

Quercetin 2,3-dioxygenase (QDO) enzyme catalyzes the degradation of flavonols by incorporating both atoms of dioxygen. HNO, nitroxyl or azanone, is isoelectronic with $^1O_2$, and acts as a reactive species for enzymatic and non-enzymatic cleavage of flavonols in the place of O_2, in which N is regioselectively found in the ring-cleaved product. Kinetic and thermodynamic analysis of the nitroxygenation of a series of flavonols with HNO have been conducted to get insights of the mechanism of enzymatic and non-enzymatic nitroxygenation. It turns out that in the QDO enzyme catalyzed reaction the possible involvement of a quinone methide tautomer of the flavonol substrates rationalizes the site of nitroxyl N-atom incorporation into the product; while in the non-enzymatic reaction the determined standard state energy (ΔG^o) and activation free energy, as well as the low entropic energy of reaction, are consistent with a proposed single electron transfer (SET) rate determining step.

In order to mimic flavonol dioxygenase catalyzed oxygenation of flavonols, a series of Ru(II) bis-bipyridyl flavonolate complexes $[Ru^{II}(bpy)_2(3\text{-hydroxyfla}^R)]^+$ (R = *p*-OMe, *p*-

Me, *p*-H, *p*-Cl), $[Ru^{II}(bpy)_2(3,7\text{-dihydroxyfla})]^+$ and $[Ru^{II}(bpy)_2(5\text{-hydroxyfla})]^+$ were designed and synthesized as functional models to investigate the oxidative cleavage of ligand flavonolate by oxygen and nitroxyl. Treatment of dry CH_3CN solutions of complexes with O_2 under light leads to oxidative O-heterocyclic ring opening of the coordinated substrate flavonolate, resulting in the formation of $[Ru^{II}(bpy)_2bpg^R]^+$ (bpg = 2-benzoyloxyphenylglyoxylate). We have been able to rule out singlet oxygen as a possible reactive intermediate. Instead, we suggest a SET (single electron transfer) mechanism between ruthenium bis-bipyridyl flavonolate complexes and oxygen. For the formation of the oxygenation product $[Ru^{II}(bpy)_2bpg^R]^+$, we were able to detect a 1,2-dioxetane intermediate by chemiluminescence spectroscopy. Both the product and the intermediate suggest that the oxygenation mechanism is through 1,2-dioxetane intermediate rather than a 1,3-endoperoxide pathway.

Enzymatic and Non-enzymatic Reactions of Flavonol and Flavonolate Ruthenium Complex with Small Molecules: HNO and O_2

by

Xiaozhen Han, B.S, M.S.

A Dissertation

Approved by Department of Chemistry and Biochemistry

_____

Patrick J. Farmer, Ph.D., Chairperson

Submitted to the Graduate Faculty of
Baylor University in Partial Fulfillment of the
Requirements for the Degree
of

Doctor of Philosophy

Approved by the Dissertation Committee

_____

Patrick J. Farmer, Ph.D., Chairperson

_____

Kevin K. Klausmeyer, Ph.D.

_____

Caleb D. Martin, Ph.D.

_____

Kevin G. Pinney, Ph.D.

_____

Zhenrong Zhang, Ph.D.

Accepted by the Graduate School

December 2016

_____

J. Larry Lyon, Ph.D., Dean

Page bearing signatures is kept on file in the Graduate School.

TABLE OF CONTENTS

LIST OF FIGURES

LIST OF TABLES

LIST OF SCHEMES

ACKNOWLEDGMENTS

First of all, I would like to express my great appreciation to Dr. Farmer, who has supported and guided me through the whole graduate career. His knowledge, scientific inspiration, and commitment to the highest standards motivated me.

To my committee, I would like to thank Dr. Klausmeyer for his help in crystal examination and elucidation; Dr. Martin, for his support in each oral exam; Dr. Pinney, for his patience and help in advanced organic chemistry; Dr. Zhang, for her support and availability to my dissertation defense.

I also need to thank the Department of Chemistry at Baylor University for providing me a wonderful opportunity to learn and communicate with intelligent and friendly colleagues and friends. Thank Nancy Kallus, Adonna Cook, Virginia Hynek, and Barbara Rauls for their efforts to help every graduate student better acquire knowledge and do research. Many thanks to my colleagues in Dr. Farmer's group. We have been together experiencing ups and downs but always believing and supporting each other. Thank Murugaeson (Ravi) Kumar, Britain Bruner, Tara Clover, Michelle del'Homme, Carrie Poe, Adrian Zapata, Michael Spiegel, Ottis Scrivner and undergraduate students Rabia and Mo.

Lastly, I would like to give deep thanks to my family. No words can fully express my gratitude. Thank you so much for your support, encouragement and love which makes me strong to overcome all the difficulties. You are my all and I would do everything I can to support you too.

DEDICATION

To my parents
May you be healthy, happy and getting older slowly

CHAPTER ONE

An Introduction of Nitroxygenation and Oxygenation of Flavonols

Nitroxygenation of Flavonols

Flavonols are a broad class of natural products that have been extensively studied for their antioxidant activity in the food and health sciences.[1-3] They have also been shown to have other multiple biological and pharmacological activities, including antiviral,[4] anti-inflammtory,[5-7] anti-allergy, and anticancer properties.[8-11] Flavonols are easily degraded by microorganisms, especially by fungi. In nature, quercetin dioxygenase (QDO), a type of flavonol dioxygenase (FDO), catalyzes the oxidative degradation of flavonols to a depside (phenolic carboxylic acid esters) with concomitant evolution of carbon monoxide, shown in Scheme 1.1.[12] In this dissertation, we will focus on favonols and investigate their nitroxygenation and oxygenation reactivity to elucidate the mechanism of enzyme flavonol dioxygenases (FDOs).

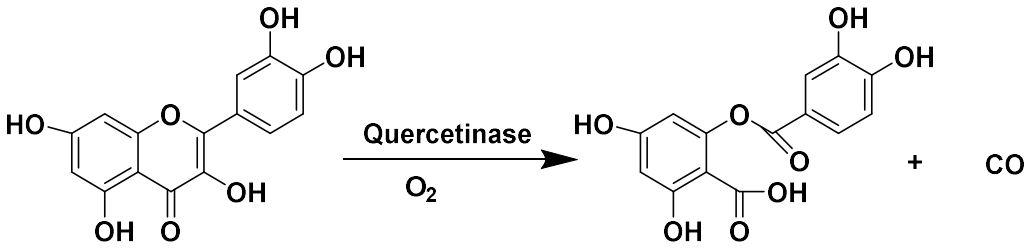

Scheme 1.1 The reaction between quercetin and oxygen catalyzed by QDO

Nitroxyl, HNO, is the reduced and protonated congener of NO, which is isoelectronic with singlet O_2. HNO displays biological effects distinct from that of NO, for example as an enzyme inhibitor and ionotropic agent that may be used in the treatment of heart failure.[13-18] HNO is very reactive and cannot be isolated because of its rapid dimerization generating N_2O between pH 2 and 11 (Equation 1).[19] Thus, HNO must be produced by the decomposition of donor compounds in the reaction.[20] By far the most widely used HNO donors are Angeli's salt (sodium trioxodinitrate, $Na_2N_2O_3$), AS, which produces HNO between pH 4 to 8, and benzylsulfohydroxamic acid or Piloty's acid, which generates HNO upon deprotonation at a pH > 8 (Equation 3).[21]

$$2HNO \rightarrow [H_2N_2O_2] \rightarrow N_2O + H_2O \qquad [1]$$

$$HN_2O_3^- \leftrightarrows HNO + NO_2^- \quad \text{pH 4–8} \qquad [2]$$

$$RSO_2NHO^- \leftrightarrows RSO_2^- + HNO \quad \text{pH 8–13} \qquad [3]$$

Previous work in the Farmer group showed that various O_2-binding globins trap free HNO in solution.[15] Thus they hypothesized that HNO might similarly interact with O_2-dependent oxygenases and substitute oxygen in enzymes. In 2011, Farmer's group reported the unprecedented substitution of HNO for dioxygen in the activity of Mn-substituted Quercetin Dioxygenase, Mn-QDO, resulting in the incorporation of both heteroatoms of HNO regioselectively into the product, Scheme 1.2.[14] In these reactions, HNO is generated *in situ* from a precursor, and in the presence of enzyme and substrate, and like oxygenation, cleaves the central O-heterocyclic ring to release CO. The reaction likely proceeds through

an analogous depsidic product, which decomposes to give the observed 2,4,6-trihydroxybenzoic acid and 3,4-dihydroxybenzonitrile products.

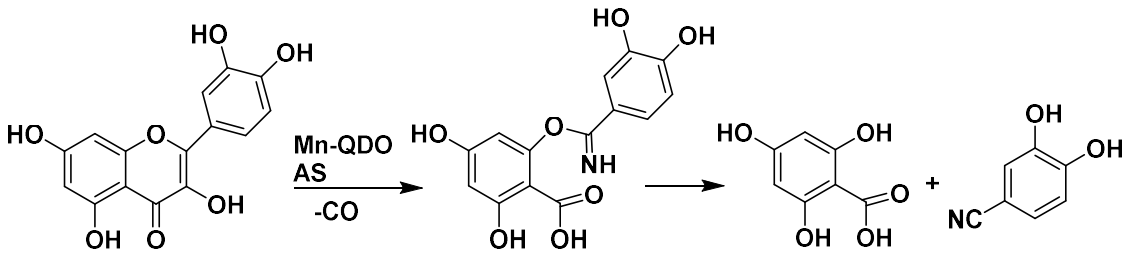

Scheme 1.2 Nitroxygenation of quercetin by HNO

The unique regioselectivity of N incorporation into the product is analogous to the recently described nitroso aldol reactions.[22-28] The nitroxygenation of flavonols by HNO as catalyzed either by enzyme (Mn-QDO) or base will be explored in detail in Chapters Two and Three. Kinetic and thermodynamic analysis of the nitroxygenation of a series of flavonols provides insight into the mechanism of enzymatic and non-enzymatic nitroxygenation.

Oxygenation of Flavonols

Since 1971, the FDOs from various fungus have been discovered with different metal ion as cofactors, shown in Table 1.[29-35] Crystal structure of quercetin dioxygenase (QDO) purified from culture filtrate of *Aspergillus* or *Pullularia* has been characterized and shows it is a copper or iron containing metalloenzyme.[31,33] The mononuclear Cu or Fe active sites of quercetin dioxygenase have the structure which is the distorted trigonal-bipyramidal geometry, and the metal ion is coordinated by three histidine imidazoles, one water molecule, and one carboxylate group of Glu. When the flavonol is coordinated with

enzyme, the metal environment undergoes a transition to a square pyramidal geometry, where the substrate is bound as a monodentate ligand via the deprotonated 3-hydroxyl group. It is proposed that this coordination motif enables the formation of a bridging peroxo species from which dioxygenase-type oxidative carbon-carbon bond cleavage occurs (Scheme 1.3a).[36-38] Notably, the oxygen activation step may involve electron transfer from ligand flavonolate to oxygen in order to generate a Cu (II) superoxide binding species, or a complex having Cu(I) flavonoxy radical (Scheme 1.3b), or flavonol radical and super oxide through outer sphere electron transfer (Scheme 1.3c).

Table 1.1 Flavonol dioxygenase with different metal cofactors found in various fungi and bacteria since 1971

Species	M(II)	Year
Aspergillus flavus	Cu	1971
Aspergillus niger	Cu	1999
Aspergillus japonicus	Cu	2002
Bacillus subtilis	Fe	2004
	Mg, Mn, Fe, Co, Ni, Cu & Cd	2005
	Mn, Co & Fe	2006
Streptomyces sp. Fla	Fe, Ni & Co	2008

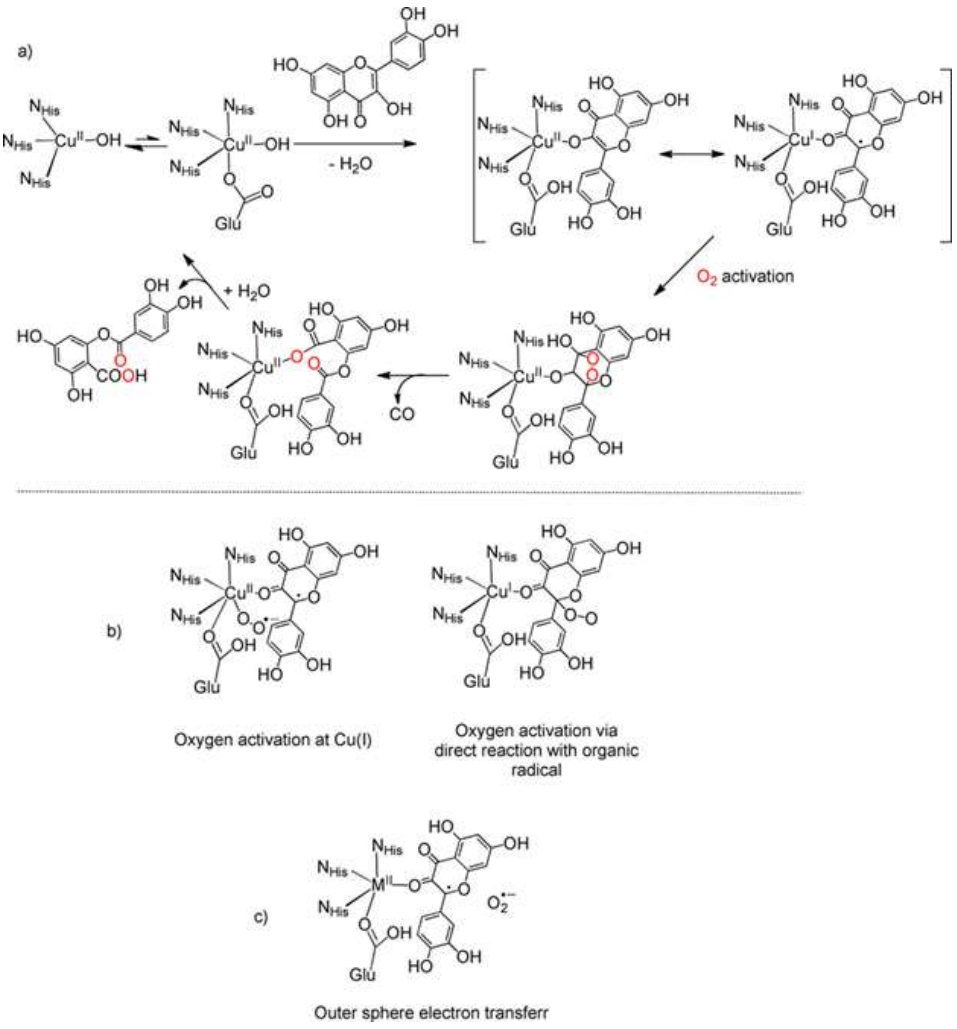

Scheme 1.3 (a) Proposed reaction pathway in fungal FDOs (b) Possible sites for O_2 activation in copper-containing fungal FDOs. (c) Proposed outer sphere electron transfer reactivity of metal-coordinated flavonol with O_2 in bacterial FDOs [22]

The role of the metal ion in catalyzing the oxygenation of flavonol has been difficult to assess. To elucidate the mechanistic route of oxidative cleavage of flavonol by flavonol dioxygenase, many flavonolate (fla^-) divalent metal complexes of iron, copper, cobalt, nickel, zinc and manganese have been synthesized and used to mimic FDO enzyme catalyzed oxygenation reaction.[39-42]

Speier's group reported a series of metal (Mn, Fe, Co, N, and Cu) flavonolate complexes, shown in Scheme 1.4.[39] The study showed enzyme – like oxygenation of the coordinated flavonolate ligand resulted in the formation of endoperoxide which decomposed by loss of carbon monoxide resulting in the corresponding depside. They found the degree of the delocalization of π-electrons in the metal-flavonolate chelate ring indicated by the shift of the absorption band (π-π*) of the coordinated flavonolate has a linear correlation with oxygenation reactivity, suggesting the role of the metal ion in the active site of FDOs may be to control the orientation of bound substrates, to contribute to modulating the reduction potential of the bound flavonol, rather than to participate directly in redox chemistry.

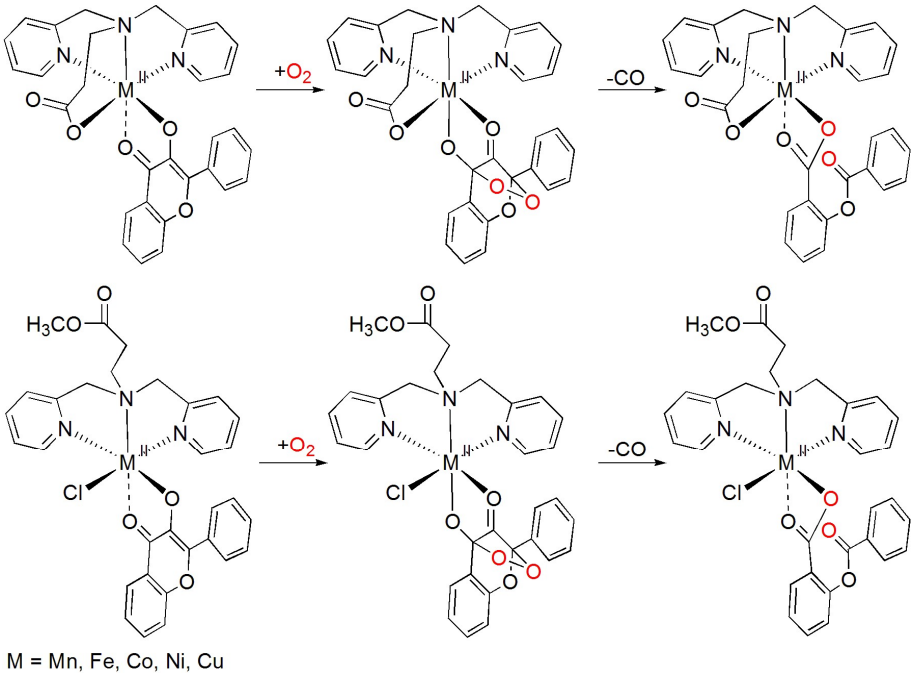

Scheme 1.4 Oxidative cleavage of $[M^{II}(fla)(L^1)]$, and $[M^{II}(fla)(L^2)X]$ (X = Cl or ClO_4) complexes in DMF [39]

Sun's group studied a series of M^{II}-flavonolate complexes containing a carboxylate ligand as structural and functional models of enzyme substrate complexes of various metal (II) – containing FDOs, shown in Scheme 1.5.[42] These model complexes exhibit relatively high reactivity in the oxidative ring-opening of the bound flavonolate at a lower temperature (70 °C) compared to Speier complexes (80 °C), presumably due to the supporting carboxylate group, and the reactivity of different metal complexes is in the order of Fe > Cu > Co > Ni > Zn > Mn. The differences on the reactivity among them may be attributed to the Lewis acidity of the metal ion and its coordination environment.

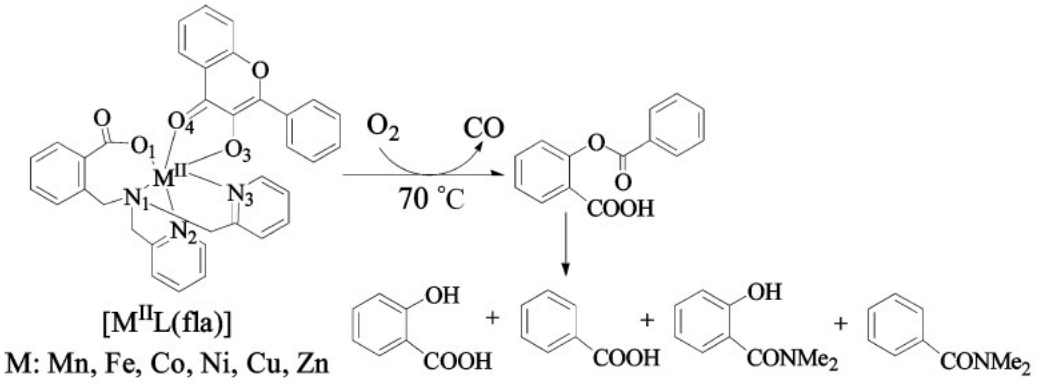

Scheme 1.5 Dioxygenation reaction of M^{II}-flavonolate complexes with a N_3O supporting ligand and their reaction products [42]

Berreau's group investigated photochemical oxygenations using flavonolate metal complexes. They reported group 12 metal (Zn^{II}, Cd^{II} and Hg^{II}) flavonolate complexes undergoing dioxygenase-type reactivity and CO release when irradiated with UV light (Scheme 1.6).[41] In 2013, they also described the photochemical reactivity of Ru^{II} (η^6-p-cymene) flavonolate compound upon irradiation with UV or visible light, in which the

photo-induced loss of the p-cymene ligand initiated oxygenation of the flavonolate ligand and release of carbon monoxide, as in the native dioxygenation reactions, shown in scheme 1.7.[43] However, the mechanism of photo-induced oxygenation of ligand flavonolate was not investigated and the intermediate endoperoxide through 1,3-addition route or 1,2-dioxetane by 1,2-addition route generated during oxygenation was unknown (Scheme 1.8).

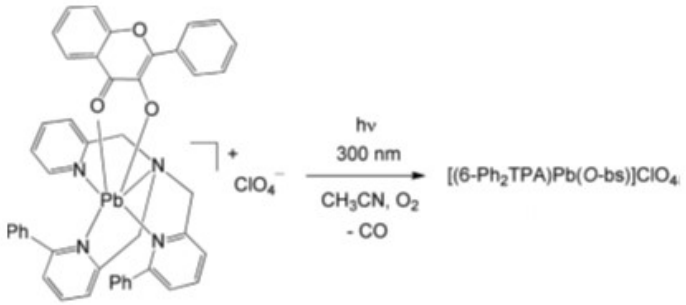

Scheme 1.6 Photo-induced oxygenation of Pb(II) flavonolate complex [41]

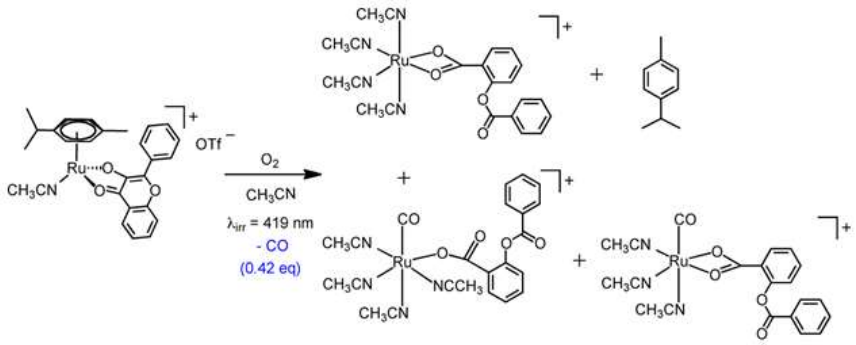

Scheme 1.7 Photo-induced reactivity of $[Ru^{II}(\eta^6\text{-}p\text{-cymene})(CH_3CN)(fla)]^+$ upon irradiation at 419 nm in aerobic CH_3CN [43]

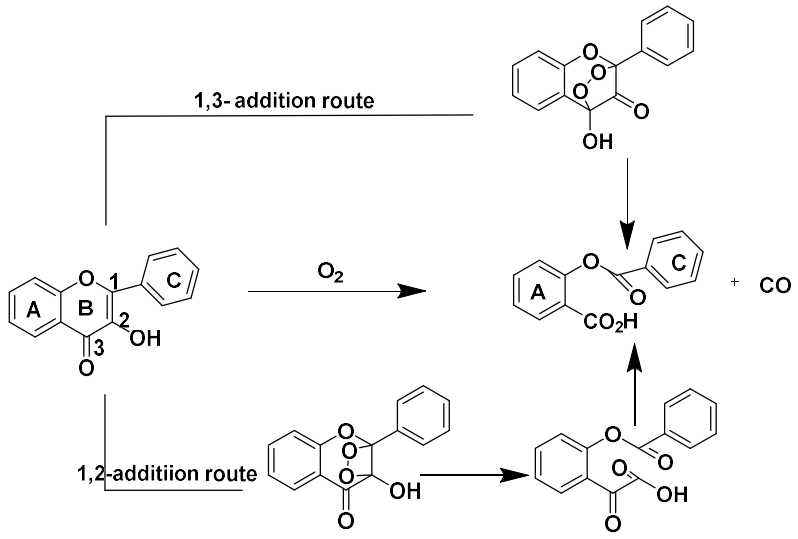

Scheme 1.8 Two different routes of oxygenation of flavonol by native QDO

As is known, photo-activation is a promising approach for modulating the reactivity of Ru^{II} compounds. The Farmer group previously reported unexpected C – H activation of a pendant methyl group in Ru(II)-dithiomatol complexes upon oxidation, as shown in Scheme 1.9.[44,45] The observed C-based oxidations are unusual in that the two S sites on the dithiomatol ligand were unaffected. Peroxidation of the free ligands yield the S-extruded ketone products rather than C-oxidization. It is clear that the coordination of the ligand to the $[Ru(bpy)_2]^{2+}$ backbone is crucial for the observed reactivity. Chapters Four and Five describe a series of ruthenium bis-bipyridyl flavonolate complexes which undergo photo-oxidation in presence of oxygen. We characterized a unique Ru-bound 2-benzoatophenylglyoxylate complex as the product, resulting from a 1,2 dioxetane intermediate, and also investigated the mechanism of oxygenation, specifically distinguishing between energy transfer and electron transfer mechanisms.

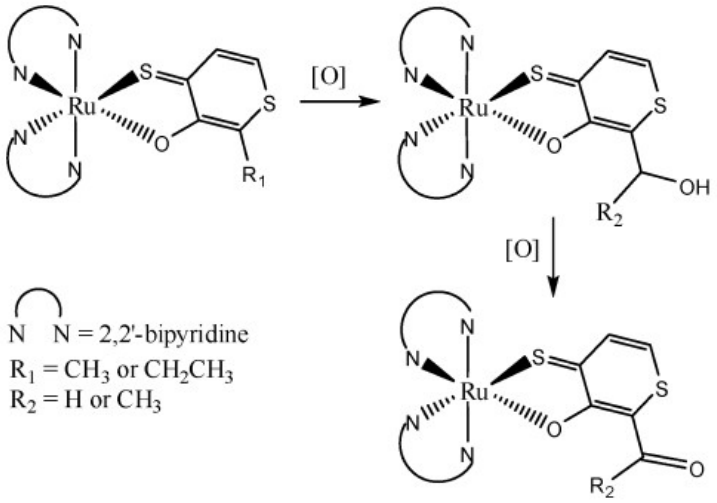

Scheme 1.9 C-H activation of Ru(II) – dithiomatol complexes [45]

In the following publications, for Chapter Two "HNO as Oxygen Substitute in Enzymes", the first author is responsible for the 90% of work described, the second author is responsible for 10% of work (product analysis of enzymatic reaction) and the third author or corresponding author is responsible for editing the manuscript and communicating with publisher; for Chapter Three "Nitroxygenation of Quercetin by HNO", the first author is responsible for 90% of work described, the second author is responsible for 10% of work (product analysis) and the third author or corresponding author is responsible for editing manuscript and communicating with publisher; for Chapter Four "Characterization of Initial Intermediate Formed during Photo-induced Oxygenation of Ruthenium(II) Bis(bipyridyl) Flavonolate Complex", the first author responsible for 90% of work described, the second author is responsible for 10% of work (crystal structure analysis) and the third author or corresponding author is responsible for editing manuscript and communicating with publisher.

References

1. Pietta, P. G. *J. Nat. Prod.* **2000**, *63*, 1035-1042.

2. Rice-Evans, C. A.; Miller, N.; Paganga, G. *Free Radical Biol. Med.* **1996**, *20*, 933-956.

3. Cotelle, N.; Bernier, J. L.; Catteau, J. P.; Pommery, J.; Wallet, J. C.; Gaydou, E. M. *Free Radical Biol. Med.* **1996**, *20*, 35-43.

4. Guohua, C.; Emin, S.; Ronald, L. *Free Radical Biol. Med.* **1997**, *22*, 749-760.

5. Van Hoof, L.; Van den Berghe, D. A.; Hatfield, G. M.; Vlietinck, A. J. *Planta Med.* **1984**, *50*, 513-517.

6. Brasseur, T. *J. Pharm. Belg.* **1989**, *44*, 235-241.

7. Wei, B. L.; Lu, C. M.; Tsao, L. T.; Wang, J. P.; Lin, C. N. *Planta Med.* **2001**, *67*, 745-747.

8. Fischer, M.; Mills, G. D.; Slaga, T. J. *Carcinogenesis* **1982**, *3*, 1243-1245.

9. Huang, M.; Ferraro, T. In *Phenolic Compounds in Food and their Effect on Health II*, Huang, M. T., Ho, C. T., Lee, C. Y., Eds.; ACS Symposium Series; American Chemical Society: Washington, DC, **1992**; Chapter 2, p 507.

10. Huang, M. T.; Wood, A. W.; Newmark, H. L.; Sayer, J. M.; Yagi, H.; Jerina, D. M.; Conney, A. H. *Carcinogenesis* **1983**, *4*, 1631-1637.

11. Musialik, M.; Kuzmicz, R.; Litwinienko, G. *J. Org. Chem.*, **2009**, *74*, 2699-2709.

12. Wollenweber, E. *Flavonoids: Advances in Research*; Harborne, J. B.; Mabry, T. J., Eds.; Chapman&Hall: London, UK, **1982**.

13. Demaster, E. G.; Redfern, B.; Nagasawa, H. T. *Biochem. Pharmacol.* **1998**, *55*, 2007-2015.

14. Kumar, R. M.; Zapata, A.; Ramirez, A.; Bowen, S.; Francisco, W.; Farmer, J. P. *Proc. Natl. Acad. Sci.* **2011**, *108*, 18926-18931.

15. Kumar, M. R. Farmer, P. J. *Biochemistry*, **2009**, *48*, 5018–5025.

16. Fukuto, J. M. *Chem. Res. Toxicol.* **2005**, *18*, 790–801.

17. Fukuto, J. M.; Switzer, C. H.; Miranda, K. M.; Wink, D. A. Annu. Rev. Pharmacol. Toxicol. **2005**, *45*, 335–355.

18. Shafirovich, V.; Lymar, S. V. *J. Am. Chem. Soc.* **2003**, *125*, 6547–6552.

19. Lymar, S. V.; Shafirovich, V.; Poskrebyshev, G. A. *Inorg. Chem.* **2005**, *44*, 5212–5221.

20. Hughes, M. N.; Cammack, R. *Methods Enzymol.* **1999**, *301*, 279–287.

21. King, S. B.; Nagasawa, T. *Methods Enzymol.* **1999**, *301*, 211–220.

22. Momiyama, N.; Yamamoto, H. *Chem. Commun.* **2005**, 3514.

23. Lewis, J.W.; Meyer, P. L.; Ormerod, J. A. *J. Chem. Soc., Perkin Trans.* **1972**, *20*, 2521-2524.

24. Sasaki, T.; Ishibashi, Y.; Ohno, M. *Chem. Lett.*, **1983**, *12*, 863-866.

25. Sasaki, T.; Mori, K.; Ohno, M. *Synthesis*, **1985**, *3*, 280-282.

26. Momiyama, N.; Yamamoto, H. *Org. Lett.*, **2002**, *4*, 3579-3582.

27. Kawasaki, M.; Li, P.; Yamamoto, H. *Angew. Chem. Int. Ed.*, **2008**, *47*, 3795-3797.

28. Momiyama, N.; Yamamoto, H. *J. Am. Chem. Soc.*, **2005**, *127*, 1080.

29. Oka, T.; Simpson, F. J. *Biochem. Biophys. Res. Commun.* **1971**, *43*, 1.

30. Hund, H. K.; Breuer, J.; Lingens, F.; Hüttermann, J.; Kappl, R.; Fetzner, S. *Eur. J. Biochem.* **1999**, *263*, 871.

31. Fusetti, F.; Schroter, K. H.; Steiner, R. A.; van Noort, P. I.; Oijning, T.; Rozeboom, H. J.; Kalk, K. H.; Egmond, M. R.; Dijkstra, B. W. *Structure* **2002**, *10*, 259.

32. Bowater, L.; Fairhurst, S. A.; Just, V. J.; Bornemann, S. *FEBS Lett.* **2004**, *557*, 45.

33. Gopal, G.; Madan, L. L.; Betz, S.F.; Kossiakoff, A. A. *Biochemistry* **2005**, *44*, 193.

34. Merkens, H.; Kappl, R.; Jakob, R.P.; Schmid, F.X.; Fetzner, S. *Biochemistry* **2008**, *47*, 12185.

35. Merkens, H.; Fetzner, S. *FEMS Microbiol. Lett.* **2008**, *287*, 100.

36. Kooter, I. M.; Steiner, R. A.; Dijkstra, B. W.; van Noort, P. I.; Egmond, M. R.; Huber, M. *Eur. J. Biochem.* **2002**, *269*, 2971–2979.

37. 50. R.A. Steiner, R. A.; Kooter, I. M.; Dijkstra, B. W. *Biochemistry* **2002**, *41*, 7955–7962.

38. Allpress, C. J.; Berreau, L. M. *Coord. Chem. Rev.* **2013**, *257*, 3005-3029.

39. (a) Kaizer, J.; Barath, G.; Pap, J. S.; Speier, G. *Chem. Commun.* **2007**, 5235−5237. (b) Matuz, A.; Giorgi, M.; Speier, G.; Kaizer, *J. Polyhedron* **2013**, *63*, 41−49. (c) Balogh-Hergovich, É.; Kaizer, J.; Speier, G.; Fulop, V.; Parkanyi, L. *Inorg. Chem.* **1999**, *38*, 3787-3795.

40. (a) Grubel, K.; Rudzka, K.; Arif, A. M.; Klotz, K. L.; Halfen, J. A.; Berreau, L. M. *Inorg. Chem.* **2010**, *49*, 82−96. (b) Grubel, K.; Laughlin, B. J.; Maltais, T. R.; Smith, R. C.; Arif, A. M.; Berreau, L. M. *Chem. Commun.* **2011**, *47*, 10431−10433.

41. (a) Barhacs, L.; Kaizer, J.; Speier, G. *J. Mol. Catal. A.* **2001**, 172, 117−125. (b) Kaizer, J.; Pap, J.; Speier, G.; Párkányi, L. *Eur. J. Inorg. Chem.* **2004**, 2253−2259. (c) Balogh-Hergovich, É.; Kaizer, J.; Pap, J.; Speier, G.; Huttner, G.; Zsolnai, L. *Eur. J. Inorg. Chem.* **2002**, 2287−2295.

42. (a) Sun, Y. J.; Huang, Q. Q.; Zhang, J. J. *Inorg. Chem.*, **2014**, *53*, 2932-2942. (b) Sun, Y. J.; Huang, Q. Q.; Tano, T.; Itoh, S. *Inorg. Chem.*, **2013**, *52*, 10936-10948.

43. Saraf, S. L.; Fish, T. J.; Bennighoff, A. D.; Buelt, A. A.; Smith, R. C.; Berreau, L. M. *Organometallics*, **2014**, *33*, 6341-6351.

44. Bruner, B.; Walker, M. B.; Zhang, D.; Selke, M.; Ghimire, M. M. M.; Omary, M. A.; Klausmeyer, K.; Farmer, P J. *Dalton Trans.* **2014***, 43,*11548-11557.

45. Backlund M.; Ziller, J.; Farmer, P. J. *Inorg. Chem.*, **2008**, *47*, 2864–2870.

CHAPTER TWO

HNO as Oxygen Substitute in Enzymes

This chapter published as: Han, X. Z.; Kumar, M. R.; Farmer, P. J. "*The Chemistry and Biology of Nitroxyl (HNO)*", Elsevier, *Amsterdam, Netherlands* **2016**, Chp. 16, 287-304

Introduction

HNO, termed nitroxyl or azanone, is the reduced and protonated congener of nitric oxide (NO). Recent work has demonstrated that HNO has distinct biological effects as compared with NO, such as the ability to elevate plasma levels of calcitonin gene-related peptide (CGRP), thus serving as a positive cardiac inotrope.[1-4] HNO is thought to target metallo- and thiol- containing proteins, often as an inhibitor or modifier of enzyme or protein function. Evidence of HNO modulation of thiol-containing enzymes first emerged from studies with the anti-alcoholism drug cyanamide, which is an aldehyde dehydrogenase (ALDH) inhibitor used therapeutically as an alcohol-aversive agent (Temposil) in Europe, Canada, and Japan.[5] Cyanamide is oxidized by peroxidases to generate HNO, which subsequently reacts with the active-site cysteine thiolate in ALDH, inhibiting the enzyme reversibly through disulfide formation or irreversibly through sulfonamide formation.[6]

HNO has also been shown to act as an activator or signaling agent promoting enzyme activity for heme-containing soluble guanylyl cyclase, sGC, the primary receptor for NO, which stimulates cyclic GMP (cGMP) production.[7,8] As with NO, vasorelaxant responses to HNO are accompanied by an increase in cGMP and are impaired by the sGC inhibitor

1H-[1,2,4]oxadiazolo[4,3-a]quinoxalin-1-one (ODQ), indicating that HNO does target sGC.[9] It remains to be determined, however, whether HNO itself directly activates sGC or first requires oxidation to NO, or if it targets the oxidized, NO-insensitive sGC isoform, which is often found with disease.[10,11]

Rarer, though, are enzymes which utilize HNO as a substrate. The first reported example was Superoxide Dismutase (SOD), an enzyme whose native function is to rapidly disproportionate superoxide (O_2^-), generating H_2O_2 and O_2. Fridovich reported that SOD facilitates the interconversion of NO and HNO.[12] When cyanamide and catalase were used to generate HNO in the presence of oxidized SOD Cu(II), NO was measured by its conversion of oxyhemoglobin to methemoglobin. When reduced SOD Cu (I) was exposed to NO anaerobically, HNO was trapped by methemoglobin forming nitrosylmyoglobin. When NO was generated by 3-morpholinosydnonimine hydrochloride in the presence of SOD, HNO or a similar reductant was formed, Scheme 2.1. Also, the activation of sGC by Angeli's salt ($Na_2N_2O_3$), a donor of HNO, implied that HNO reduces SOD to produce NO. In one study, Angeli's salt had no significant effect on sGC activity in the absence of superoxide dismutase (SOD). With SOD, Angeli's salt caused biphasic sGC activation that was accompanied by the formation of NO.[13]

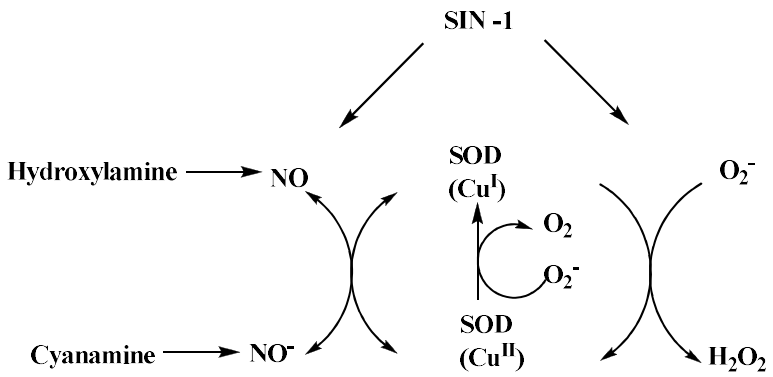

Scheme 2.1 Reaction pathways involving SOD and NO

Nitroxygenase activity. HNO is isoelectronic with O_2 and it is efficiently trapped by O_2 binding proteins like myoglobin and hemoglobin.[14] Therefore, we hypothesized that HNO may inhibit or turnover oxygenases or dioxygenases in the place of O_2, and thus allow a unique approach to study the mechanism of such enzymes. Non-heme dioxygenases catalyze an amazing variety of complex oxidations, including oxidative cleavage of carbon-carbon bonds, monohydroxylation and dihydroxylation reactions.[15] Among them, some of particular interest are dioxygenases which can catalyze the oxidative cleavage of aromatic substrates as part of bacterial aromatic degradation pathways.[16]

Quercetin 2,3-dioxygenase (QDO) is an important oxygenase in the metabolism of flavonols. Its enzymatic turnover oxidatively cleaves the central ring of the flavonol quercetin producing the depside 2-protocatechuoylphloro- glucinolcarboxylic acid and carbon monoxide.[17]

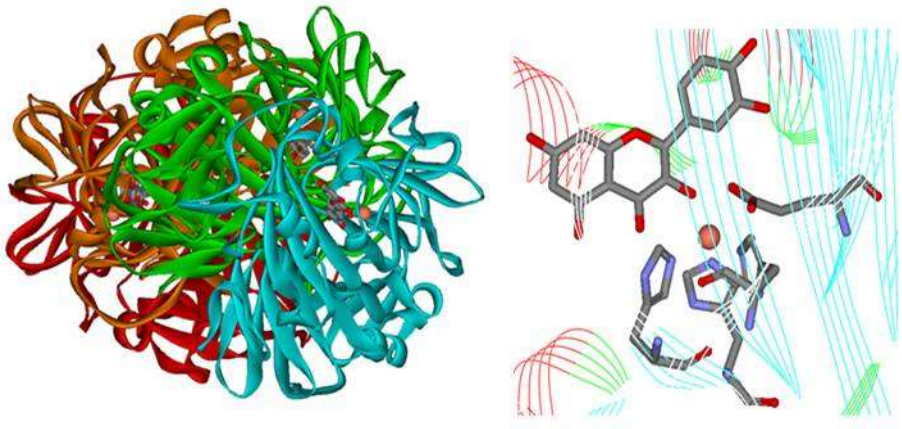

Figure 2.1 The crystal structures of QDO from *Bacillus subtilis*. The Fe atom is shown as red sphere. Also shown are the substrate quercetin, three histidines and Glu69 which all bind to the Fe(II) within the active site.

QDOs from *A. japonicus* and *B. subtilis* have been crystallographically characterized, as shown in Figure 2.1,[18-20] and their metal-binding active sites have similar structures. The Cu(II) active site of resting 2,3-QDO from *A. japonicus* (homo bicupin glycoprotein) exhibits two distinct geometries: a distorted trigonal bipyramidal geometry consisting of three histidine imidazoles (His66, His68, and His112), one water molecule and a carboxylate group of Glu73 (minor conformation 30%), and a distorted tetrahedral geometry without the direct coordinative interaction between copper(II) ion and the carboxylate group of Glu73 (major conformation 70%). In its principal conformation, Glu73 acts as a hydrogen bond acceptor for the metal-bound water molecule. The substrate quercetin is bound to the copper(II) ion through the deprotonated 3-hydroxy group of flavonolate, with displacement of the water molecule, forming an ES (enzyme–substrate) complex with a distorted square pyramidal geometry under anaerobic conditions.

The active site of the Fe(II) containing 2,3-QDO from *B. subtilis* (hetero bicupin glycoprotein) has a distorted trigonal-bipyramidal geometry consisting of three histidine imidazoles (His62, His64, and His103), a water molecule and one Glu69 at a 2.10 Å distance in the N-terminal cupin motif, and the other has a square pyramidal geometry consisting of three histidines (His234, His236, His275), a water molecule, and a weakly coordinating Glu241 at a 2.44 Å distance in the C terminal cupin motif. Metal-ion substitution experiments have shown that the catalytic activity of the Mn(II)- and Co(II) -containing enzymes were 35 and 24 fold more active, respectively, than the Fe(II)-containing native enzyme.[17] Thus, Mn(II) is proposed as the a preferred metal cofactor for 2,3-QDO from *B. subtilis*.

We demonstrated that HNO can replace O_2 in the catalytic turnover of the Mn(II)-substituted QDO from *B. subtilis*; this "nitroxygenase activity" results in the incorporation of both N and O into products derived from quercetin.[21] An analogous non-catalytic reaction of quercetin and HNO also occurs under base catalyzed conditions in the absence of enzyme, producing the same products, which can be rationalized from a depside-intermediate similar to that generated in the reaction of quercetin and dioxygen, Scheme 2. This is the first demonstration of the nitroxygenase activity using HNO as a substrate, and we believe it may have significance in the pharmacology of HNO. In this report, we further analyze this reactivity by comparing the nitroxygenase activity of the Mn(II)-substituted QDO with a series of flavonoid substrates.

Experimental

Materials. Angeli's salt was purchased from Cayman chemicals and used as received. Quercetin, myricetin, galangin and other flavonols shown in the text and 3,4-dihydroxy benzonitrile were purchased from Tokyo Chemical Industry America and checked for purity by ^{1}H NMR and ^{13}C NMR.

Enzyme expression and purification. Mn -substituted quercetin dioxygenase (QDO) was prepared by growing *Escherichia coli* BL21 (DE3) carrying plasmid pQuer4, grown in M9 minimal medium. Each culture was induced to express protein by the addition of 50 mg/L isopropyl-ß-D- thiogalactopyranoside. The Mn-QDO was selectively generated by supplementation of the media with 1 mM $MnCl_2$. Cells were harvested and the protein purified, except the protein was eluted from the DEAE-Sephacel column stepwise with 125 mM NaCl in 50 mM Tris buffer, pH 7.5 (wash buffer) and 175 mM NaCl in 50 mM Tris buffer, pH 7.5 (elution buffer). Also, the DEAE-Sepharose column was omitted from the purification procedure. Enzymatic activity for isolated batches was assayed at 380 nm in a standard spectroscopic assay using quercetin as a substrate. Active samples were analyzed for purity by SDS-PAGE electrophoresis. The purest, most active samples were pooled and concentrated and the buffer was exchanged to 50 mM phosphate buffer (pH 7.0) by centrifugation in a Vivaspin 15R centrifugal filter unit (10,000 molecular weight cutoff). Protein concentration was determined by a Bradford assay, and enzyme was stored in 10% glycerol at -20 °C.

CO trapping by deoxyMyoglobin. A home-built long-necked quartz cuvette with a side arm attached to a 25 mL round bottom flask was used to trap the CO by deoxy-myoglobin. In the cuvette was added 11 μM deoxymyoglobin in IP buffer, pH 7.0. For the non-enzymatic

reaction, quercetin (33 μM) in IP buffer, pH 8 was added to the round-bottom flask. The reaction was initiated by adding Angeli's salt (327 μM) to the quercetin. The progress of the reaction was monitored by the shift in Soret absorbance from 434 to 423 nm, confirming formation of CO-Fe^{II}Mb.

Kinetic Measurements: the nonenzymatic reaction of HNO with flavonols. Assay reactions between flavonol and HNO-precursor AS were carried out in a screw-capped UV cuvette and monitored by following the decrease of the substrate absorbance at 380 nm. An initial estimate of the rate of decomposition of Angeli's salt was determined by a natural log of concentration vs. time plot, and this value was used as a starting point in the subsequent simulations using REACT for Windows, Version 1.2.

Assays of Mn-QDO nitroxygenase activity. Assay reactions with varying amounts of flavonol, Mn-QDO, and the HNO-precursor AS were carried out in a screw-capped UV cuvette and monitored by following the decrease of the substrate absorbance at 380 nm. In a typical assay, 13.7 μM flavonol is mixed with 8.5 nM of enzyme in deareated IP buffer at pH 7; the reaction is initiated by the addition of a stock AS solution to give final concentration of 137 μM. The reaction was initiated by gently shaking the cuvette before placing it in the spectrometer, followed by observing the loss of absorbance at 380 nm.

Results

Six flavonoid antioxidants were tested for the nitroxygenase reactivity, the flavonols quercetin, myricetin, galangin, the flavone luteolin, the flavanonol taxifolin, and the flavanol catechin, shown in Scheme 2.2. In typical anaerobic enzymatic assays, premade solutions of the substrate flavonol in DMSO and the Mn-QDO in sodium phosphate buffer at pH 7 were mixed. The reaction was initiated by the addition of a stock Angeli's salt (AS)

at high pH. The reaction of substrate was quantitated by the loss of its absorbance ca. 380 nm, as shown in Figure 2.2. After completion, the reaction solutions were analyzed by liquid chromatography mass spectrometry (LC-MS). A series of analogous non-enzymatic anaerobic base-catalyzed assays were performed to compare with enzyme-catalyzed reactions, and analyzed in the same fashion.

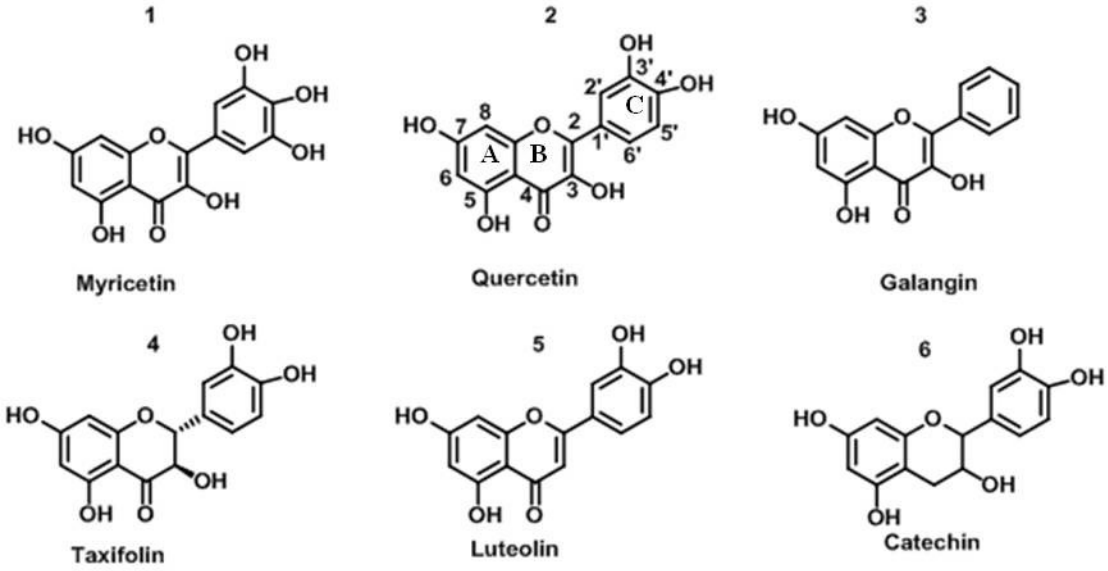

Scheme 2.2 Structures of flavonoids used

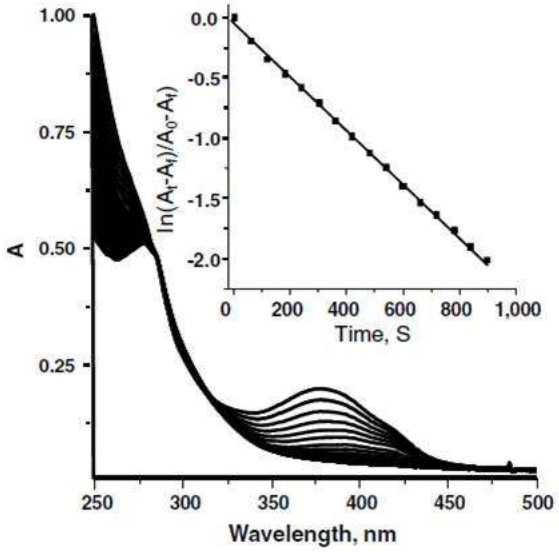

Figure 2.2 Absorbance spectrum of reaction of HNO (137 μM) with Mn-QDO (8.5 μM) showing the decrease of quercetin (13.8 μM) absorbance at 380 nm over time. Inset shows a plot of $\ln(A_t - A_f) / (A_0 - A_f)$ versus time data (▪), with a best fit line through data points

Of the tested flavonoids, only the true flavonols myricetin, quercetin and galangin react with AS. As a control, we tested the reactivity of the flavonols with NO_2^- and NH_2OH, possible decomposition byproducts of AS, but no reactions were observed on the timescale of the HNO based activity, Figure 2.3.

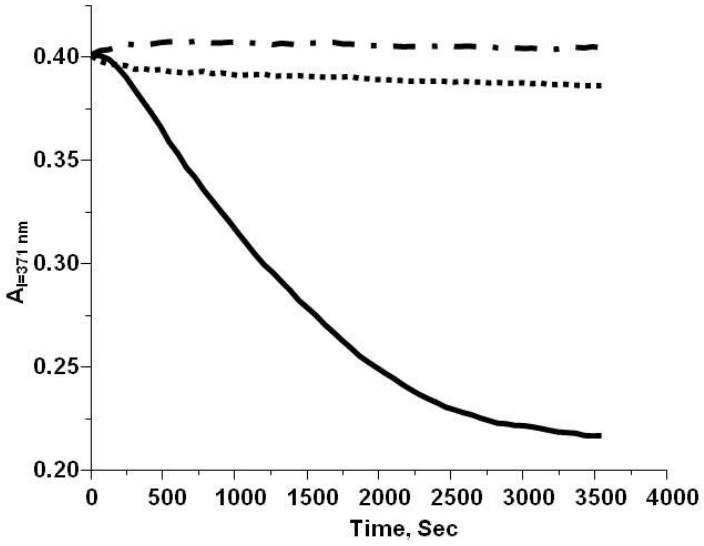

Figure 2.3 Time course UV-Vis spectra of reactions of quercetin with HNO (solid), NO_2^- anion (dash-dot) and NH_2OH (dot) in the presence of enzyme

For the three reactive substrates, analysis of negative ion LC-MS data of the product mixtures from enzymatic and non-enzymatic assays gives similar results. The substrate is completely converted to a new product ion, 134 m/z, that matches a $C_7H_4O_2N^-$ anion; LC-MS retention time and fragmentation pattern is consistent with 3,4-dihydroxybenzonitrile, an as confirmed with authentic sample of the product. The use of ^{15}N-labeled AS (specifically $Na_2[O^{15}N^{14}NO_2^{-2}]$) in which only the HNO precursor is labeled results in ^{15}N-labeled product with 135 m/z peak observable in LC-MS, Figure 2.4. The generation of CO during these reactions was confirmed by the conversion of a solution of deoxymyoglobin to its ferrous CO adduct upon exposure to the head gas above the assay mixture, Figure 2.5. Although not observed in the MS, it is assumed that an initial depside-like product, 2-iminomethoxy-3,4–dihydroxyphenyl -4,6-dihydroxybenzoate, undergoes a 1,3 proton transfer to generate the observed nitrile and phenolic products. An analogous

hydrolytic cleavage of the depside ester produced under typical QDO turnover is seen at basic pH, Scheme 2.3, resulting in carboxylic and phenolic products.

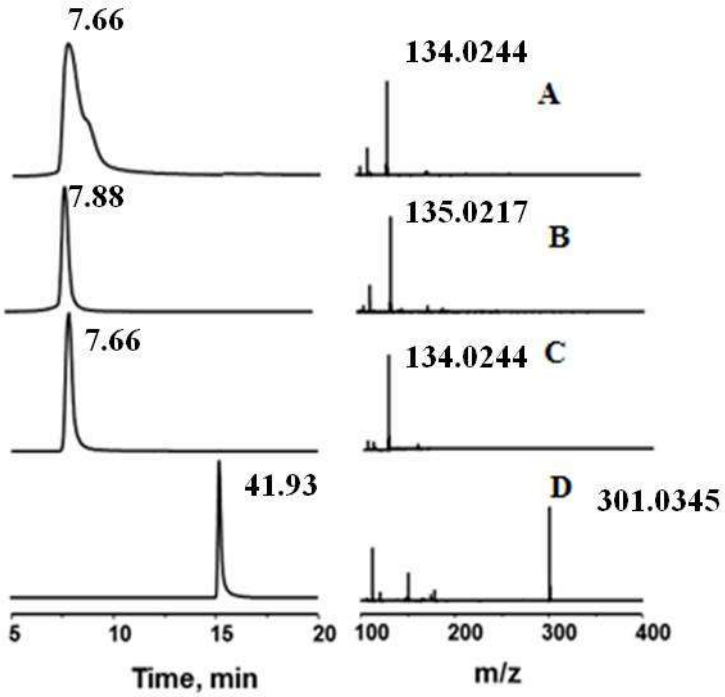

Figure 2.4 LC-MS analysis of reaction mixtures. Total ion chromatograms (left) and mass spectra (right) of product mixtures from: A) authentic 3,4-dihydroxy benzonitrile; B) the reaction of labeled Angeli's Salt, $Na_2{}^{15}NONO_2$ with quercetin; C) the reaction of unlabeled Angeli's Salt, $Na_2N_2O_3$, with quercetin; D) the substrate quercetin

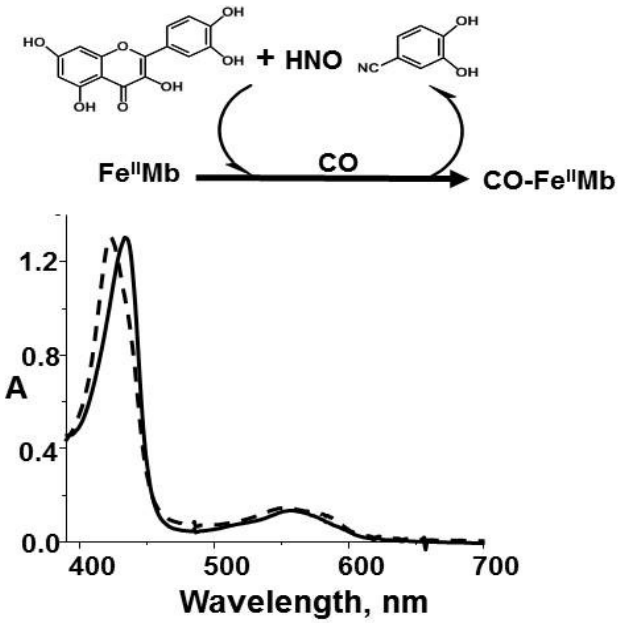

Figure 2.5 Absorbance spectra illustrating the formation of CO-Fe^{II}Mb (dotted line) by trapping of CO by deoxy-myoglobin (solid line) released in the reaction of quercetin (0.033 mM) with AS (0.327 mM); a simplified reaction scheme is shown at top

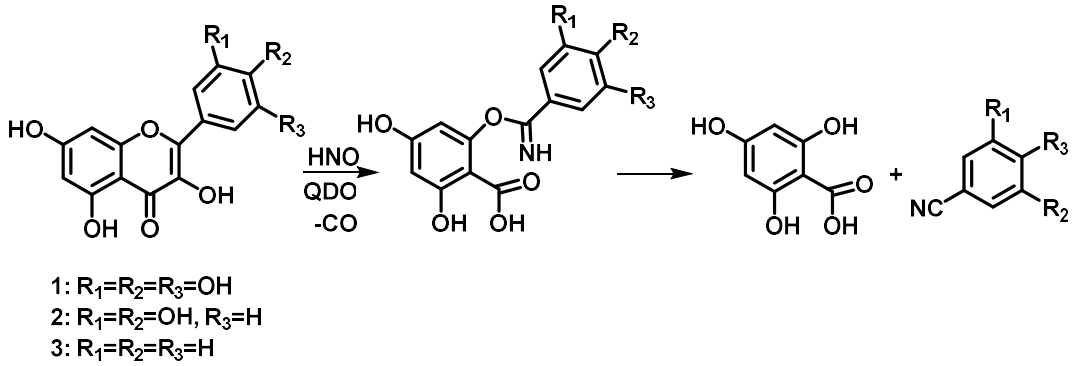

Scheme 2.3 Products of the enzymatic and non-enzymatic reaction between flavonols and AS

Kinetic analyses of the enzymatic and non-enzymatic reactions were performed and analyzed by using the sequential reactions described in Equations 1- 6. Rate analysis of the reaction between flavonol (Hfla) and HNO is complicated due to the slow decomposition rate of the HNO-donor AS and the competitive dimerization of free HNO. The dimerization of free HNO results in the formation of N_2O.[22] Equations 1-4 describe the nonenzymatic reaction between flavonol (Hfla) and HNO, while Equations 1, 2 and 5, 6 relate to the enzyme-catalyzed reaction.

$$HN_2O_3^- \longrightarrow HNO + NO_2^- \quad (1)$$

$$HNO + HNO \longrightarrow N_2O + H_2O \quad (2)$$

$$Hfla \rightleftharpoons fla^- + H^+ \quad (3)$$

$$fla^- + HNO \longrightarrow Product \quad (4)$$

$$Hfla + QDO \rightleftharpoons fla^-/QDO\ complex \quad (5)$$

$$fla^-/QDO\ complex + HNO \longrightarrow Product + QDO \quad (6)$$

A first-order rate constant at 25ºC of 7.0×10^{-4} s^{-1} for Equation 1 was calculated by Guggenheim's method, derived from plots of the first-order rate constants versus the concentrations of AS in controlled temperature bath reactions. This value is somewhat larger than the published constant for this reaction of 6.75×10^{-4} s^{-1} at room temperature, but was derived under conditions equivalent to those of the subsequent determinations. The widely reported bimolecular rate constant of the dimerization in Equation 2 of 8.00×10^6 $M^{-1}s^{-1}$ was used.[22]

The dependence of the non-enzymatic reactivity on basic conditions suggests that the substrate must be deprotonated, Equation 3, preceding its reaction with HNO. All of the substrates used have reported pK_a of flavonols in the range of the onset of HNO reactivity, shown in Table 2.1.[23] There is some variability in the reported pK_as of flavonols and related polyhydroxylic antioxidants,[24] the values used are mid-range within those reported. Likewise, there is much variability in reported oxidation potentials of the substrate flavonols; selected values used here are for general comparison, given in Table 2.1.[25]

Table 2.1 Enzymatic and nonenzymatic reaction rate constants between flavonols and AS at room temperature, as well as reported p*K*a and oxidation potentials of each flavonol

Flavonol	Enzyme catalyzed[a]	Base catalyzed[a]	pK_a[b]	E_{ox}[c]
	k_6($M^{-1}s^{-1}$)x10^4	k_4($M^{-1}s^{-1}$)x10^4		(V vs Ag/AgCl)
1 (m)	1.97 (+/ -0.09)	1.79 (+/-0.03)	6.5	-0.030
2 (q)	3.32 (+/-0.12)	1.10 (+/-0.05)	7.1	0.020
3 (g)	5.60 (+/-0.11)	0.86 (+/-0.04)	7.2	0.280

[a] Average of three trials (error in parenthesis). [b] Data from reference 23. [c] Oxidation potentials determined by column electrolysis, from reference 25.

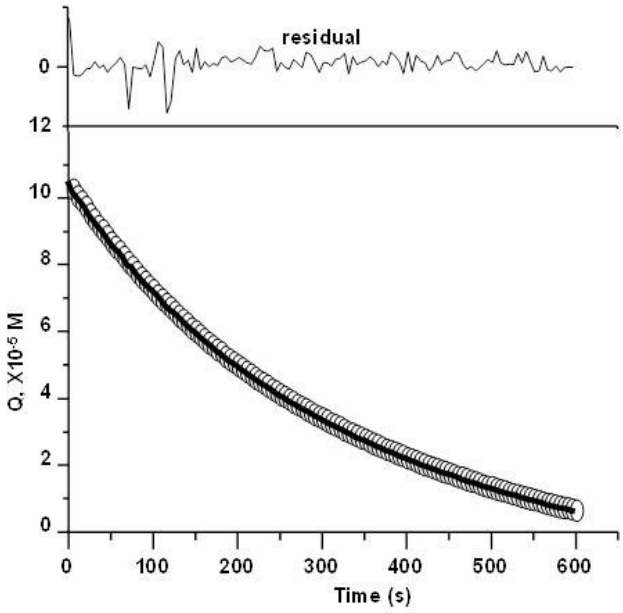

Figure 2.6 A plot of best fit kinetic model (line) vs. data absorbance at 380 nm (circles). A residual plot of (model minus data) over time is shown at top

The Henderson–Hasselbalch equilibrium was used to estimate the percentages of deprotonated flavonol (fla^-) in pH 8 buffer: 96% for myricetin, 93% for quercetin and 87% for galangin. These percentages were used to adjust substrate flavonate concentrations when solving for the second-order rate constants (k_4) of Equation 4 from kinetic data using the software, REACT for Windows,[26] as illustrated in Figure 2.6 and reported in Table 2.1 as an average of three trials. For comparison, the rate constant for the non-enzymatic dioxygenation of quercetin, Equation 7, was determined under equivalent conditions as k_7 = 0.46 $M^{-1}S^{-1}$, dramatically slower than that of nitroxygenation. Likewise, a difference of ca. 10^5 is found between psuedo bimolecular rates reported for the enzymatic dioxygenase and nitroxygenase reaction of Mn-QDO.[21]

$fla^- + O_2 \longrightarrow$ Product (7)

For the Mn-QDO catalyzed reactions (Equations. 1, 2 and 5, 6), the rate constants of the Equations 1 and 2 were obtained by the same method as in the non-enzymatic reactions, following the loss of absorbance at 380 nm at 25ºC. Previous studies had determined a Michealis constant, $K_{M,}$ of ca. 4 μM for the formation of the quercetin/QDO complex, Equation 5.[17,21] To determine the bimolecular rate constants given, quantitative formation of the flavonolate/QDO complex is assumed under conditions equivalent to that used for quercetin, i.e., at concentrations of substrate in > 100-fold excess to the enzyme. Using the same modeling REACT program, the rate constants for Equation 6 was obtained for each substrate, listed in Table 2.1 as an average of three trials.

Discussion

The substrates chosen in Scheme 1 were intended to test for structural dependences that might distinguish nitroxygenase reactivity from the corresponding dioxygenase reactivity. As with native QDO activity, only the true flavonols reacted with AS either enzymatically or nonenzymatically; the other flavonoids luteolin, taxifolin and catechin. Thus the structural requirements for dioxygenase and nitroxygenase reactivities are to have an alpha hydroxy-ketone functionality at the 3 and 4 position, as well as a double bond between C2 and C3.

Both dioxygenase and nitroxygenase reactivity also have similar bimolecular rate constants for enzyme catalyzed reactions at neutral or acidic pH as compared with the corresponding non-enzymatic reactions at high pH.[21] But there is a large difference in rates between the two reactivities, the nitroxygenase reactivity is ca. 10^5 times faster that of the dioxygenase reactivity both enzymatically and non-enzymatically. This is to be expected, as HNO is much more electrophilic than dioxygen, and also reacts from a singlet ground

state rather than the triplet ground state of dioxygen; the required spin-flip results in a substantial kinetic barrier to dioxygenation reactions.[21,27]

In the nonenzymatic reactions, the interaction of flavonolate and HNO may be initiated by an initial electron transfer,[28,29] or by nucleophilic attack of the anionic substrate on HNO,[30] as have been proposed for the corresponding dioxygenation reactions. In both scenarios, the reaction rate should be affected by the pK_a of flavonol and thermodynamic potential of the flavonate anion HOMO. The determined rate constants for Equation 4 do appear to follow to the substrate's assigned pK_a and oxidation potential, but the enzymatic rates run counter to both trends which may suggest a different mechanistic path is involved.

In the enzymatic reaction, the Mn-QDO and flavonol must first combine to form a complex, which assumes prior coordination of the flavonolate with the Mn(II) within the QDO active site. Steric hindrance within the binding pocket might favor a less bulky flavonol; the data seems most consistent with this hypothesis. Galangin, **3**, having the least number of hydroxyl groups undergoes the enzymatic nitroxygenase reaction almost six times faster than the non-enzymatic reaction. Myricetin, **1**, having the highest number of hydroxyl groups, reacts at comparable rates under both conditions tested.

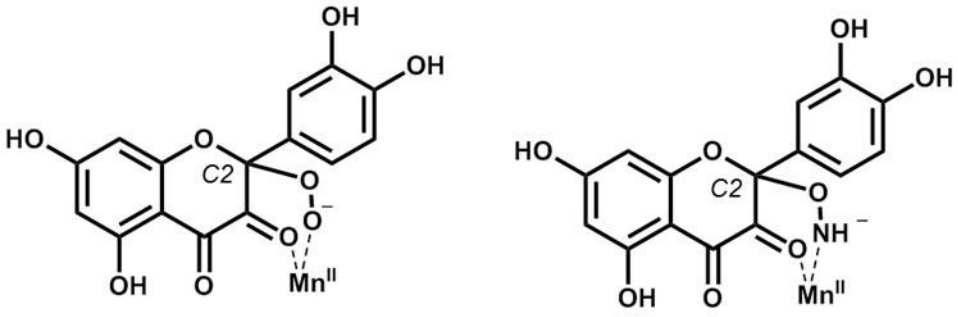

Scheme 2.4 Possible way of HNO and O_2 binding to Mn-QDO

For Mn-QDO catalyzed mechanism, it remains unclear whether HNO binds to the Mn cofactor in QDO enzyme prior to its insertion into the substrate. In most previously proposed mechanisms for QDO native activity, the β-O atom of a metal-bound superoxide attacks the C2 position which initiates the ring-opening reaction sequence, Scheme 2.4. All known metal-ion complexes of HNO are N-bound; thus an analogous nitroxygenase reaction mechanism would predict the β-O atom of a metal-bound aminoxyl radical attacks this site. But the observed products derive from N-atom incorporation at the C2 position, counter to the prediction and perhaps more consistent with a direct reaction of the activated substrate with HNO.

Importantly, only the Mn- substituted QDO enzyme undergoes nitroxygenase reactivity; samples of Fe(II) and Co(II) QDO did not show demonstrable activity.[21] Such selectivity argues for a metal-mediated mechanism, in which both the HNO and the substrate flavonolate are bound to the metal prior to product formation, rather than a metal-activation of the substrate, in which the metal-coordinated flavonolate reactions directly with HNO.

Similar questions of substrate vs. metal ion initiation have been raised in the native QDO reactivity, where reactivity is seen for several metal ions including Fe(II), Co(II), Mn(II) and Cu(II).[17] A true tertiary complex of substrate/metal ion/dioxygen has recently been characterized in a similar non-heme dioxygenase homoprocatechuate 2,3-dioxygenase (HPCD).[16] The substrate 4-nitrocatechol and dioxygen were characterized bound to the active-site Mn ion in distinct intermediate states by both EPR and Mossbauer spectroscopy; the various radical intermediates seen a sequential oxidation and reduction of the metal ion may occur during enzymatic turnover. An important distinction in the

proposed HPCD mechanism is that the Mn-bound superoxide attacks via a 4-centered cyclic transition state, rather than the 6-atom cyclic intermediate proposed for QDO, as shown in Scheme 2.5A.

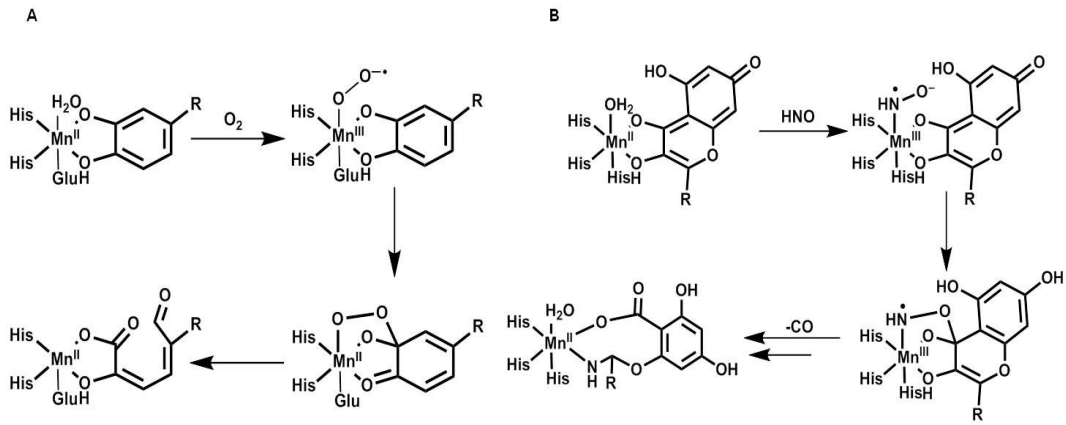

Scheme 2.5 Proposed reaction pathway for Mn-QDO catalyzed reactions of flavonols and HNO and HPCD catalyzed reactions for the reaction between 4-nitrocatechol and dioxygen

For such a mechanistic sequence to apply to the nitroxygenase reaction of Mn-QDO, a tautomeric quinone methide must be formed in ring A of the flavonol, as shown in Scheme 2.5B, which would be favored by metal binding at the two oxygen appended to positions C4 and C3. The substrate quinone methide allows attack of the Mn(III) – aminoxyl radical adduct at the C4 position, analogous to that of the dioxygenase mechanism. The plausibility of such a tautomeric substrate intermediate is supported by recent a NMR study which suggests that the C7 hydroxyl is the most acidic site in flavonoids, even in the presence of additional hydroxyls at positions C3, C5, or C6.[24] Thus the reactive flavonolate anionic species likely has quinone methide character in both the

enzymatic and non-enzymatic reactions. To our knowledge, such an intermediate has not been previously proposed, and ongoing tests of its viability in both the dioxygenase and nitroxygenase reactions are in progress.

Conclusions

The unprecedented substitution of HNO for dioxygen in the enzymatic turnover of Mn-QDO has been described, termed nitroxygenase activity, which results in the regioselective incorporation of both N and O atoms into the flavonol-derived products, as well as CO release. A similar nonenzymatic reaction of the flavonolates with HNO is observed at high pH. Rate analysis studies imply that nitroxygenase reactivity of Mn-QDO depends mainly on steric hindrance of flavonol under conditions tested, while the base-catalyzed reaction appears to depend strongly on the pK_a and oxidation potential of flavonol. The possible involvement of a quinone methide tautomer of the flavonol substrates was used to rationalize the site of nitroxyl N-atom incorporation into the product.

References

1. Paolocci, N.; Saavedra, W. F.; Miranda, K. M.; Martignani, C., Isoda, T.; Hare, J. M.; Espey, M. G.; Fukuto, J. M.; Feelisch, M.; Wink, D. A.; Kass, D. A. "Nitroxyl anion exerts redox-sensitive positive cardiac inotropy *in vivo* by calcitonin gene-related peptide signaling." *Proc. Natl. Acad. Sci.*, **2001**, *98*, 10463-10468.

2. Paolocci, N.; Katori, T.; Champion, H. C.; St John, M. E.; Miranda, K. M.,; Fukuto, J. M.; Wink, D. A.; Kass, D. A. "Positive inotropic and lusitropic effects of HNO/NO^- in failing hearts: Independence from β-adrenergic signaling." *Proc. Natl. Acad. Sci.*, **2003**, *100*, 5537-5542.

3. Paolocci, N.; Jackson, M. I.; Lopez, B. E.; Miranda, K.; Tocchetti, C. G.; Wink, D. A.; Hobbs, A. J.; Fukuto, J. M. "The pharmacology of nitroxyl (HNO) and its therapeutic potential: not just the Janus face of NO." *Pharmacol. Ther.*, **2007**, *113*, 442- 458.

4. Dai, T.; Tian, Y.; Tocchetti, C. G.; Katori, T.; Murphy, A. M.; Kass, D. A.; Paolocci, N.; Gao, W. D. "Nitroxyl increases force development in rat cardiac muscle." *J. Physiol.,* **2007**, *580*,951-960.

5. Kappaka V.; Thomposon, D. C.; Chen, Y.; Vasiliou, V. "Aldehyde dehydrogenase inhibitors: a comprehensive review of the pharmacology, mechanism of action, substrate specificity, and clinical application." *Pharma. Rev.*, **2012**, *64*,520-539.

6. DeMaster, E. G.; Redfern, B.; Nagasawa, H. T. "Mechanisms of inhibition of aldehyde dehydrogenase by nitroxyl, the active metabolite of the alcohol deterrent agent cyanamide." *Biochem. Pharmacol.*, **1998**, *55*, 2007-2015.

7. Irvine, J. C.; Ritchie, R. H.; Favaloro, J. L.; Andrews, K. L.; Widdop, R. E.; Kemp-Harper, B. K. "Nitroxyl(HNO): the Cinderella of the nitric oxide story." *Trends Pharmacol. Sci.*, **2008**, *29*, 601-608.

8. Irvine, J. C.; Cao, N.; Gossain, S.; Alexander, A.; Love, J. E.; Qin, C.; Horowitz, J. D.; Kemp-Harper, B. K.; Ritchie, R. H. "HNO/cGMP-dependent antihypertrophic actions of isopropylamine-NONOate in neonatal rat cardiomyocytes: potential therapeutic advantages of HNO over NO." *Am. J. Physiol. Heart Circ Physiol.*, **2013**, *305*, H365-H377.

9. Chin, K. Y.; Qin, C.; Kemp-Harper, B. K.; Woodman, O. L.; Ritchie, R. H. "The concomitant coronary vasodilator and positive inotropic actions of the nitroxyl donor Angeli's salt in the intact rat heart: contribution of soluble guanylyl cyclase-dependent and -independent mechanisms." *Br. J. Pharmacol.*, **2014**, *7*, 1722-1734.

10. Miller, T.M.; Cherney, M.E.; Franco, N.; Farmer, P.J.; King, S.B.; Hobbs, A.J.; Miranda, K.; Burstyn, J.N.; Fukuto, J.M. "The effects of nitroxyl (HNO) on soluble guanylate cyclase activity: Interactions at ferrous heme and cysteine thiols." *J. Biol. Chem.* **2009**, *284*, 21788-21796.

11. Irvine, J. C.; Favaloro, J. L.; Kemp-Harper, B. K. "NO^- activates soluble guanylate cyclase and K_v channels to vasodilate resistance arteries." *Hypertension,* **2003,** *41,* 1301-1307.

12. Liochev, S. I.; Fridovich, I. "Nitroxyl (NO^-): a substrate for superoxide dismutase." *Archives of Biochemistry and Biophysics*, **2002**, *402*, 166-171.

13. Zeller, A.; Wenzl, M.; Beretta, M.; Stessel, H.; Russwurm, M.; Koesling, D.; Mayer, B. "Mechanism underlying activation of soluble guanylate cyclase by the nitroxyl donor angeli's salt." *Mol. Pharmacol.*, **2009**, *76*, 1115-1122.

14. (1) Kumar, R. M.; Pervisky, D.; Chem, L.; Poulos, T.; Kundu, S.; Hargrove, M. S.; Rivera, E. J.; Diaz, A.; Colon, J. L.; Farmer, J. P. "Nitrosyl hydride (HNO) as an O_2 analogue: long-lived HNO-adducts of ferrous globins." *Biochemistry,* **2009**, *48*, 5018-5025. (2) Reisz, J. A.; Bechtold, E.; King, S. B. "Oxidative heme protein-mediated nitroxyl (HNO) generation." *Dalton Trans.*, **2010**, *39*, 5203-5212.

15. Bugg, T. "Dioxygenase enzymes: catalytic mechanisms and model chemistry." *Tetrahedron*, **2003**, 59, 7075 – 7101.

16. Bugg, T.; Ramaswamy, S. "Non-heme iron-dependent dioxygenases: unraveling catalytic mechanisms for complex enzymatic oxidations." *Curr. Opin. Chem. Biol.*, **2008**, *12*, 134-140.

17. Schaab, M. R.; Barney, B. M.; Francisco, W. A. "Kinetic and spectroscopic studies on the quecetin 2,3-dioxygenase from *Bacillus subtilis*." *Biochemistry*, **2006**, *45*, 1009-1016.

18. Fusetti, F.; Schroter, K. H.; Steiner, R. A.; Noort, P.; Pijing, T.; Rozeboom, H. J.; Kalk, K. H.; Egmond, M. R.; Dijkstra, B. W. "Crystal structure of the copper-containing quercetin 2,3-dioxygenase from *Aspergillus japonicus*." *Structure*, **2002**, *10*, 259-268.

19. Gopal, B.; Madan, L. L.; Betz, S. F.; Kossiakoff, A. A. "The crystal structure of a quercetin 2,3-dioxygenase from *Bacillus subtilis* suggests modulation of enzyme activity by a change in the metal ion at the active site." *Biochemistry*, **2005**, *44*, 193-201.

20. Sun, Y. J.; Huang, Q. Q.; Zhang, J. J. "Series of structural and functional models for the ES (enzyme-substrate) complex of the Co(II)-containing quercetin 2,3-dioxygenase." *Inorg. Chem.*, **2014**, *53*, 2932-2942.

21. Kumar, R. M.; Zapata, A.; Ramirez, A.; Bowen, S.; Francisco, W.; Farmer, J. P. "Nitrosyl hydride (HNO) replaces dioxygen in nitroxygenase activity of manganese quercetin dioxygenase". *Proc. Natl. Acad. Sci*., **2011**, *108*, 18926-18931.

22. Shafirovich, V.; Lymar, S. V. "Nitroxyl and its anion in aqueous solutions: Spin states, protic equilibria, and reactivities toward oxygen and nitric oxide." *Proc. Natl. Acad. Sci*., **2002**, *99*, 7340-7345.

23. Lunte, C.; Sanli, S. "Determination of eleven flavonoids in chamomile and linden extracts by capillary electrophoresis." *Anal. Methods*, **2014**, *6*, 3858-3864.

24. Musialik, M.; Kuzmicz, R.; Litwinienko, G. "Acidity of hydroxyl groups: An overlooked influence on antiradical properties of flavonoids." *J. Org. Chem.,* **2009**, *74*, 2699-2709.

25. Yang B.; Kotani A.; Arai, K.; Kusu, F. "Estimation of the antioxidant activities of flavonoids from their oxidation potentials." *Anal. Sci.*, **2001**, *17*, 599-604.

26. a) *REACT for Windows, Version 1.2*; Manka, M. J., Ed.; Alchemy Software, Wesley: Chapel, FL, 2001; b) Braun, W.; Herron, J. T.; Kahaner, D.K. "Acuchem: A computer program for modeling complex chemical reaction systems." *Int. J. Chem. Kinet.*, **1988**, *20*, 51-62.

27. Costas, M.; Mehn, M. P.; Jensen, M. P.; Que, L. "Dioxygen activation at mononuclear nonheme iron active sites: enzymes, models, and intermediates." *Chem. Rev.*, **2004**, *104*, 939-986.

28. Kaizer, J.; Speier, G. "Radical-initiated oxygenation of flavonols by dioxygen." *J. Mo.l Catal. A: Chem.,* **2001**, *171*, 33-36.

29. Balogh-Hergovich, E.; Speier, G. "Kinetics and mechanism of the base-catalyzed oxygenation of flavonol in DMSO-H_2O solution." *J. Org. Chem.*, **2001**, *66*, 7974-7978.

30. Nishinaga, A.; Tojo, T.; Tomita, H.; Matsuura, T. "Base-catalyzed oxygenolysis of 3-hydroxyflavones." *J. Chem. Soc. Perkin Trans.*, **1979**, *10*, 2511-25.

CHAPTER THREE

Nitroxygenation of Quercetin by HNO

This chapter published as: Han, X. Z.; Kumar, M. R.; Farmer, P. J. *Tetrahedron Letters*, **2016**, *57*, 399-402

Introduction

Quercetin and other flavonoids are antioxidants found in fresh fruits and vegetables that have been shown to play an important preventative role in cardiovascular diseases and aging.[1-3] A number of enzymes have been found which decompose flavonoids by reaction with dioxygen, Scheme 3.1.[4,5] The same reaction occurs non-enzymatically, though typically at higher pH.[4]

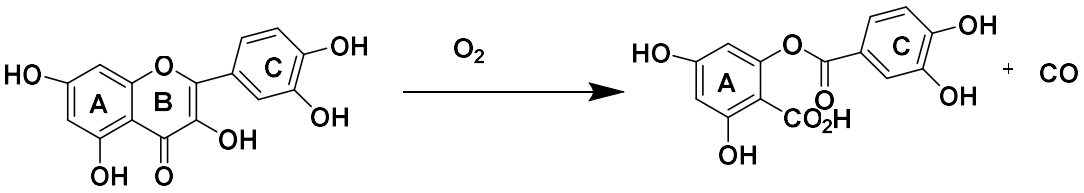

Scheme 3.1 Decomposition of quercetin by O_2

In a series of mechanistic studies, the Speier group proposed that in organic solvents the non-enzymatic reaction proceeds by an way of a rate-limiting single electron transfer (SET) between the deprotonated flavonol and oxygen, but in protic solvents a second slower bimolecular reaction competes.[5] Metal complex models for the enzymatic reactions have also examined by Speier[6] and others.[7,8] In both the free or metal-bound non-enzymatic

oxygenations, the reactions are typically observed at temperatures above 70 ^{0}C, with reported activation free energies of greater than 24.1 kcal/mol.[5a,6f]

Nitroxyl, HNO, is the reduced and protonated congener of NO, which is isoelectronic with singlet O_2. HNO displays biological effects distinct from that of NO, for example as an enzyme inhibitor[9] and ionotropic agent that may be used in the treatment of heart failure.[10] Recently, we reported the unprecedented substitution of HNO for dioxygen in the activity of Mn-substituted Quercetin Dioxygenase, Mn-QDO, resulting in the incorporation of both heteroatoms of HNO regioselectively into the product, Scheme 3.2.[9] In these reactions, HNO is generated *in situ* from a precursor, and in the presence of enzyme and substrate, and like dioxygenation, cleaves the central O-heterocyclic ring to release CO. The reaction likely proceeds through an analogous depsidic product **2,** which decomposes to give the observed 2,4,6-trihydroxybenzoic acid and 3,4-dihydroxybenzonitrile products. Importantly, like dioxygenation, a non-enzymatic nitroxygenation of quercetin with HNO proceeds at high pH yielding the same regioselective products, again suggesting the deprotonated quercetinate anion is the dominant reactant.

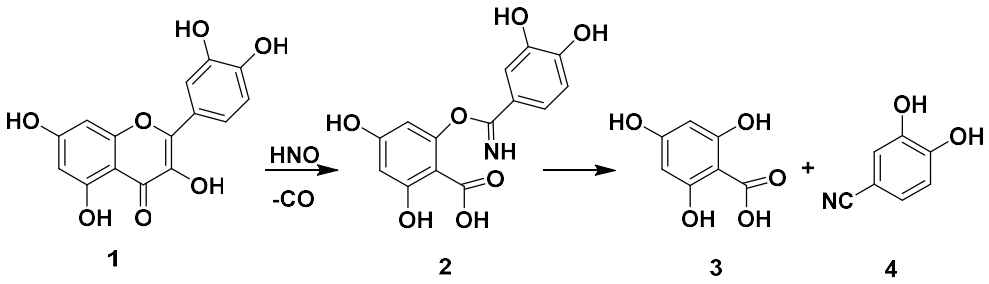

Scheme 3.2 Mn-QDO catalyzed nitroxygenation of quercetin

The coupling of HNO to an enolic carbon center is similar to the so-called nitroso aldol reactions, NA, in which nitroso compounds couple with activated ketones and aldehydes yielding both O- or N-bound adducts, Scheme 3.3.[11] The early examples of these aldol condensations utilized nitrosobenzene and strongly activated enolates or silyl enol ethers, typically yielding N-bound hydroxyamino products.[12-14] More recent work by Yamamoto and coworkers have shown a much wider scope of NA reactivity,[15] with Lewis-acid catalysis yielding O-bound aminooxy adducts.[16-17] These reactions are proposed to occur through bimolecular nucleophilic attack, rather than outersphere SET.

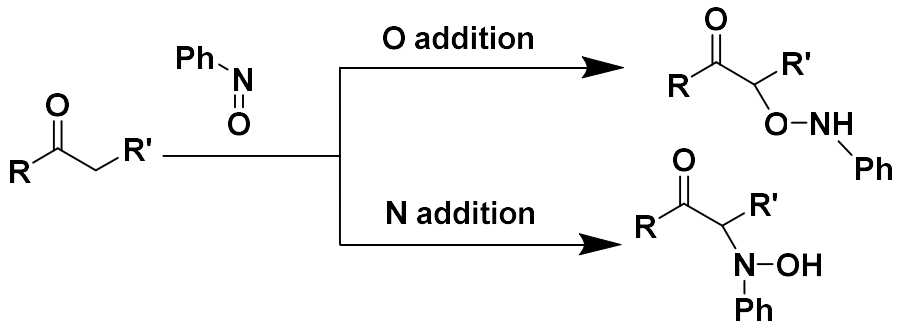

Scheme 3.3 O addition and N addition in nitroso aldol reaction

Experimental

Materials. Angeli's salt was purchased from Cayman chemicals and used as received. Quercetinshown in the text was purchased from Tokyo Chemical Industry America and checked for purity by ^{1}H NMR and ^{13}C NMR. Deuterium oxide (D_2O), 99.9 atom % D, was purchased from Sigma-Aldrich.

The kinetic reaction between Quercetin and HNO. Assay reactions between Quercetin and HNO-precursor AS were carried out in a screw-capped UV cuvette and monitored by

following the decrease of the substrate absorbance at 380 nm. An initial estimate of the rate of decomposition of Angeli's salt was determined by a natural log of concentration vs. time plot, and this value was used as a starting point in the subsequent simulations using REACT for Windows, Version 1.2. UV-vis spectra were recorded with an Agilent Technologies diode array spectrophotometer 8453.

Results and Discussion

In this report, we investigate the kinetics and thermodynamics of the non-enzymatic reaction to address questions regarding the mechanism of nitroxygenation. Reactions between quercetin and HNO were monitored by the decay of the quercetin absorption band with λ_{max} of 400 nm, as shown in Figure 3.1. The majority of experiments were run at pH 8.0 in phosphate buffer, conditions at which quercetin (p*K*a = 7.1)[18] is almost 90% deprotonated and compatible with the use of Angeli's Salt (AS) as a stable source of HNO. Under analogous conditions, no side reaction of quercetin with the byproduct NO_2^-, was seen on the timescale of the measured reactivity.

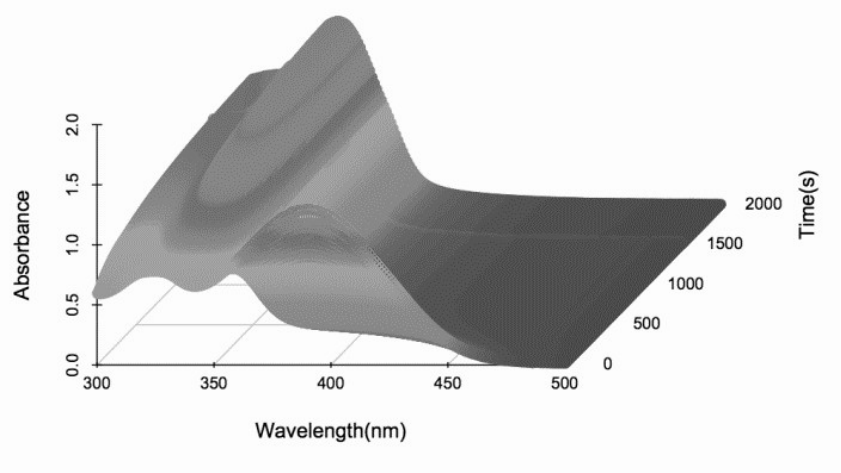

Figure 3.1 Absorbance spectra obtained over the course of reaction of quercetin (0.04 mM) with HNO donor Angeli's salt (1.00 mM) in pH 8.0 sodium phosphate buffer at 298 K

$$HN_2O_3^- \longrightarrow HNO + NO_2^- \quad (k_1) \qquad (1)$$

$$HNO + HNO \longrightarrow N_2O + H_2O \quad (k_2) \qquad (2)$$

$$Q^- + HNO \longrightarrow \text{Product} \quad (k_3) \qquad (3)$$

The reaction sequence in Equations 1-3 was used to model the kinetic data. These reactions are complicated by the slow release of HNO from AS, and its competitive dimerization forming N_2O.[19] The temperature dependence under our conditions for the first-order rate constant k_1 for Equation 1 was obtained following the loss of absorbance of Angeli's salt at 250 nm, in both H_2O and D_2O solutions, summarized in Table 3.1. A literature value for the bimolecular rate of Equation 2, $k_2 = 8 \times 10^6$ $M^{-1}s^{-1}$, was assumed unchanged under these conditions. [9,19]

Table 3.1 Temperature dependence of AS decomposition

T/K	k_1 (s^{-1})[a]	
	HNO	DNO
288	5.0×10^{-4}	4.0×10^{-4}
293	7.0×10^{-4}	6.0×10^{-4}
298	1.8×10^{-3}	1.5×10^{-3}
303	2.6×10^{-3}	2.3×10^{-3}
308	3.4×10^{-3}	2.8×10^{-3}

[a] experimental variance within 5%.

The temperature dependence of the second-order rate constant of Equation 3, k_3, was obtained by converting absorbance data to concentration vs time and then fitting the data to the reaction sequence using REACT for Windows, Version 1.2, Figure 3.2.[20] Table 3.2 gives the determined rate constants for analogous reactions of HNO and DNO, the latter being the assumed reactant in D_2O solution.

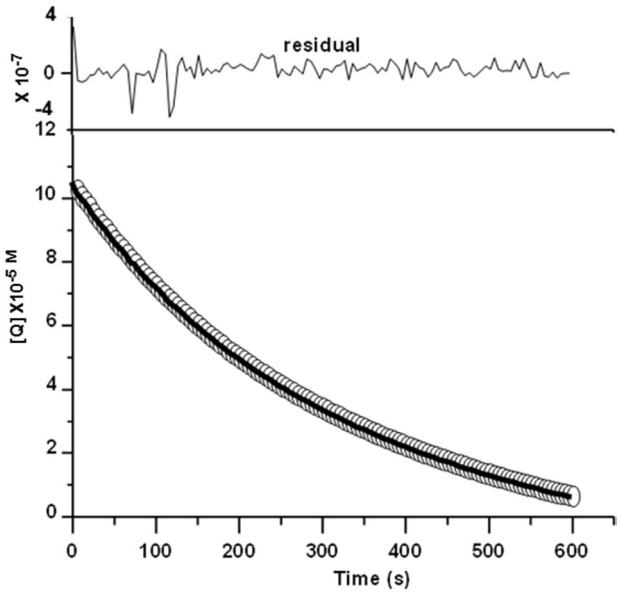

Figure 3.2 Overlay of modeled (dot) and experimentally-derived (dash) concentrations for a typical reaction, with residual plot above

Table 3.2 Temperature dependence of k_3

	$k_3(M^{-1}s^{-1})^a \times 10^4$	
T/K	HNO	DNO
288	0.782 (± 0.15)	0.418 (± 0.13)
293	1.10 (± 0.05)	0.573 (± 0.08)
298	1.34 (± 0.09)	0.852 (± 0.07)
303	1.85 (± 0.07)	1.32 (± 0.05)
308	2.49 (± 0.12)	2.06 (± 0.09)

[a] experimental variance is within 5%, average of three trials (error in parenthesis).

Using the data in Table 3.2, the activation enthalpy ($\Delta H^{\neq}$) and activation entropy ($\Delta S^{\neq}$) for the reaction were derived from Eyring plots of $\ln(k_2/T)$ versus the reciprocal of the absolute temperature ($1/T$), respectively, and are given in Table 3.3 for reactions in both H_2O and D_2O. Analysis of the variable temperature kinetic data on this reaction obtains an activation free energy $\Delta G^{\neq}$ of 11.8 kcal/mol, shown in Table 3. The kinetic isotope effect, KIE, derived from rate constants obtained in H_2O and D_2O solutions is 1.92 at 293K. This value suggests, as well as the relatively small entropic energies of activation, suggest that no bonds are made or broken in the rate-determining step.

Table 3.3 Determined activation parameters at 20 ºC for Equation 3.

	$\Delta H^{\neq}$	$\Delta S^{\neq}$	$-T\Delta S^{\neq}$	$\Delta G^{\neq}$
	kcal/mol	cal/mol K[a]	kcal/mol	kcal/mol[b]
HNO	9.38 (± 0.04)	-8.27 (± 0.03)	2.42	11.80
DNO	13.61 (± 0.02)	5.07 (± 0.04)	-1.48	12.13

[a] From intercepts of the Eyring plots.

[b] From the equation $\Delta G^{\neq} = \Delta H^{\neq} - T\Delta S^{\neq}$.

$$Q^- + O_2 \longrightarrow \text{Product} \quad (k_4) \qquad (4)$$

For comparison, the bimolecular rate constant of dioxygenation, k_4, at 293K is 0.46 $M^{-1}s^{-1}$, ca. 10^4 slower than that of nitroxygenation. Likewise, the reported enzymatic dioxygenation reaction of quercetin by Mn-QDO was ca. 10^4 slower than the analogous

nitroxygenation.[9,21] Thus nitroxygenation appears to be fundamentally and significantly more facile than dioxygenation in these reactions.

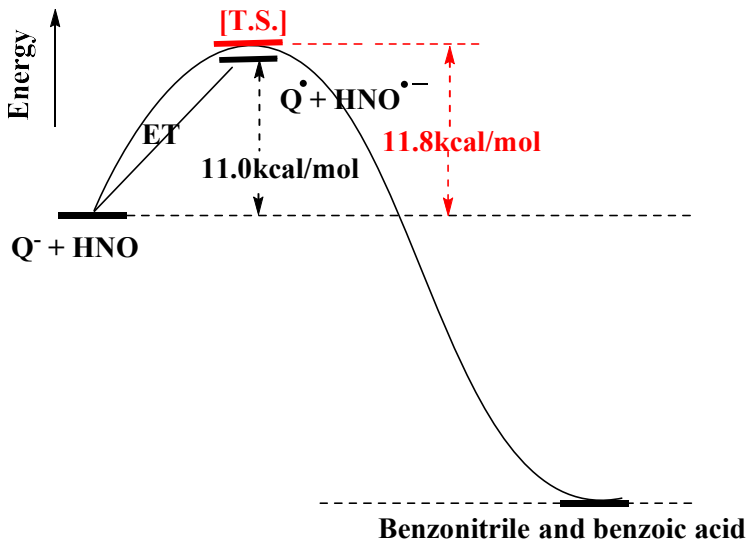

Figure 3.3 Reaction coordinate diagram for Equation 3 showing determined activation energy in red, and calculated value for initial outer-sphere electron transfer mechanism.

$$\Delta G^{o} = F[E^{o}(QH^{+/0} - E^{o}(HNO^{0/-})] \qquad (5)$$

Further insight is obtained by application of the Nernst relationship, Equation 5, utilizing the reported potentials vs NHE for quercetin oxidation (0.26 V) and HNO reduction (-0.22V),[22-24] which obtains the theoretical energy for single electron transfer (SET) of 11.0 kcal/mol. This value is quite close to that of the determined $\Delta G^{\neq}$ for the non-enzymatic nitroxygenation, and thus is consistent with an initial single electron transfer, SET, as the rate-determining step, illustrated in Figure 3.3. One product of SET

would be HNO^-, the aminoxyl radical anion, at an estimated reduction potential of 0.52 V NHE,[25] as compared to that of superoxide at –0.33 V from O_2.[26] Thus the accelerated rate of nitroxygenation vs. oxygenation can be attributed to the difference in driving force for the rate determining SET step.

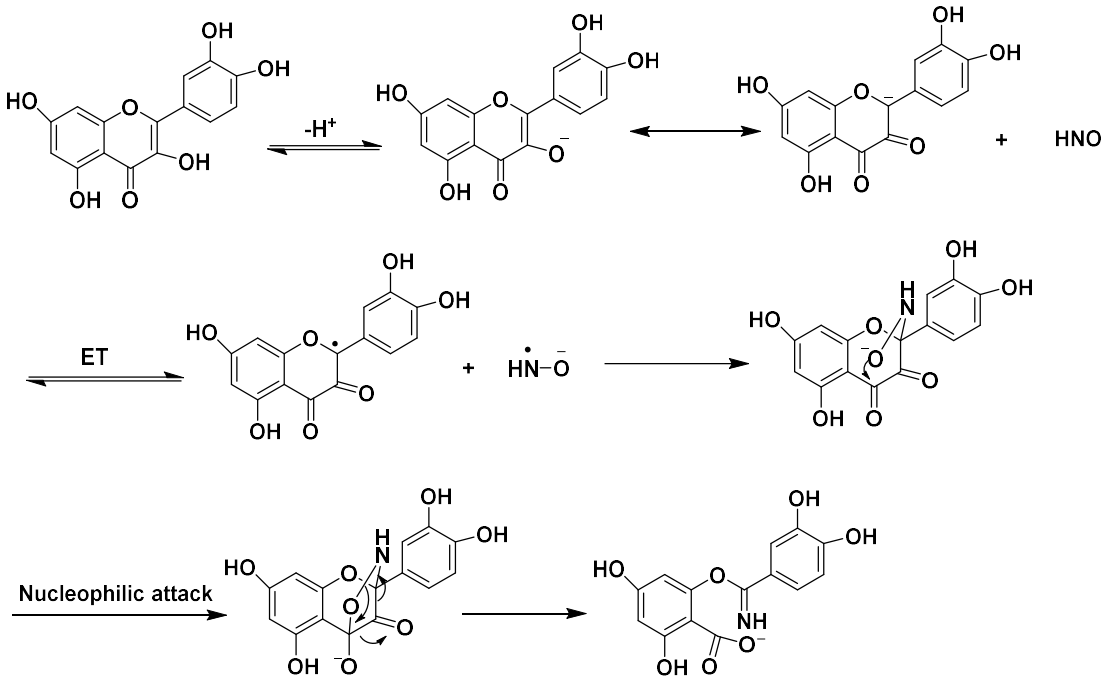

Scheme 3.4 Proposed mechanism of nitroxygenation of quercetin by HNO

These results are consistent with the proposed mechanism shown in Scheme 3.4. In this sequence, quercetin is first deprotonated, generating an anion with substantial electron density located on C2 of the central ring. The rate-limiting electron transfer between quercetinate and HNO produces a quercetin radical and the aminoxyl radical anion, HNO^- · Radical-radical coupling generates an N-oxyamino anion; this key intermediate may also

be generated by nucleophilic attack of a C2-based carbanion on HNO, analogous to the nitroso aldol reactions. But the relatively small entropy of activation suggest no bond formation in the rate-determining step, thus supporting the outersphere SET mechanism.[27,28] The incipient N-oxyamino anion then undergoes an intramolecular nucleophilic attack at the C4 carbonyl, releasing CO and forming the proposed depsidic intermediate which decomposes to the observed products.

Conclusions

The nitroxygenation of quercetin with HNO is much more facile than the comparable dioxygenation, some 1000-fold faster at room temperature than an analogous dioxygenation at 70 ^{0}C. Thermodynamic analysis yields an activation barrier very similar to that predicted for a rate-determining SET step; the difference in rates may be attributed to a large difference in SET driving force. The unique regioselectivity of nitroxygenation may be of use in organic synthesis, as well as to provide mechanistic insight in comparison to analogous dioxygenation reactions.

References

1. Dragsted, L.; Strube M.; Larsen, J. *Pharmacology & Toxicology.* **1993**, *72*, 116-135.

2. Bors, W.; Heller, W.; Stettmaier K. *Handbook of Antioxidants.* **1996**, 409-466.

3. Shahidi F. and Wanasundara P. *Critical Reviews in Food Science and Nutrition.* **1992**, *32*, 67-103.

4. a) Schaab, M. R.; Barney, B. M.; Francisco, W. A. *Biochemistry*, **2006**, *45*, 1009-1016. b) Fusetti, F.; Schroter, K. H.; Steiner, R. A.; Noort, P.; Pijing, T.; Rozeboom, H. J.; Kalk, K. H.; Egmond, M. R.; Dijkstra, B. W. *Structure*, **2002**, *10*, 259-268. c) Gopal, B.; Madan, L. L.; Betz, S. F.; Kossiakoff, A. A. *Biochemistry*, **2005**, *44*, 193-201.

5. a) Hergovich, E. B. and Speier G. *J. Org. Chem.* **2001**, *66*, 7974-7978. b) Czaun, M.; Speier, G. *Tetrahedron Lett*. **2002**, *43*, 5961-5963. c) Czaun, M.; Speier, G.; Kaizer, J.; Farkas, E. *Tetrahedron* **2013**, *69*, 6666-6672.

6. a) Pap, J. S.; Kaizer, J.; Speier, G. *Coord. Chem. Rev*., **2010**, *254*, 781-793. b) Balogh-Hergovich, E.; Speier, G.; Argay, G. *J. Chem. Soc. Chem. Commn.*, **1991**, 551-552. c) Matuz, A.; Giorgi, M.; Speier, G.; Kaizer, J. *Polyhedron*, **2013**, *63*, 41-49. d) Lippai, I.; Speier, G. *J. Mol. Cata. A:*, **1998**, *130*, 139-148. e) Balogh-Hergovich, E.; Kaizer, J.; Speier G.; Hutter, G.; Jacobi, A. *Inorg. Chem.*, **2000**, *39*, 4224-4229. f) Balogh-Hergovich, E.; Kaizer, J.; Sperier, G.; Fulop, V.; Parkanyi, L. *Inorg. Chem.* **1999**, *38*, 3787-3795.

7. a) Grubel, K.; Rudzka, K.; Arif, A. M.; Klotz, K. L.; Halfen, J. A.; Berreau, L. M. *Inorg. Chem*., **2010**, *49*, 82-96. b) Berreau, L. M.; Borowski, T.; Grubel, K.; Allpress, C. J.; Wikstrom, J. P.; Germain, M. E.; Rybak-Akimova, E. V.; Tierney, D. L. *Inorg. Chem.*, **2011**, *50*, 1047-1057. c) Szajna-Fuller, E.; Rudzka, K.; Arif, A. M.; Berreau, L. M. *Inorg. Chem*., **2007**, *46*, 5499-5507. d) Grubel, K.; Fuller, A. L.; Chambers, B. M.; Arif, A. M.; Berreau, L. M. *Inorg. Chem*., **2010**, *49*, 1071-1081.

8. a) Nishinaga, A.; Tojo, T.; Matsuura, T. *J. Chem. Soc., Chem. Commun.* **1974**, 896-897. b) Nishinaga, A,; Numada, N.; Maruyama, K. *Tetrahedron Lett.* **1989**, *30*, 2257-2258. C) Nishinaga, A.; Kuwashige, T.; Tsutsui, T.; Mashino, T.; Maruyama, K. *J. Chem. Soc., Dalton Tran.* **1994**, 805-810.

9. Kumar, M.; Zapata, A.; Ramirez, A.; Bowen, S.; Francisco, W.; Farmer, P. *Proc. Natl. Acad. Sci*. **2011,** *108*, 18926-18931.

10. Demaster, E. G.; Redfern, B.; Nagasawa, H. T. *Biochem. Pharmacol.* **1998**, *55*, 2007-2015.

11. Momiyama, N.; Yamamoto, H. *Chem. Commun.* **2005**, 3514.

12. Lewis, J.W.; Meyer, P. L.; Ormerod, J. A. *J. Chem. Soc., Perkin Trans.* **1972**, *20*, 2521-2524.

13. Sasaki, T.; Ishibashi, Y.; Ohno, M. *Chem. Lett.*, **1983**, *12*, 863-866.

14. Sasaki, T.; Mori, K.; Ohno, M. *Synthesis*, **1985**, *3*, 280-282.

15. Momiyama, N.; Yamamoto, H. *Org. Lett.*, **2002**, *4*, 3579-3582.

16. Kawasaki, M.; Li, P.; Yamamoto, H. *Angew. Chem. Int. Ed.*, **2008**, *47*, 3795-3797.

17. Momiyama, N.; Yamamoto, H. *J. Am. Chem. Soc.*, **2005**, *127*, 1080.

18. Lunte, C.; Sanli, S. *Anal. Methods*, **2014**, *6*, 3858-3864.

19. (a) Shafirovich, V.; Lymar. S. *J. Am. Chem. Soc.* **2003**, *125*, 6547-6552. (b) Lymar, S. V.; Shafirovich, V.; Poskrebyshew, G. A. *Inorg. Chem.* **2005**, *44*, 5212-5221.

20. *REACT for Windows, Version 1.2*; Manka, M. J., Ed.; Alchemy Software, Wesley: Chapel, FL, 2001; as described in Braun, W.; Herron, J. T.; Kahaner, D.K. *Int. J. Chem. Kinet.* **1988**, *20*, 51-62.

21. Schaab, M. R.; Barney, B. M.; Francisco, W. A. *Biochemistry*, **2006**, *45*, 1009-1016.

22. Shafirovich V. and Lymar S. V. *Proc. Natl. Acad. Sci*. **2002,** *99*, 7340-7345.

23. Yang B.; Kotani A.; Arai, K.; Kusu, F. *Anal. Sci.* **2001**, *17*, 599-604.

24. Yang B.; Arai K.; Kusu F. *Anal. Sci.* **2001**, *17*, 987-989.

25. Lind, J.; Merenyi, G. *J. Phys. Chem. A* **2006**, *110*, 192-197.

26. Wood, P.M. *Biochem. J.* **1988** *253*, 287–289.

27. Han X. Z.; Parker, V. D. and Zhu, X. Q. *J. Org. Chem.* **2012**, *77*, 6520-6529.

28. (a) Page, M.; Williams, A. Organic and Bio-organic Mechanism; Longman: Harlow, UK, 1997; Chapter 3, pp. 52-79. (b) Williams, A. *Acc. Chem. Res.* **1984**, *17*, 425–430. (c) Williams, A. *Acc. Chem. Res*. **1989**, *22*, 387–392. (d) Williams, A. *Adv*. *Phys. Org. Chem*. **1991**, *27*, 1.(e) Williams, A. *J. Am. Chem. Soc.* **1985**, *107*, 6335–6339.

CHAPTER FOUR

Characterization of Initial Intermediate Formed during Photo-induced Oxygenation of the Ruthenium (II) Bis(bipyridyl) Flavonolate Complex

This chapter published as: Han, X. Z.; Klausmeyer, K. K.; Farmer, P. J. *Inorg. Chem.* **2016**, *55*, 7320-7322

Introduction

Flavonol dioxygenases (FDOs) are non-heme metalloenzymes that incorporate both atoms of dioxygen into a targeted flavonol.[1] A well-studied example is the family of quercetin dioxygenases (QDOs), which catalyze the oxidation of the flavonol quercetin with dioxygen, cleaving the central heterocyclic ring and releasing CO.[2] A variety of QDOs have been characterized with diverse metal cofactors such as Cu, Fe, Mn, and Co.[3] Free flavonols undergo similar reactivity with oxygen at high temperature under basic conditions, also generating the phenolic carboxylic acid esters and CO.[4] Two pathways have been proposed for these oxygenations, one through a 1,3-endoperoxide intermediate (route a) and the other through a 1,2-dioxetane intermediate (route b), shown in Scheme 4.1.[5]

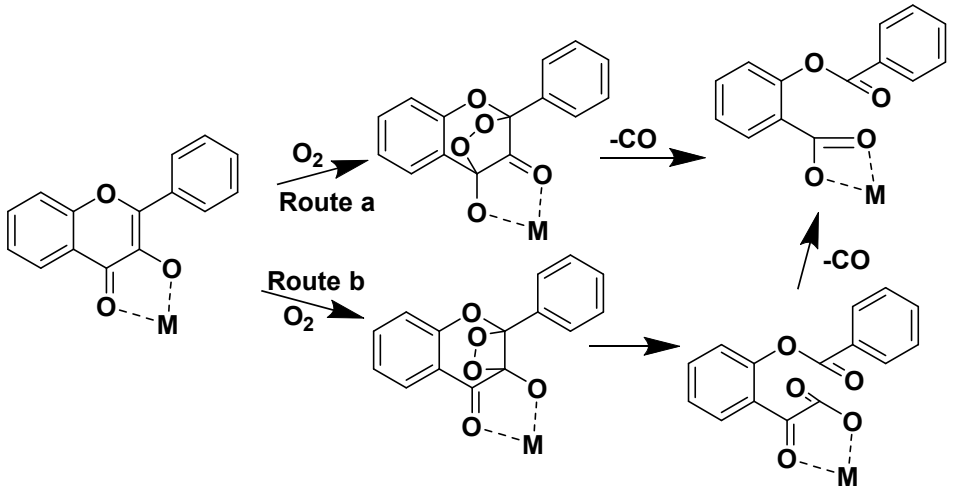

Scheme 4.1 Two pathways of oxygenation of flavonolate metal complex

The role of the metal ion in catalyzing these reactions has been difficult to assess; for instance, autoxidation reactions of potassium and zinc flavonolate have been found to form enzyme-like products.[6] To investigate these metal-catalyzed reactions, flavonolate (fla^-) complexes of copper, cobalt, nickel and manganese have been synthesized.[7-9] Like the free flavonols, these metal flavonolate complexes typically require high temperature (70 – 130 ^oC) to induce deoxygenation. . Alternatively, in certain cases photo-induced oxygenations of metallo-flavonolate complexes also generate similar mixtures of ring-cleaved products under mild condition.[5,10]

We have previously used $[Ru^{II}(bpy)_2X]^+$ complexes to explore the redox reactivity of metal-coordinated ligands, most recently demonstrating unusual photochemically induced C-H bond activation in a $[Ru^{II}(bpy)_2(dithiomaltolate)]^+$ complex.[11] These low spin d^6 complexes are quite inert, which allows characterization of ligand transformations, such as the peroxygenation, O-atom exchange and S extrusion of Ru-coordinated

dithiocarbamates.[12] Herein we report on a Ru-coordinated flavonolate model, $[Ru^{II}(bpy)_2fla][BF_4]$ (fla = 3-oxy-2-phenylchromen-4-onate), complex **1,** which undergoes photo-induced oxygenation of the flavonolate ligand.

Experimental

Materials. The flavonol ligand, 3-hydroxyflavone, cis-dichloro(2,2' – bipyridine)ruthenium(II) ($Ru(bpy)_2Cl_2$) and other chemicals used in this work were purchased from Sigma-Aldrich. Air-sensitive manipulations were carried out using Schlenk techniques or in an anaerobic dry glovebox. All common laboratory solvents are of reagent grade, dried and degassed using standard techniques. Manipulations requiring anaerobic conditions were carried out under nitrogen on a Schlenk line or in a glovebox.

Physical measurements. UV-vis spectra were recorded with an Agilent Technologies diode array spectrophotometer 8453. Emission and excitation spectra were recorded on a Hitachi F-4500 fluorescence spectrometer. FI-IR spectra were recorded with a Nicolet 6700 spectrophotometer. Crystallographic data was collected at 110 K on a Bruker X8 Apex using Mo-K radiation (λ = 0.71073 Å). The data were processed using the Bruker AXS SHELXTL software, version 6.10.40. Accurate complex mass spectra were obtained on an Accela Bundle Liquid Chromatograph (LC) coupled to a Thermo Electron Linear Trap Quadropole Orbitrap Discovery mass spectrometer. NMR spectra were recorded on a Varian 500 NMR system in CD_3CN. Redox potentials were measured by cyclic voltammetry under anaerobic conditions using a CHI-760B potentiostat in dry-degassed CH_3CN with 0.1 M tetrabutylammonium hexafluorophosphate ($TBAPF_6$) as the supporting electrolyte. Measured potentials were corrected using a MV^{2+} standard, with the

$MV^{2+}/MV^{\cdot+}$ couple set to -446 mV NHE. Elemental analyses were performed by Atlantic Microlabs Inc., Norcross, GA. EPR experiment of the oxygenation reaction was examined under N_2 at 100 K by using a EMX Plus Spectrometer (Billerica, MA) equipped with a EMX Plus spectrometer equipped with a EMX Plus and EMX micro standard resonator (Bruker model ER 4102ST). No signal was observed. Low-temperature measurements were taken using an Oxford ESR900 cryostat and an Oxford ITC 503 temperature controller.

Synthesis of [Ru^{II}(bpy)$_2$fla][BF_4], complex 1. Samples of $Ru(bpy)_2Cl_2$ (0.95 mmol) and 3-hydroxyflavone (1.00 mmol) and excess triethylamine were placed in a three – neck flask with 10 ml ethanol. The three-neck flask was fitted with a condenser, and an inert atmosphere was established using standard Schlenk techniques. The reaction was brought to refluxed state and stirred under N_2 for 14hrs. The mixture was then poured into 200 ml of deionized H_2O, and an excess of $NaBF_4$ was added. The purple product was collected on a Buchner funnel under vacuum filtration. The compound was purified using a basic alumina column and CH_2Cl_2/CH_3CN as the eluent. The yield 0.55g, 79% yield, after purification. The complex was stable in solid and dark condition. The complex was crystallized in $CHCl_3$/hexane under dark condition, forming purple cubic crystals suitable for X-ray diffraction. [Ru^{II}(bpy)$_2$fla][BF_4]. UV-vis λ_{max} (CH_3CN)/nm (ε / M^{-1} cm^{-1}): 370 (11228), 520 (7669). ESI MS: m/z (pos.) 651.10. Anal. Calcd for $C_{35}H_{25}N_4O_3RuBF_4$: C, 57.00; H, 3.42; N, 7.68. Found: C, 57.00; H, 3.42; N, 7.60. ^{1}H NMR (500 MHz, CD_3CN): δ 9.03 (d, *J*= 6.9 Hz,1H), 8.83 (d, *J*= 5.1 Hz,1H), 8.50 (m, 4H), 8.42 (d, *J*= 7.9 Hz, 1H), 8.39 (d, *J*= 7.8 Hz, 1H), 8.06 (t, *J*= 7.8 Hz,1H), 8.02 (t, *J*= 7.9 Hz, 1H), 7.95 (d, *J*= 5.8 Hz,

1H), 7.85 (d, *J*= 5.9 Hz, 1H), 7.82 (m, 2H), 7.75 (d, *J*= 5.8 Hz, 1H), 7.73 (m, 2H), 7.60 (t, *J*= 7.0 Hz, 1H) 7.53 (t, *J*= 7.2 Hz, 1H), 7.38 (m, 4H), 7.19 (t, *J*= 6.0 Hz, 1H), 7.16 (t, *J*= 5.9 Hz, 1H).

Synthesis of [Ru^{II}(bpy)$_2$bpg] [BF_4] (bpg = 2-benzoyloxyphenylglyoxylate), complex 2. Large-scale photolysis experiment was carried out using an Oriel Apex Quartz Tungsten Halogen Source with a 150 W Xe Arc Lamp and 400 nm filter. [Ru^{II}(bpy)$_2$ fla][BF_4] (50 mg) was put in a one – neck flask with 20 ml acetonitrile. Bubble oxygen into flask which was placed in an ice bath for 10 mins. The flask with ice bath was taken to Xe lamp with a filter (only pass ≥ 400 nm) in front of lamp and stirred under O_2 for 20 mins. Then the red product was collected by evaporation. [Ru^{II}(bpy)$_2$bpg][BF_4], yielding 46 mg, or 88% isolated yield, after exhaustive drying under vacuum. UV-vis λ_{max} (CH_3CN)/nm (ε / M^{-1} cm^{-1}): 340 (7254), 475 (6677). ESI MS: m/z (pos.) 683.09. Anal. Calcd for $C_{35}H_{25}N_4O_5RuBF_4$: C, 54.68; H, 3.27; N, 7.28. Found: C, 54.42; H, 3.22; N, 7.26. ^{1}H NMR (500 MHz, CD_3CN): δ 9.56 (d, *J*= 6.3 Hz,1H), 9.29 (d, *J*= 6.2 Hz,1H), 8.48 (d, *J*= 8.1 Hz, 1H), 8.42 (d, *J*= 8.1 Hz, 1H), 8.30 (t, *J*= 7.6 Hz, 2H), 8.18 (d, *J*= 8.5 Hz, 1H), 8.13 (d, *J*= 8.1 Hz, 1H), 8.07 (d, *J*= 8.2 Hz, 2H), 7.80 (m, 2H), 7.76 (m, 1H), 7.72 (m, 2H), 7.60 (m, 3H), 7.56 (t, *J*= 5.4 Hz, 2H) 7.25 (m, 2H), 7.19 (d, *J*= 6.1 Hz, 1H), 7.14 (m, 2H).

Photo-induced oxygenation of the free flavonolate. To assess the photochemical reactivity of the free flavonolate anion, trimethylamine was added dropwise to a 5 mM solution flavonol in anaerobic acetonitrile. The resulting red solution was diluted to 50 uM and characterized by UV-vis, shown in Figure 1in red. Oxygen was bubbled through the red

solution for 10 mins, and then the solution was irradiated with Xe lamp with a filter (only pass ≥ 400 nm) for an additional 20 mins. The absorbance spectrum of the resulting reaction solution suggests no oxygenation occurs.

Results and Discussion

The target complex was synthesized by widely utilized method, heating a solution of $Ru(bpy)_2Cl_2$ in the presence of excess ligand.[11] Complex **1** is stable in solid state, but reacts over time in aerobic solutions. Pure complex **1** was obtained by utilizing strict anaerobic purification on basic alumina column and a single crystal suitable for X-ray diffraction studies obtained by slow evaporation of a $CHCl_3$ solution. The determined structure is shown in Figure 4.1 with some selected bond distances. Crystallographic data of the complex are summarized in Table 4.1 and Table 4.2.

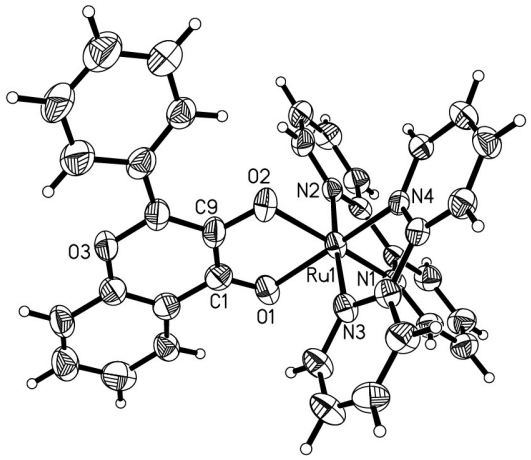

Figure 4.1 Crystal structure of the $[Ru^{II}(bpy)_2(fla)]^+$ cation, complex **1**

Table 4.1 Crystal data and structure refinement for complex **1**

Empirical formula	C35 H25 B F4 N4 O3 Ru
Formula weight	737.47
Temperature (K)	150(2)
Crystal system	Triclinic
Space group	P -1
a (Å)	12.8932(6)
b (Å)	13.3868(7)
c (Å)	13.8876(7)
α (°)	117.522(2)
β (°)	94.824(2)
γ (°)	105.152(2)
V ($Å^3$)	1992.19(18)
Z	2
D_{calcd} ($g\ cm^{-3}$)	1.229
Absorption coefficient (mm^{-1})	0.446
$2\theta_{max}$ (°)	26.390
Reflections collected	39921
Independent reflections	8147 [R(int) = 0.0293]
Final R indices [I > 2sigma(I)]	R1 = 0.0636, wR2 = 0.1664
R indices (all data)	R1 = 0.0710, wR2 = 0.1745
Goodness-of-fit on F^2	1.147

Table 4.2 Selected bond lengths (Å) and bond angles (°) for complex **1**

Ru(1)-N(4)	2.023(3)
Ru(1)-N(1)	2.024(3)
Ru(1)-N(3)	2.043(4)
Ru(1)-N(2)	2.055(3)
Ru(1)-O(2)	2.059(3)
Ru(1)-O(1)	2.098(3)
O(1)-C(1)	1.266(6)
O(2)-C(9)	1.360(6)
C(8)-C(9)	1.402(6)
N(4)-Ru(1)-N(1)	93.86(12)
N(4)-Ru(1)-N(3)	79.48(13)
N(1)-Ru(1)-N(3)	96.11(13)
N(4)-Ru(1)-N(2)	99.65(13)
N(1)-Ru(1)-N(2)	79.51(13)
N(3)-Ru(1)-N(2)	175.49(13)
N(4)-Ru(1)-O(2)	92.28(13)
N(1)-Ru(1)-O(2)	171.89(13)
N(3)-Ru(1)-O(2)	90.22(14)
N(2)-Ru(1)-O(2)	94.24(13)
N(4)-Ru(1)-O(1)	170.22(12)
N(1)-Ru(1)-O(1)	93.43(13)
N(3)-Ru(1)-O(1)	93.28(13)
N(2)-Ru(1)-O(1)	88.08(13)
O(2)-Ru(1)-O(1)	81.10(13)
C(1)-O(1)-Ru(1)	110.4(3)
C(9)-O(2)-Ru(1)	109.1(3)
C(7)-O(3)-C(8)	120.2(4)

In this structure, metal center has a distorted octahedral geometry involving two oxygen of flavonolate (O(1) in Figure 4.1, the carbonyl, and O(2), the 3-oxyl), and four nitrogen

atoms of bipyridyl ligands. The structure of the Ru-bound flavonolate is only mildly perturbed. The carbonyl C(1) – O(1) bond at 1.266(6) Å is slightly elongated to that of the free flavonol at 1.232 (3) Å; [13] and likewise, the oxylic C(9) – O(2) bond at 1.360(6) Å, is close to that observed in the flavonol at 1.357(3) Å.[13] But the C(8)-C(9) double bond length at 1.402(6) Å is longer than that in the free flavonol at 1.363(4) Å, suggesting that Ru coordination may promote reactivity at this site.

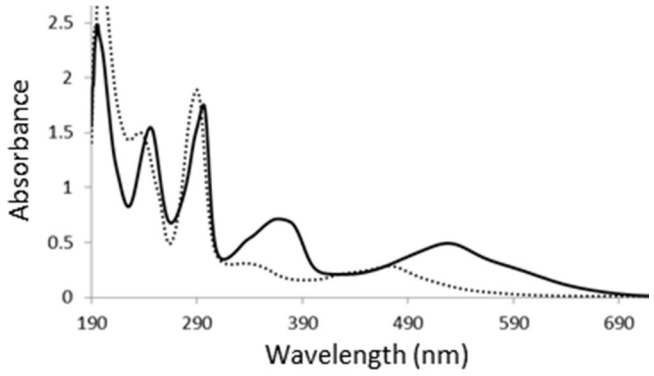

Figure 4.2 UV-vis absorbance of **1** in aerobic CH_3CN before (solid line) and after (dotted line) decomposition

In benchtop aerobic solutions, compound **1** degrades rapidly, Figure 4.2**,** but no degradation occurs in the absence of light. ESI-MS analysis of the degradation mixture shown in Figure 4.3 identified a dioxygenated product, as well as products resulting from the loss of CO and cleavage of the depside ligand, Scheme 4.2**.** This sequence is consistent with reported transformations of other metal flavonolate complexes in presence of oxygen.[7-10]

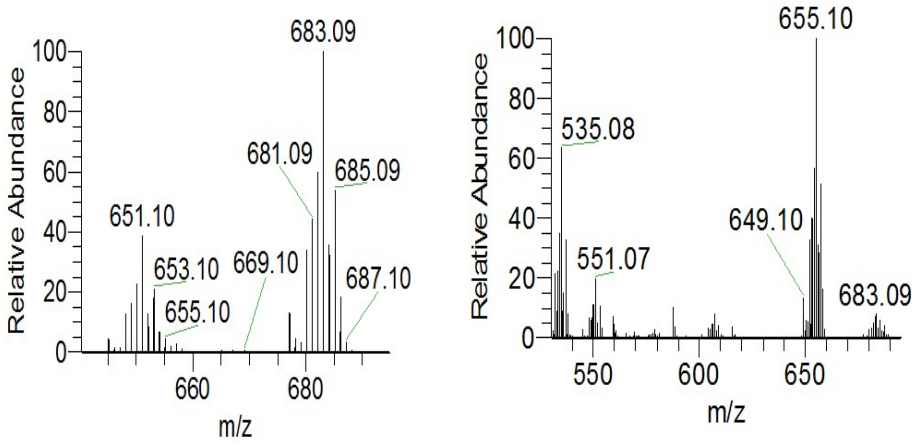

Figure 4.3 ESI MS characterization of the reaction products formed by aerobic degradation of **1** (m/z 683.09) under Xe lamp illumination. Product mixture spectra (left) after two minutes, and (right) after 5 minutes

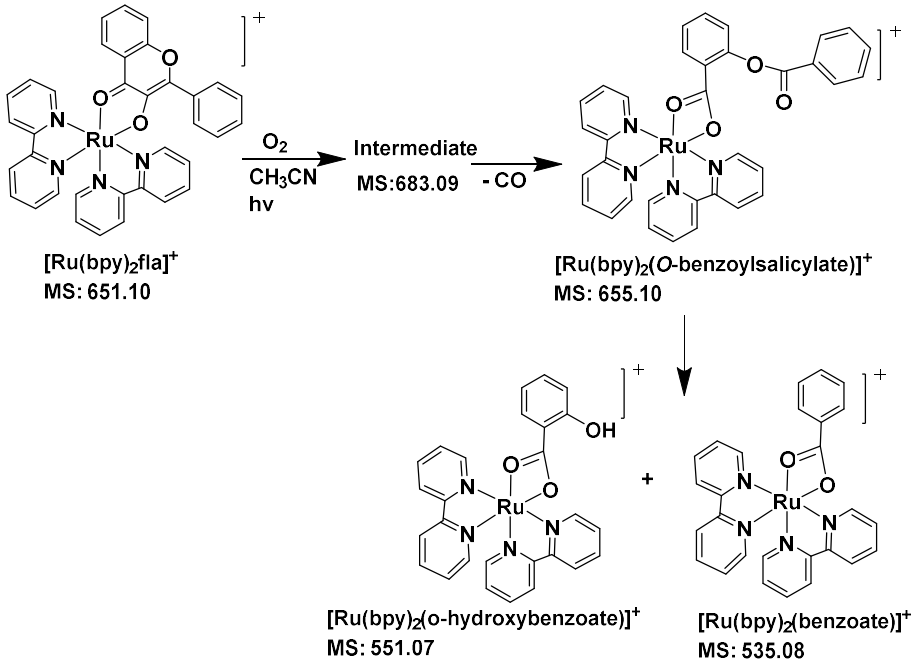

Scheme 4.2 Reaction sequence of ruthenium flavonolate complex with O_2

The action spectra of complex **1** is shown in Figure 4.4; excitation of a transition centered at 410 nm, attributable to the flavonolate, elicits an emission at 466 nm. This behavior strongly resembles that described for Cd^{2+} and Hg^{2+} flavonolate complexes which also undergo light-induced dioxygenation and CO release.[7b] With the assumption that this excitation is critical to the dioxygenation, we sought to limit unwanted excitations that might lead to the other decomposition products. Indeed, O_2 saturated solutions of **1** in an ice bath illuminated using a 400 nm cut-on filter yielded a single dioxygenated product, complex **2** (ESI-MS, m/z = 683.09). Complex **2** is stable at low temperature, but decomposes upon illumination or over time in solution to yield the same mixture of products shown in Scheme 4.2 and Figure 4.5. A sample of complex **2** was dissolved in MeCN and left at room temperature under room light for one day. Subsequent ESI-MS analysis of the resulting decomposition mixture demonstrated decomposition by loss of CO and cleavage of the depside ligand (o-benzoylsalicylate) into o-hydroxybenzoate and benzoate. This method generated sufficient quantities of complex **2** for a variety of characterizations.

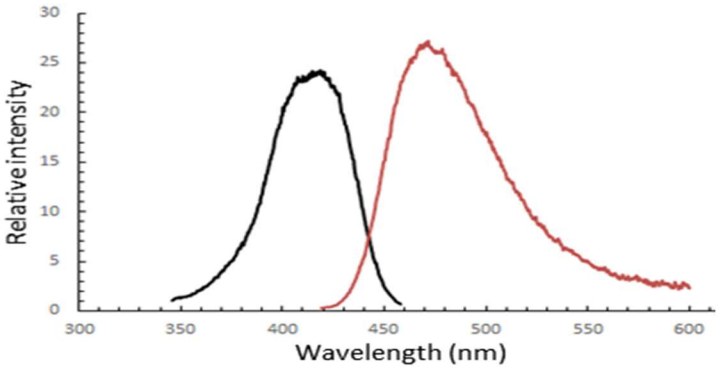

Figure 4.4 The normalized action and emission spectrum of complex **1** in CH_3CN, black line: excitation, red line: emission

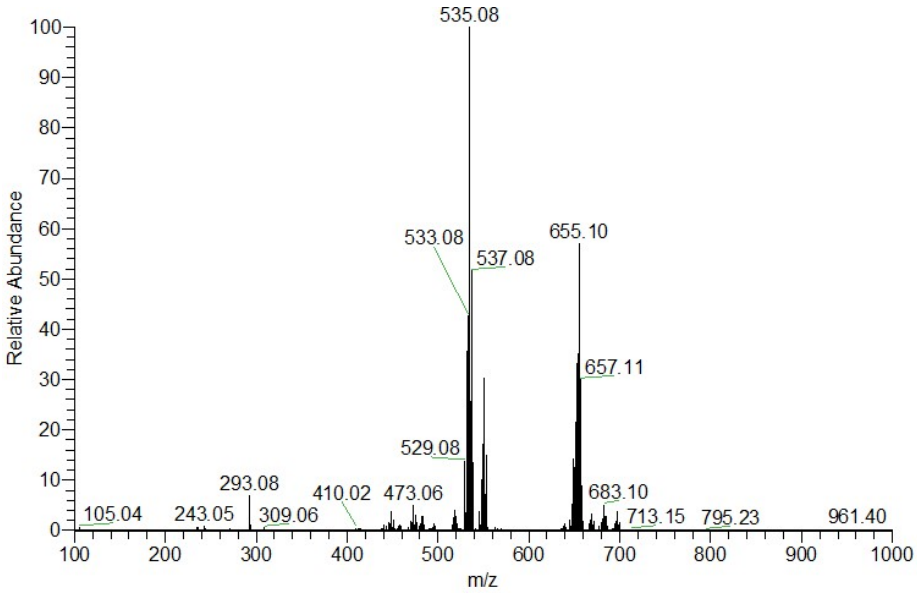

Figure 4.5 ESI-MS of decomposition of complex 2 in MeCN at room temperature

IR spectra of complexes 1 and 2, illustrated in Figure 4.6 imply significant structural changes occur in the flavonolate ligand; spectra of the deoxygenated complex 2 show increase in number and absorbance of bands in the ketone region from 1600-1750 cm^{-1}. Importantly, no band is seen in the ν_{CO} stretch region from 1900 - 2100 cm^{-1}, which would be indicate extruded CO had been trapped by coordination to the Ru, has been observed in previous Ru-flavonolate oxygenations.[10]

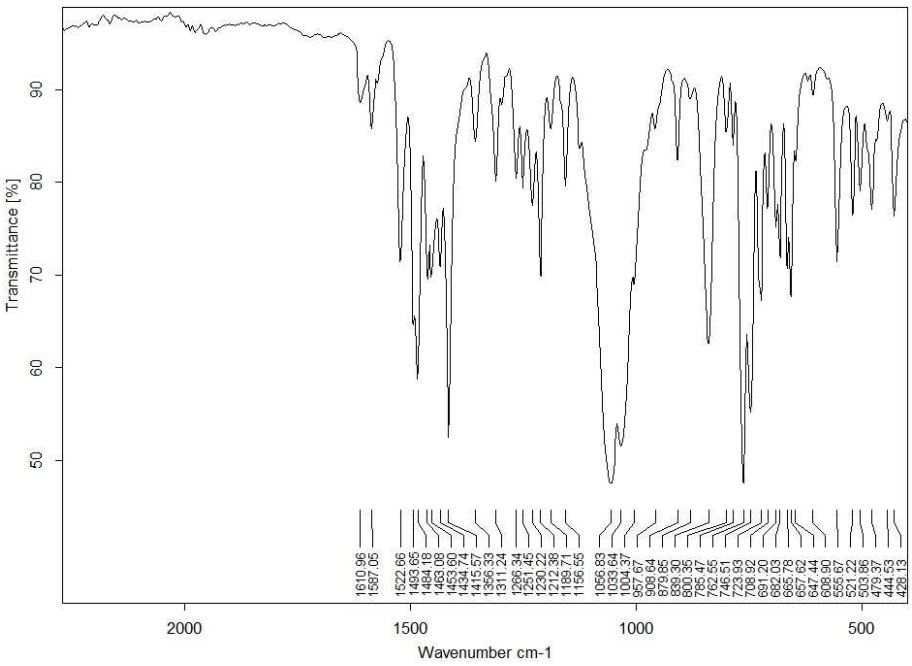

(a)

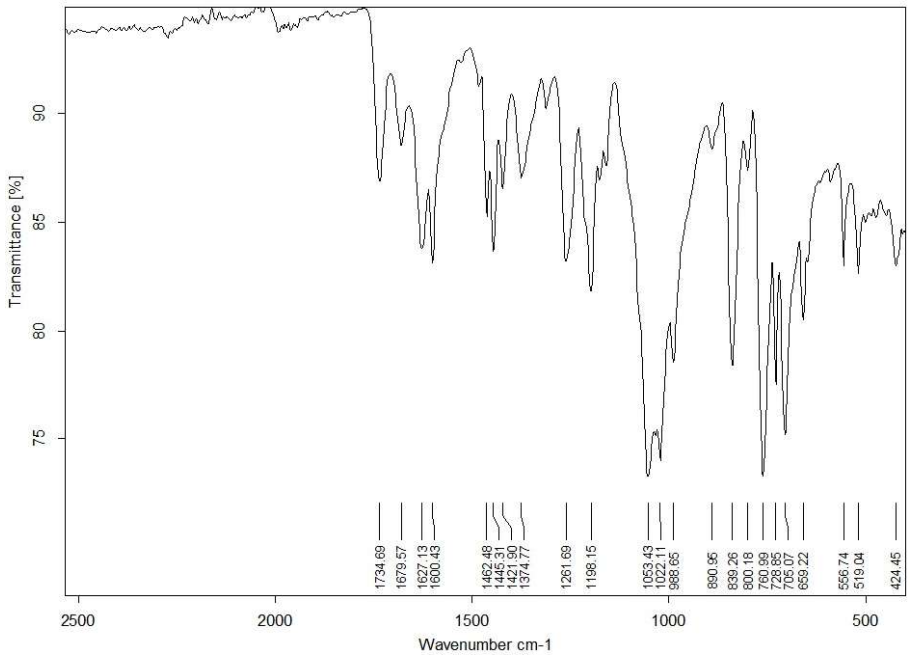

(b)

Figure 4.6 FT-IR spectra of complex 1(a) and complex 2 (b)

Cyclic voltammograms of complex **1** and **2** display reversible oxidations assignable to the Ru^{II}/Ru^{III} redox couple, shown in Figure 4.7. Again, there is a large shift of ca. 400 mV in Ru-based potential resulting from the oxidation, very similar to that observed upon oxidation of $[Ru^{II}(bpy)_2(dithiomaltolate)]^+$ complex,[11] implying the ligand has become more electron withdrawing.

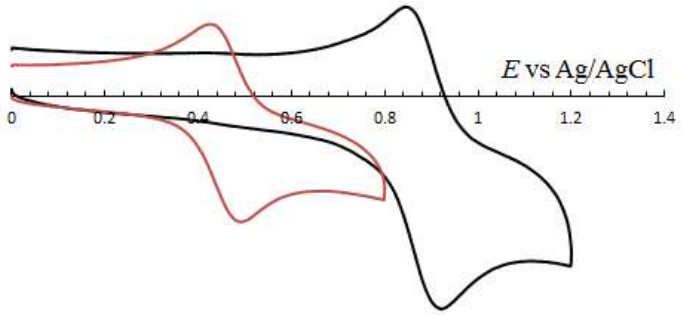

Figure 4.7 Cyclic voltammograms of complex 1 (red line) and complex 2 (black line), conditions: 0.1 M TBAPF6 in anaerobic CH_3CN

More conclusive structural information is obtained from the NMR analysis of the complexes. Selective regions of ^{1}HNMR and ^{13}CNMR spectra for complexes **1** and **2** are shown in Figure 4.8. The ^{1}HNMR and ^{13}CNMR spectra of **1** and **2** have equal numbers of proton and carbon signals, in agreement with ESI-MS that imply they differ only by the addition of O_2. Characteristic upfield proton peaks at 9.05 and 8.82 ppm for **1**, and 9.55 and 9.28 ppm for **2**, are ascribable to position 16 and 35 protons which are closest to the flavonolate ligand.

In the ^{13}CNMR spectra, both **1** and **2** have 10 quaternary carbons: 4 (C20, C21, C30, C31) from bipyridyl and 6 (C1, C2, C7, C8, C9, C10) from the flavonolate or 2-

benzoatophenylglyoxylate. The ^{13}CNMR spectrum of **2** has new peaks characteristic of a ketone (C1, 191.8 ppm), an acid group (C9, 172.3 ppm), and an ester group (C8, 164.9 ppm), which suggests complex **2** to be $[Ru^{II}(bpy)_2bpg]^+$ (bpg: 2-benzoyloxyphenylglyoxylate), as shown in Scheme 4.3, consistent with previous literature.[14] In addition, there are 25 tertiary carbons, all of which were assigned by ^{1}H-^{1}H COSY and ^{1}H – ^{13}C HSQC, shown in Figure 4.9 and Figure 4.10. The assignments of all carbons were confirmed by carbon – proton long – range couplings obtained from ^{1}H – ^{13}C HMBC spectrum, shown in Figure 4.11.

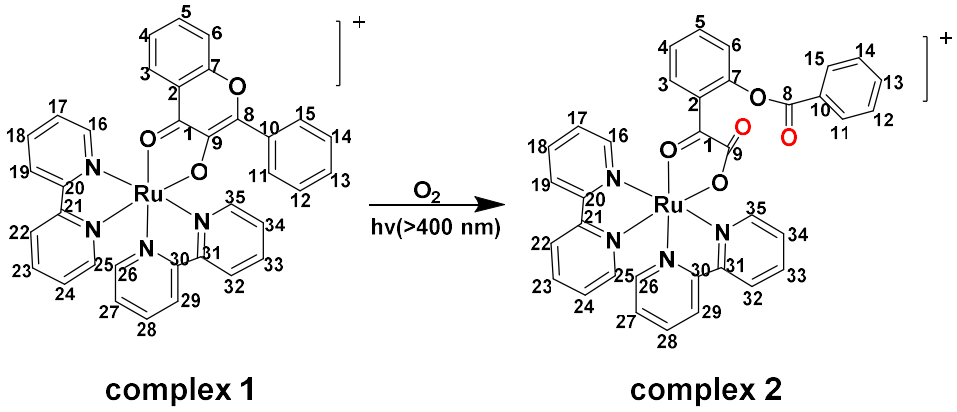

Scheme 4.3 Photo-induced oxygenation of complex 1 to complex 2

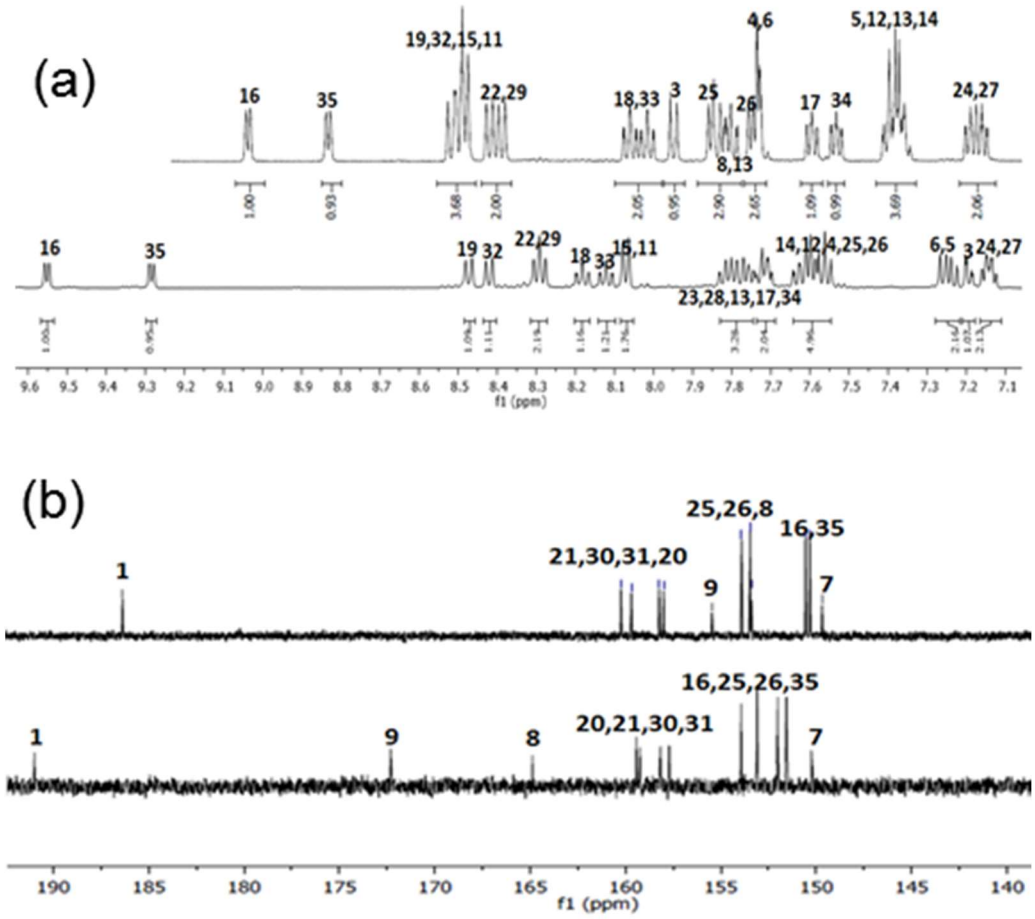

Figure 4.8 (a) ^{1}HNMR and (b) ^{13}CNMR spectra **1** and **2** in selected regions showing characteristic peaks which allowed structural assignment, numbering as in Scheme 4.3

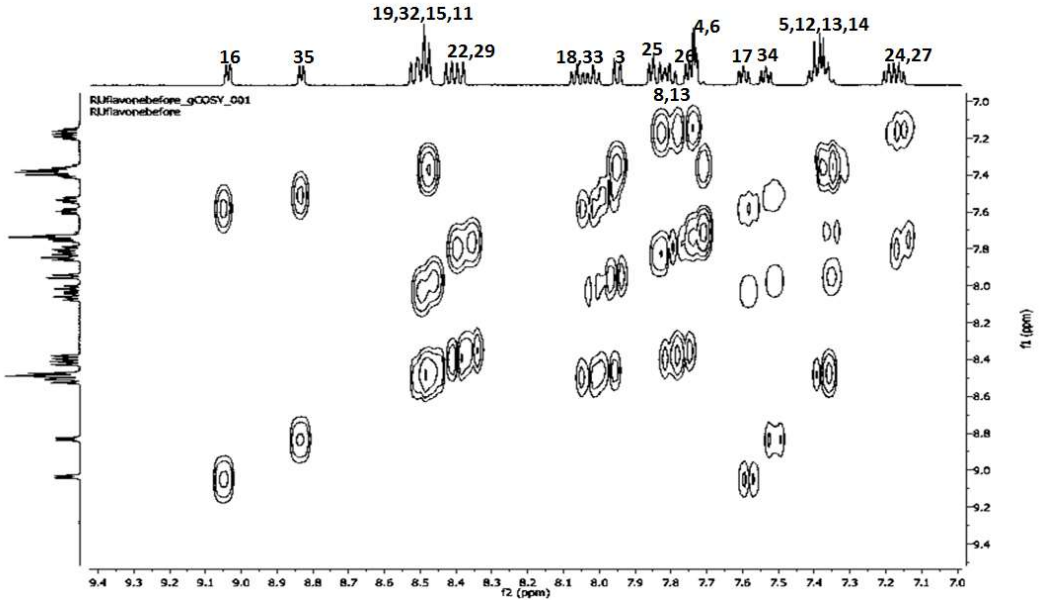

(a)

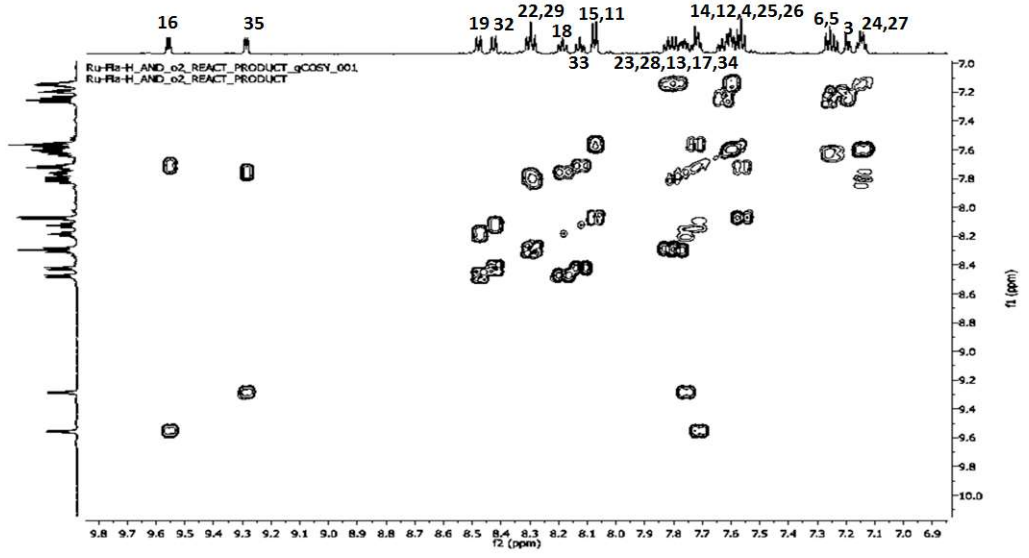

(b)

Figure 4.9 2D ^{1}H-^{1}H COSY of complex 1 (a) and complex 2 (b)

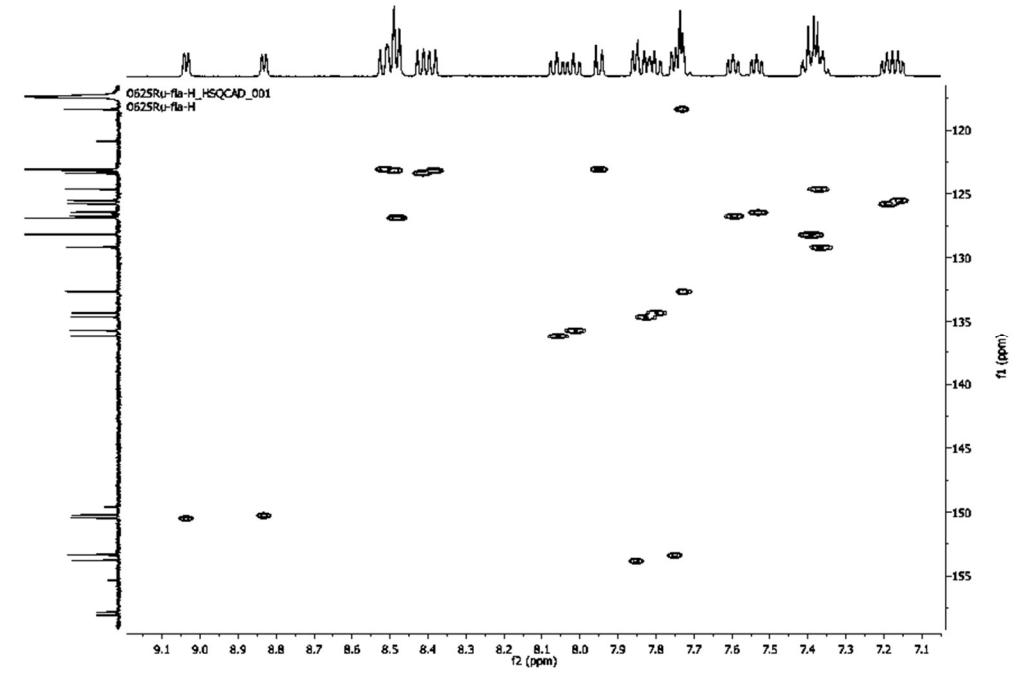

(a)

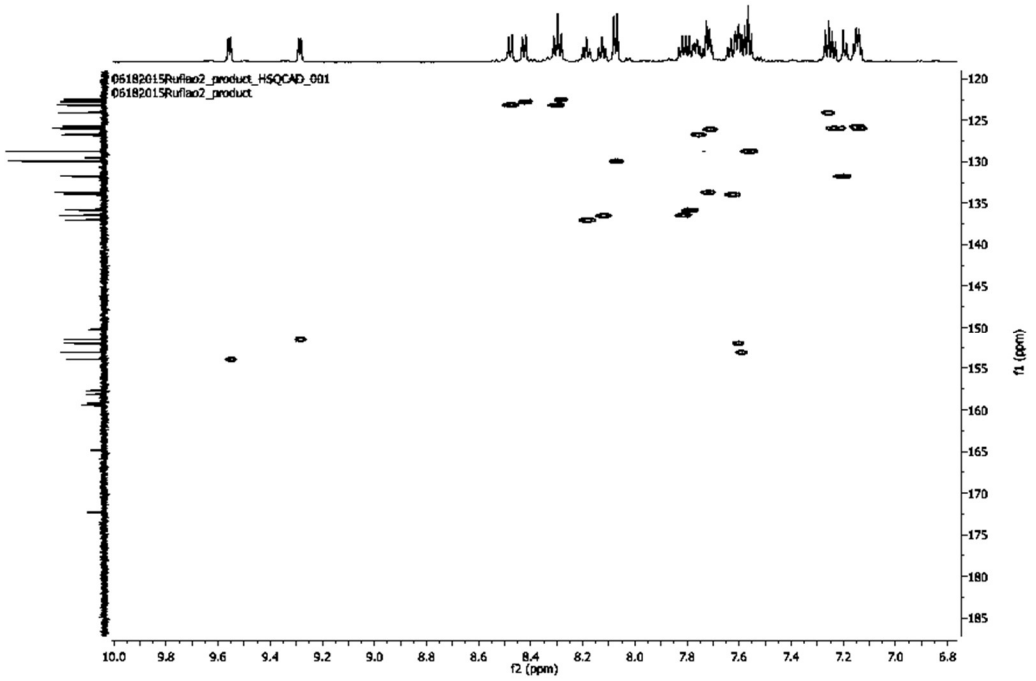

(b)

Figure 4.10 HSQC ^{13}C-^{1}H of complex 1(a) and complex 2(b)

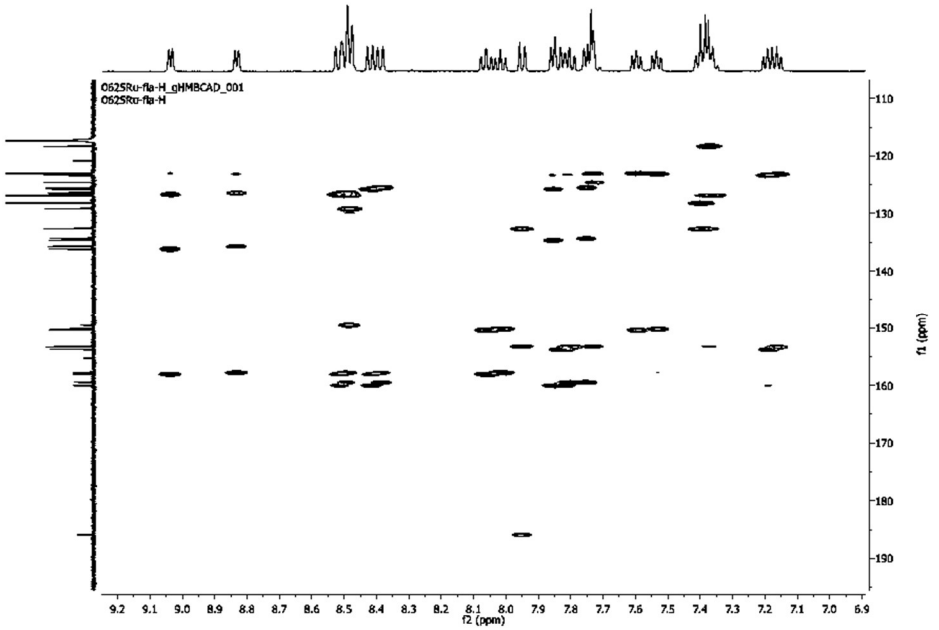

(a)

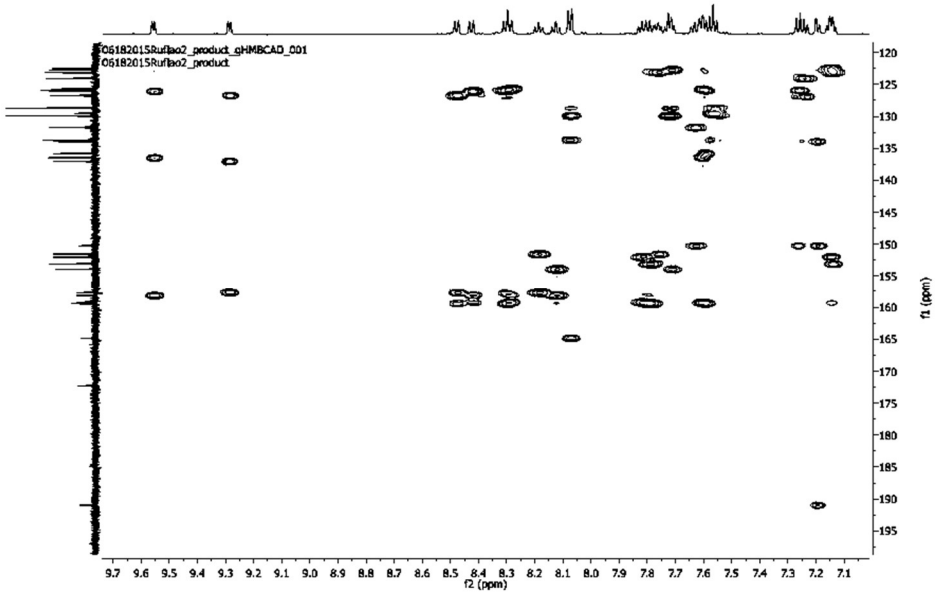

(b)

Figure 4.11 HMBC ^{1}H-^{13}C of complex 1(a) and complex 2(b)

The structure of complex **2** is unexpected as it suggests a 1,2-dioxetane pathway, Scheme 4.1**,** rather than the 1,3-endoperoxide path typically proposed for these reactions. Additional support for a 1,2-dioxetane pathway was obtained by observation of a distinctive chemiluminescence during the oxygenation of 1, illustrated in Figure 4.12, [15] as previously reported for certain Cu diflavonolate complexes. [5b] Similar 1,2-dioxetane products have been observed in reactions of free flavonol with superoxide anion.[14b,c] Using deoxygmyoglobin as a trap, we also confirm that decomposition of **2** leads to CO release and a mixture of other cleavage product characteristic of the natural reactivity, shown in Figure 4.13.

An anaerobic solution of 0.1 mM complex **1** in MeCN was transferred into a quartz cuvette, and placed into a fluorescence spectrometer (Hitachi F-4500) in chemiluminescence mode (with no excitation source). The solution was bubbled with O_2, concurrent with the acquisition of the emission spectrum below, was recorded over a 5 minute interval, which clearly supports the production of a 1,2 dioxetane intermediate, Figure 4.12.

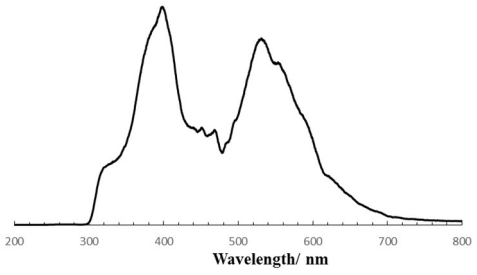

Figure 4.12 Chemiluminescence spectrum of the emitted light during the oxygenation of complex **1** in MeCN

The assessment of CO formation during the decomposition of complex 2 utilized a home-built reaction vessel with a long-necked quartz cuvette attached via side arm to a 10 mL round bottom flask. A 6.2 μM sample of deoxymyoglobin in 3 mL pH 7.0 phosphate buffer was added to the cuvette; a 2 mM of solution of complex **2** in MeCN was added to the round-bottom flask and the reaction was initiated by Xe lamp. The generation of CO-Fe^{II}Mb, via diffusion of CO through the side arm, was observed by a shift of the Soret absorbance peak from 434 to 423 nm, illustrated Figure 4.13.

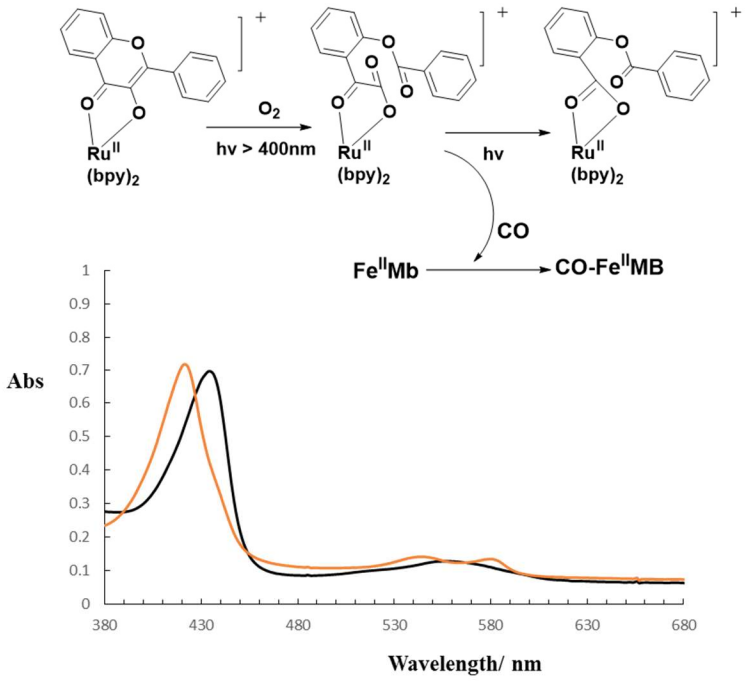

Figure 4.13 UV-Vis spectra of formation of CO-Fe^{II}Mb (red line) from CO trapping by deoxy-myoglobin (black line)

Conclusions

A flavonolate Ru(II) complex $[Ru^{II}(bpy)_2fla][BF_4]$ was synthesized to model the reactivity of the flavonol dioxygenases. Treatment of dry CH_3CN solutions of $[Ru^{II}(bpy)_2fla][BF_4]$ with O_2 under light leads to oxidative O-heterocyclic ring opening of the coordinated substrate flavonolate, resulting in the formation of $[Ru^{II}(bpy)_2(carboxylate)][BF_4]$ (carboxylate = *O*-benzoylsalicylate or benzoate) species, as determined by ESI MS. Moderation of the excitation and temperature allowed isolation and characterization of an intermediate, $[Ru^{II}(bpy)_2bpg][BF_4]$ (bpg = 2-benzoyloxyphenylglyoxylate), generated by 1,2 addition of O_2 to the central flavonolate ring.

References

1. a) Buongiorno, D.; Straganz, G. D. *Coord. Chem. Rev*. **2013**, *257*, 541-563. b) Costas, M.; Mehn, M. P.; Jensen, M. P.; Que, L. Jr. *Chem. Rev.* **2004**, *104*, 939-986.c) Kovaleva, E. G.; Lipscomb, J. D. *Nat. Chem. Biol.* **2008**, *4*, 186 –193.

2. a) Fusetti, F.; Schröter, K. H.; Steiner, R. A.; van Noort, P. I.; Pijning, T.; Rozeboom, H. J.; Kalk, K. H.; Egmond, M. R.; Dijkstra, B. W. *Structure* **2002**, *10*, 259−268. b) Bugg, T.; Ramaswamy, S. *Curr. Opin. Chem. Biol.*, **2008**, *12*, 134-140. (c) Kumar, M.; Zapata, A.; Ramirez, A.; Bowen, S.; Francisco, W.; Farmer, P. *Proc. Natl. Acad. Sci.* **2011**, *108*, 18926-18931. (d) Han, X. Z.; Kumar, M. R.; Farmer, P. J. *Tetrahedron Lett*. **2016**, *57*, 399-402.

3. a) Matuz, A.; Giorgi, M.; Speier, G.; Kaizer, J. *Polyhedron* **2013**, *63*, 41-49. b) Gopal, B.; Madan, L. L.; Betz, S. F.; Kossiakoff, A. A. *Biochemistry* **2005**, *44*, 193-201. c) Schaab, M. R.; Barney, B. M.; Francisco, W. A. *Biochemistry* **2006**, *45*, 1009–1016.

4. a) Hergovich, E. B. and Speier G. *J. Org. Chem.* **2001**, *66*, 7974-7978. b) Czaun, M.; Speier, G. *Tetrahedron Lett.* **2002**, *43*, 5961-5963. c) Czaun, M.; Speier, G.; Kaizer, J.; Farkas, E. *Tetrahedron* **2013**, *69*, 6666-6672.

5. a) Sisa, M.; Bonnet, S.L.; Ferreira, D.; Van der Weshuizen, J.H. *Molecules*, **2010**, *15*, 5196-5245. b) Balogh-Hergovich, É.; Kaizer, J.; Pap, J.; Speier, G.; Huttner, G.; Zsolnai, L. *Eur. J. Inorg. Chem.* **2002**, 2287−2295.

6. Barhacs, L.; Kaizer, J.; Speier, G. *J. Mol. Catal. A.* **2001**, *172*, 117−125.

7. a) Matuz, A.; Giorgi, M.; Speier, G.; Kaizer, *J. Polyhedron* **2013**, *63*, 41−49. b) Balogh-Hergovich, É.; Kaizer, J.; Speier, G.; Fulop, V.; Parkanyi, L. *Inorg. Chem.* **1999**, *38*, 3787-3795. c) Kaizer, J.; Pap, J.; Speier, G.; Párkányi, L. *Eur. J. Inorg. Chem.* **2004**, 2253−2259.

8. a) Grubel, K.; Rudzka, K.; Arif, A. M.; Klotz, K. L.; Halfen, J. A.; Berreau, L. M. *Inorg. Chem.* **2010**, *49*, 82−96. b) Grubel, K.; Laughlin, B. J.; Maltais, T. R.; Smith, R. C.; Arif, A. M.; Berreau, L. M. *Chem. Commun.* **2011**, *47*, 10431−10433.

9. a) Sun, Y. J.; Huang, Q. Q.; Zhang, J. J. *Inorg. Chem.*, **2014**, *53*, 2932-2942. b) Sun, Y. J.; Huang, Q. Q.; Tano, T.; Itoh, S. *Inorg. Chem.*, **2013**, *52*, 10936-10948.

10. Saraf, S. L.; Fish, T. J.; Bennighoff, A. D.; Buelt, A. A.; Smith, R. C.; Berreau, L. M. *Organometallics*, **2014**, *33*, 6341-6351.

11. a) Backlund M.; Ziller, J.; Farmer, P. J. *Inorg. Chem.*, **2008**, *47*, 2864–2870. b) Bruner, B.; Walker, M. B.; Zhang, D.; Selke, M.; Ghimire, M. M. M.; Omary, M. A.; Klausmeyer, K.; Farmer, P J. *Dalton Trans.* **2014***, 43,*11548-11557.

12. a) Szeman, N.; Ziller, J. W.;Farmer, P. J. *Inorg. Chem.* **2004**, *43*, 8301-8309. b) Szeman, N.; Backlund, M.; Farmer, P. J. *Inorg. Chim. Acta* **2009**, *362*, 4013-4016.

13. Etter, M. C.; Urbanczyk-Lipkowska, Z.; Baer, S.; Barbara, P. F. *J. Mol. Struct.* **1986**, *144*, 155−167.

14. (a) Marfak, A.; Trouillas, P; Allais, D. p.; Champavier, Y.; Calliste, C. A.; Duroux, J. L. *J. Agric. Food Chem.* **2002**, *50*, 4827-4833. (b) El-Sukkary, M.; Speier, G. *J.C.S. Chem. Comm.* **1981**, *15*,745. (c) Singh, K. N.; Kumar, R. *Indian J. Chem.* **2006**, *46B*. 1554-1557.

15. R. Hiatt, Organic Peroxides, (Ed.: D. Swern), Wiley Intersciene, New York, 1971, 2511-1516.

CHAPTER FIVE

Mechanistic Study of Photo-induced Oxygenation of the Ruthenium (II) Bis(bipyridyl) Flavonolate Complexes

Introduction

Flavonols are a broad class of natural products that have been extensively studied for their antioxidant activity in the food and health sciences.[1-3] They have also been shown to have other biological and pharmacological activities, including antiviral,[4] anti-inflammtory,[5-7] anti-allergy, and anticancer properties.[8-10] The oxidation of flavonols has been widely investigated to gain insight into their ability to quench oxidative stress. In general, the ability of flavonols to be effective antioxidants depends on three factors:[11] (1) the metal-chelating potential that is strongly dependent on the arrangement of hydroxyls and carbonyl group around the molecule; (2) the presence of hydrogen or electron-donating substituents able to reduce free radicals; and (3) the ability to delocalize the unpaired electron leading to formation of a stable phenoxyl radical. In nature, quercetin dioxygenase (QDO), a type of flavonol dioxygenase, catalyzes the oxidative degradation of flavonols to a depside (phenolic carboxylic acid esters) with concomitant evolution of carbon monoxide.[12] The crystal structures of copper and iron quercetin dioxygenases (QDOs) from *Aspergillus* or *Pullularia* have been reported.[13-15] To elucidate the mechanistic route of oxidative cleavage of flavonol by these metalloenzymes, flavonolate (fla^-) complexes of divalent iron, copper, cobalt, nickel, zinc and manganese have been used to mimic the enzyme catalyzed oxygenations.[16-19] Two pathways have been proposed

for these oxygenations, through a 1,3-endoperoxide intermediate (route a) or by a 1,2-dioxetane intermediate (route b), shown in Scheme 5.1.

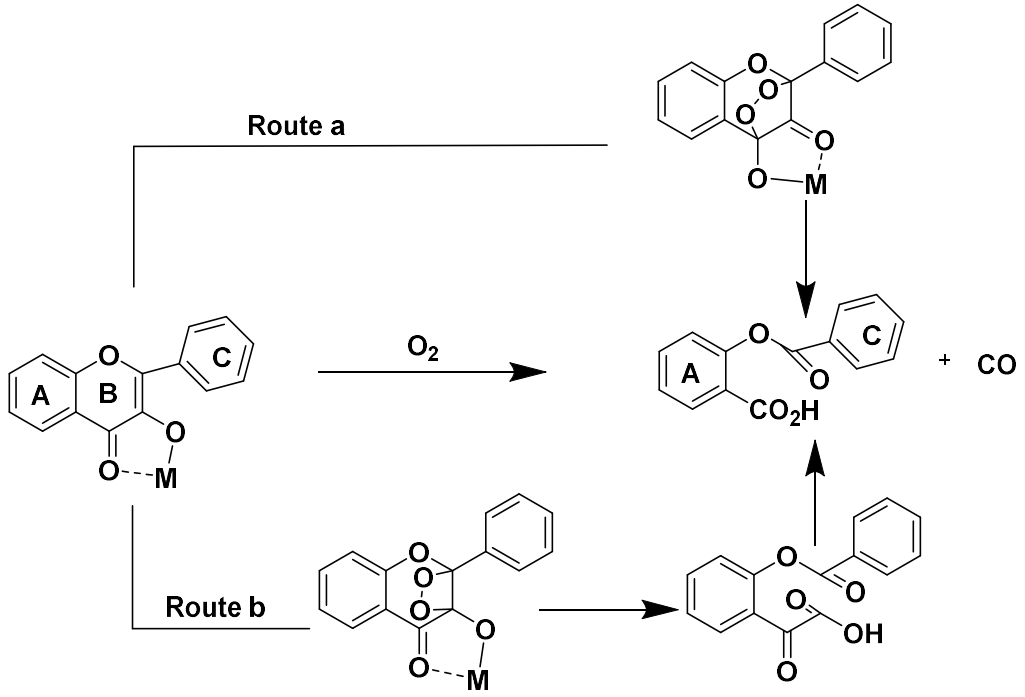

Scheme 5.1 Two different routes of oxygenation of flavonol by native QDO

Although many groups have studied the models of the QDO enzyme catalyzed oxygenation reactions, few reports have been published on the photolysis of flavonolate metal complex. In 2013, Berreau published the work of photochemical reactivity of Ru^{II} (η^6-*p*-cymene) flavonolate compound.[20] It revealed that irradiation in CH_3CN resulted in the loss of the *p*-cymene ligand and the oxidative ring cleavage of the flavonolate ligand, analogous to a typical dioxygenase-type reaction. Berreau's Ru^{II} (η^6-*p*-cymene) flavonolate complex is a good example using light irradiation to induce the oxygenations; other divalent metal (Fe, Cu, Co, Ni, Mn, Zn) flavonolate complexes require high temperature (70-80 ^oC) to undergo such dioxygenase-type reactions.[16-19]

Of photoactive Ru complexes, $[Ru^{II}(bpy)_2L]^{2+}$ is by far the best known, widely used in photochemical studies due to its redox-active luminescent state.[21-27] Previously, our group reported that a ruthenium bis-bipyridyl dithiomaltol complex, $[Ru^{II}(bpy)_2(ttma)][PF_6]$, undergoes C-H activation at a pendant alkyl position, yielding $[Ru^{II}(bpy)_2(ttma\text{-}alcohol)]^+$ and $[Ru^{II}(bpy)_2(ttma\text{-}aldehyde)]^+$ as products due to photo catalyzed chemical oxidation.[28] The observed C oxidations are unusual in that the two S sites on the dithiomaltol ligand were unaffected.

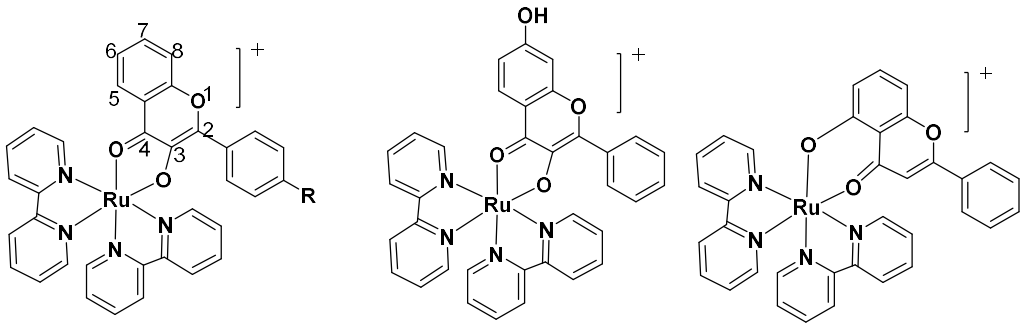

Scheme 5.2 Complexes investigated in this work

In this chapter we investigate the mechanism of oxygenation using a series of analogous Ru (II) bis-bipyridyl flavonolate complex, $[Ru^{II}(bpy)_2(3\text{-}hydroxyfla^R)]$ $[PF_6]$ (R = *p*-OMe (**1**), *p*-Me (**2**) , *p*-H (**3**) , *p*-Cl (**4**)), $[Ru^{II}(bpy)_2(3,7\text{-}dihydroxyfla)]$ $[PF_6]$ (**5**), and $[Ru^{II}(bpy)_2(5\text{-}hydroxyfla)]$ $[PF_6]$(**6**) shown in Scheme 5.2, with a focus on the effects of light and electronic nature of substituted groups on the reactivity. The initial oxygenation product of complex 3 has been previously isolated and characterized, shown in Scheme

5.3.[29] Our hope is to provide insights into the role of light in the oxygenation of natural flavonols.

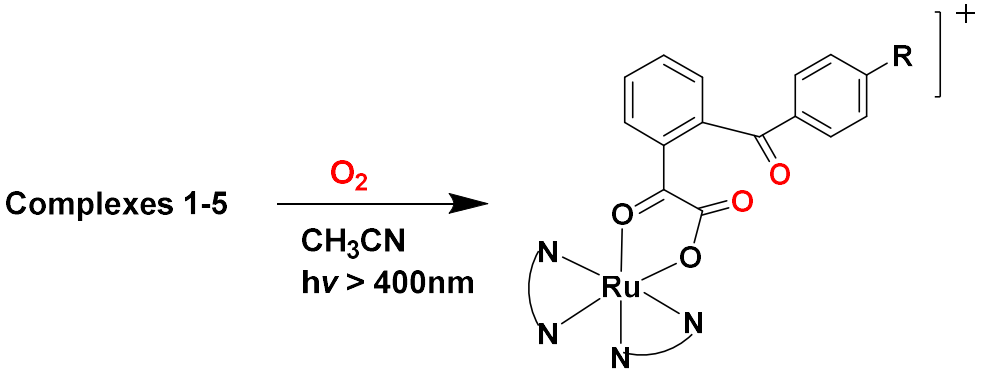

Scheme 5.3 Initial product of photo-induced oxygenation of ruthenium bis-bipyridyl flavonolate complexes

Experimental

Materials. A selection of substituted flavonol ligands, 3-hydroxyflavone, 5-hydroxyflavone, 3,7-dihydroxyflavone, 4'-methyl-3-hydroxyflavone, 4'-methoxy-3-hydroxyflavone, 4'-choloro-3-hydroxyflavone, and cis-dichloro (2,2'-bipyridineruthenium (II) ($Ru(bpy)_2Cl_2$) were obtained commercially from Sigma-Aldrich and OTAVA in high purity. 1,1-dimethyl-4,4′-bipyridinium dichloride (MV^{2+})Cl_2 and other chemicals used in this work were purchased from Sigma-Aldrich. Air-sensitive manipulations were carried out using Schlenk techniques.

Physical measurements. UV-vis spectra were recorded with an Agilent Technologies diode array spectrophotometer. Emission and excitation spectra and chemiluminescence spectrum were recorded on a Hitachi F-4500 fluorescence spectrometer. All photochemical

reactions were performed anaerobically in quartz fluorescence cells or sealed jacketed beakers. FI-IR spectra were recorded with a Nicolet 6700 spectrophotometer.

Crystallographic data was collected at 110 K on a Bruker X8 Apex using Mo-K radiation (λ = 0.71073 Å). The data were processed using the Bruker AXS SHELXTL software, version 6.10.40.

Redox potentials were measured by cyclic voltammetry under anaerobic conditions using a CHI-760B potentiostat in dry-degassed CH_3CN with 0.1 M tetrabutylammonium hexafluorophosphate ($TBAPF_6$) as the supporting electrolyte. Measured potentials were corrected using a MV^{2+} standard, with the $MV^{2+}/MV^{\cdot+}$ couple set to -446 mV NHE.

Accurate masses were resolved by an Accela Bundle Liquid Chromatograph (LC) coupled to a Thermo Electron Linear Trap Quadropole Orbitrap Discovery mass spectrometer. NMR spectra were recorded on a Varian 500 NMR system in deuterated – acetonitrile (CD_3CN). Elemental analyses were performed by Atlantic Microlabs Inc., Norcross, GA.

Photophysical and photochemical studies. Near-infrared time-resolved luminescence measurements were performed at the Selke lab at California State University, Los Angeles. The apparatus comprised of a Nd:YAG laser set to an excitation pulse of 2 ns (Minilase II, New Wave Research Inc.). A liquid nitrogen cooled Ge photodetector (Applied Detector Corporation Model 403 S) was placed at a 90 degree angle relative to the laser beam path. The detector contained a Schott colored filter (model RG850; cut-on 850 nm; Newport, USA) to block UV-Vis light and a long wave pass filter (silicon filter model 10LWF -1000; Newport, USA) which transmits at 1100 to 2220 nm, but blocks 800-954 nm. The

phosphorescence signals were digitized by an oscilloscope (LeCroy 9350 CM 500 Mhz). The data for the first 2 μs of the singlet oxygen decay were not used due to electronic interference signals from the detector. Measurements of both emission intensity and lifetime were performed in air-saturated acetonitrile solutions and solutions purged with Argon at 355 and 532 nm. The optical densities of the solutions were between 0.28 and 0.31 at the specific excitation wavelength.

Spectral and lifetime data for complexes **1-6** were obtained from the Omary lab at University of North Texas. Near-IR emission spectra of dilute acetonitrile (CH_3CN) solution of complexes **1-6** were collected by using a Photon Technology International (PTI) QuantaMaster Model QM-4 scanning spectrofluorometer equipped with a 75-watt xenon lamp, emission and excitation monochromators, excitation correction unit, and a near-infrared (NIR) photomultiplier tube (PMT) from Hamamatsu. Lifetime data were collected using a pulsed Xenon source with a pulse repetition rate of 300 pulse/sec and a PTI-supplied Gated Voltage-Controlled Integrator to interface to the NIR PMT. For the improved sensitivity in the steady state NIR- emission spectra within 800-950nm, we used a Horiba Jobin Yvon Nanolog UV-visible-NIR spectrofluorometer equipped with a PMT (for UV-visible) and InGaAs (for NIR) detectors. A right angle detection method was used for emission measurements.

Excited-state oxidation and reduction potentials were determined by the observed E^{00} for singlet spin states, and approximated for the triplet spin states based on the observed emission wavelength. Thermodynamic cycles were then drawn with the excited state reduction and oxidation potentials calculated from the equation 5.1 and 5.2.

$$E^{O} - E^{*O} = E^{00} \qquad 5.1$$

$$E^{*R} - E^{R} = E^{00} \qquad 5.2$$

Kinetic Measurements. The reactions of the complexes **1 - 6** (30 μM) with saturated O_2 in acetonitrile were carried out in a screw-capped UV cuvette and monitored by following the decrease of the ligand flavonolate absorbance at λ_{max} = 380 nm. O_2-saturated solutions of CH_3CN (8.0 mM) were prepared by bubbling dry O_2 through a solution of dry CH_3CN.[30] Solutions containing lower O_2 concentrations were prepared by diluting the saturated solution with N_2-saturated CH_3CN using gastight syringes.

Synthesis of complexes. General procedure for synthesis of complexes **1-6**: $Ru(bpy)_2Cl_2$ (0.95 mmol) and flavonol (1.00 mmol) and excess triethylamine were placed in a three – neck flask with 10 ml ethanol. The three-neck flask was fitted with a condenser, and an inert atmosphere was established using standard Schlenk techniques. The reaction was brought to refluxed state and stirred under N_2 for 14 hs. The mixture was then poured into 200 ml of deionized H_2O, and an excess of KPF_6 was added. The purple product were collected by funnel under vacuum filtration. The compounds were purified using a basic alumina column and CH_2Cl_2/CH_3CN as the eluent. Typical isolated yields obtained were over 70%. Complex **6** was crystallized in $CHCl_3$/hexane, forming purple cubic crystals suitable for X-ray diffraction.

[$Ru(bpy)_2$(3-hydroxyfla^{Cl})][PF_6] (**4**): Yield: 681 mg, 83%. Found: C, 50.38; H, 2.90; N, 6.75; Calcd for $C_{35}H_{24}F_6N_4O_3ClRuP$: C, 50.64; H, 2.91; N, 6.75. UV-vis λ_{max} (CH_3CN)/nm (ε / M^{-1} cm^{-1}): 370 (13200), 529 (8656). FT-IR (KBr, cm^{-1}): 1612 ($\nu_{C=O}$). ESI MS: m/z (pos.) 685.06. ^{1}H NMR (500 MHz, CD_3CN): δ 9.00 (d,1H), 8.82 (d,1H), 8.50 (m, 4H), 8.42 (d, 1H), 8.39 (d, 1H), 8.05 (t,1H), 8.02 (t, 1H), 7.95 (d, 1H), 7.82 (m, 3H), 7.73 (m, 3H), 7.60 (t, 1H), 7.53 (t, 2H), 7.38 (m, 3H), 7.18 (t, 1H), 7.16 (t, 1H).

[$Ru(bpy)_2$(3-hydroxyfla^{CH3})][PF_6] (**2**): Yield: 713 mg, 88%. Found: C, 53.47; H, 3.34; N, 7.03; Calcd for $C_{36}H_{27}F_6N_4O_3RuP$: C, 53.40; H, 3.36; N, 6.92. UV-vis λ_{max} (CH_3CN)/nm (ε / M^{-1} cm^{-1}): 370 (10383), 529 (6867). FT-IR (KBr, cm^{-1}): 1609 ($\nu_{C=O}$). ESI MS: m/z (pos.) 665.12. ^{1}H NMR (500 MHz, CD_3CN): δ 9.03 (d,1H), 8.83 (d,1H), 8.50 (m, 4H), 8.42 (t, 2H), 8.37 (d, 2H), 8.06 (t,1H), 8.02 (t, 1H), 7.93 (d, 1H), 7.85 (d, 1H), 7.82 (t, 2H), 7.75 (d, 1H), 7.72 (m, 2H), 7.60 (t, 1H) 7.53 (t, 1H), 7.37 (m, 1H), 7.22 (d, 2H), 7.18 (t, 1H), 7.16 (t, 1H), 2.35 (s, 3H).

[$Ru(bpy)_2$(3-hydroxyfla^{OCH3})][PF_6] (**1**): Yield: 619 mg, 74%. Found: C, 52.31; H, 3.35; N, 6.73; Calcd for $C_{36}H_{27}F_6N_4O_4RuP$: C, 52.37; H, 3.30; N, 6.79. UV-vis λ_{max} (CH_3CN)/nm (ε / M^{-1} cm^{-1}): 370 (9567), 529 (6066). FT-IR (KBr, cm^{-1}): 1602 ($\nu_{C=O}$). ESI MS: m/z (pos.) 681.19. ^{1}H NMR (500 MHz, CD_3CN): δ 9.03 (d,1H), 8.84 (d,1H), 8.48 (m, 4H), 8.42 (d, 1H), 8.39 (d, 1H), 8.06 (d,1H), 8.02 (d, 1H), 7.93 (d, 1H), 7.85 (d, 1H), 7.80 (m, 2H), 7.75 (d, 1H), 7.70 (m, 2H), 7.60 (t, 1H) 7.52 (t, 1H), 7.36 (m, 1H), 7.18 (t, 1H), 7.16 (t, 1H), 6.94 (d, 2H), 3.82 (s, 3H).

[Ru(bpy)$_2$(5-hydroxyfla)][PF_6] (**6**) : Yield: 677 mg, 85%. Found: C, 52.85; H, 3.12; N, 6.97; Calcd for $C_{35}H_{25}F_6N_4O_3RuP$: C, 52.84; H, 3.17; N, 7.04. UV-vis λ_{max} (CH_3CN)/nm (ε / M^{-1} cm^{-1}): 370 (11500), 520 (14000). ESI MS: m/z (pos.) 651.10. ^{1}H NMR (500 MHz, CD_3CN): δ 9.06 (d,1H), 8.98 (d,1H), 8.78 (d, 1H), 8.74 (d, 1H), 8.69 (d, 1H), 8.63 (d,1H), 8.21 (t, 1H), 8.15 (t, 1H), 8.05 (m, 3H), 7.96 (t, 1H), 7.91 (t, 2H), 7.77 (t, 1H), 7.67 (t, 1H) 7.59 (m, 1H), 7.55 (m, 2H), 7.34 (t, 1H), 7.28 (m, 2H), 6.82 (s, 1H), 6.62 (d, 1H), 6.52 (d, 1H).

[Ru^{II}(bpy)$_2$(3,7-dihydroxyfla)][PF_6] (**5**): Yield: 584 mg, 71%. Found: C, 51.85; H, 3.10; N, 6.91; Calcd for $C_{36}H_{27}F_6N_4O_4RuP$: C, 51.79; H, 3.10; N, 6.90. UV-vis λ_{max} (CH_3CN)/nm (ε / M^{-1} cm^{-1}): 370 (8560), 529 (4800). FT-IR (KBr, cm^{-1}): 1615 ($\nu_{C=O}$). ESI MS: m/z (pos.) 667.09. ^{1}H NMR (500 MHz, CD_3CN): δ 9.16 (d,1H), 8.97 (d,1H), 8.76 (d, 1H), 8.72 (d, 1H), 8.67 (d, 1H), 8.63 (d,1H), 8.47 (d, 2H), 8.16 (t, 1H), 8.09 (t, 1H), 8.02 (d, 1H), 7.92 (t, 3H), 7.84 (d, 1H), 7.74 (t, 1H) 7.67 (t, 1H), 7.31 (m, 5H), 7.05 (s, 1H), 6.92 (d, 1H).

Results and Discussion

*Synthesis and Characterization of Complexes **1 – 6***

The synthesis of the Ru (II) bis-bipyridyl flavonolate complexes followed previously described methods.[21,28,29] For example, complex **1** [Ru^{II}(bpy)$_2$(3-hydroxyfla^{OCH3})] [PF_6] was prepared by mixing 1 equiv of $Ru^{II}(bpy)_2Cl_2$ with 1.2 equiv of ligand flavonol and 2.0 equiv of trimethylamine in ethanol under N_2. The reaction was brought to refluxed state and stirred under N_2 for 14 hrs. The resulting complexes were isolated as purple, diamagnetic PF_6^- salts. All of the complexes are relatively stable as solids but react with O_2 in air when dissolved. The complexes have all been characterized by ^{1}H NMR, UV-vis,

FT-IR, cyclic voltammetry, mass spectrometry, and for complex **6**, and previously for complex **3** by X-ray crystallography, shown in Figure 5.1, Figure 5.2 and Figure 5.3.

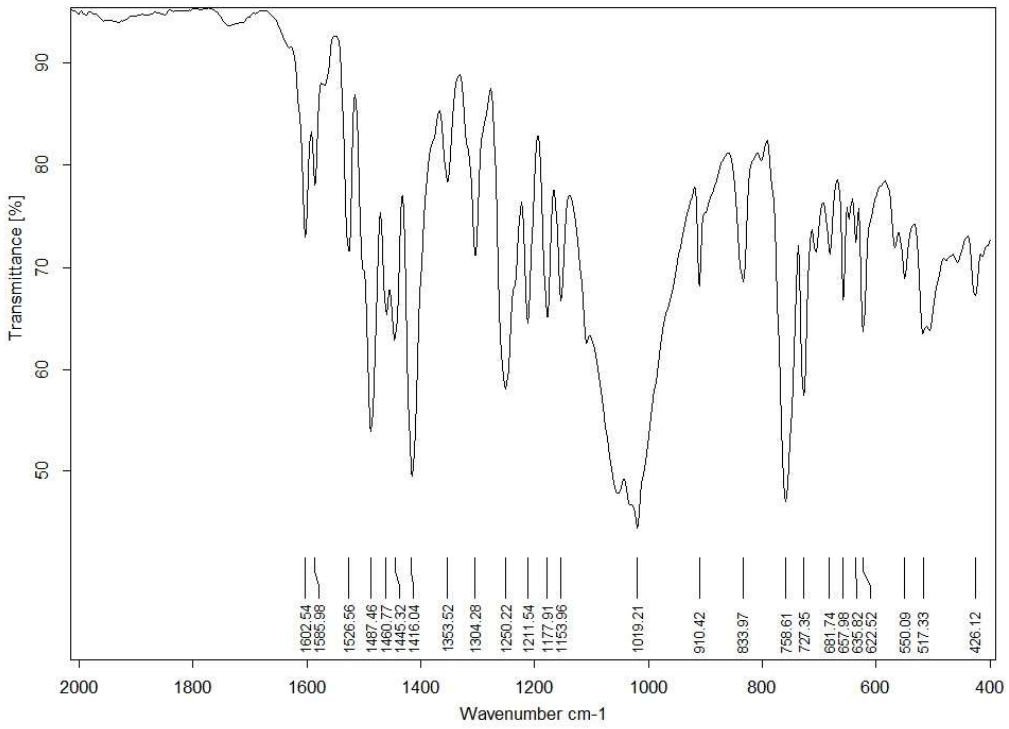

Figure 5.1 FT-IR spectrum of complex **1**

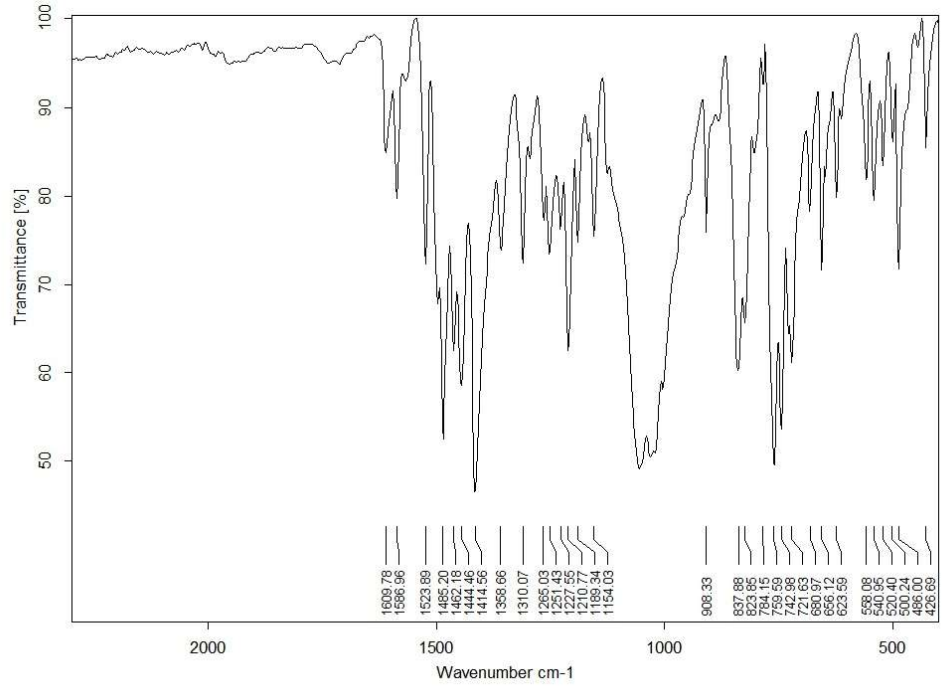

Figure 5.2 FT-IR spectrum of complex **2**

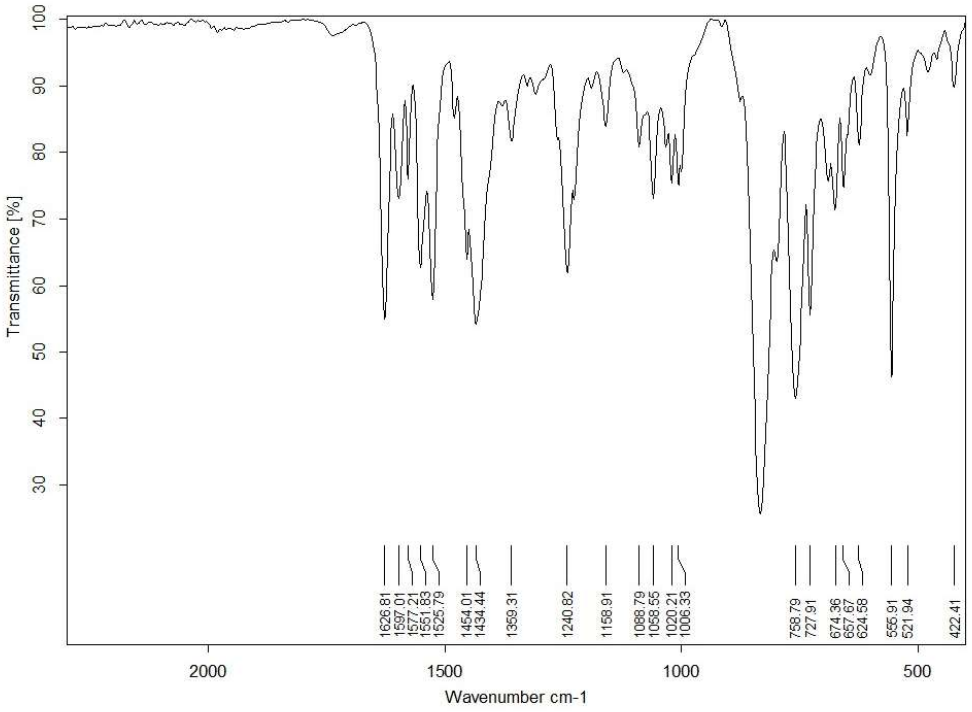

Figure 5.3 FT-IR spectrum of complex **6**

The [1]HNMR spectra of complexes **1-6** in d-acetonitrile exhibits peaks at the region from 8.8 to 9.2 pm which is due to the fact that they are close to position 3 oxygen (C-O) and position 4 oxygen (C=O) and these two oxygens would make their neighbor protons more electron deficient, shown in Figure 5.4, Figure 5.5, Figure 5.6, Figure 5.7, Figure 5.8.

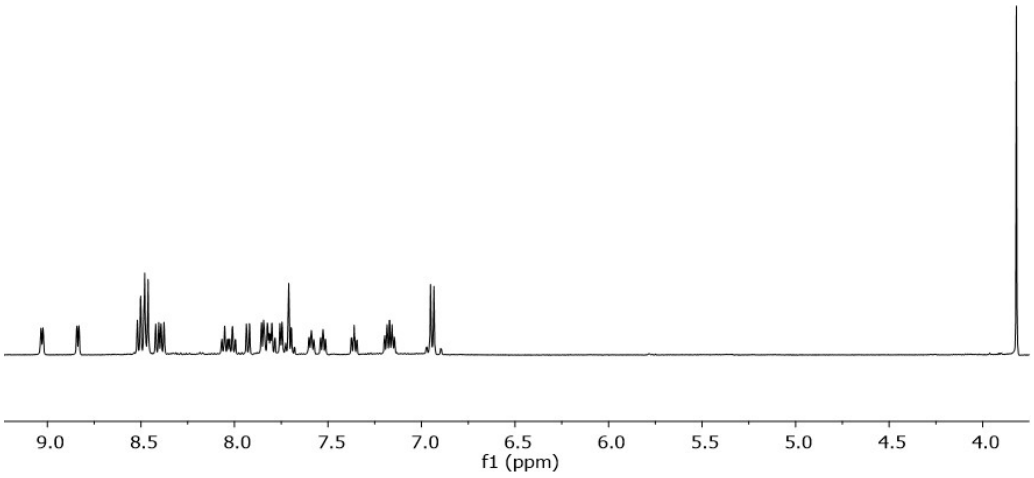

Figure 5.4 [1]H NMR spectrum of complex **1**

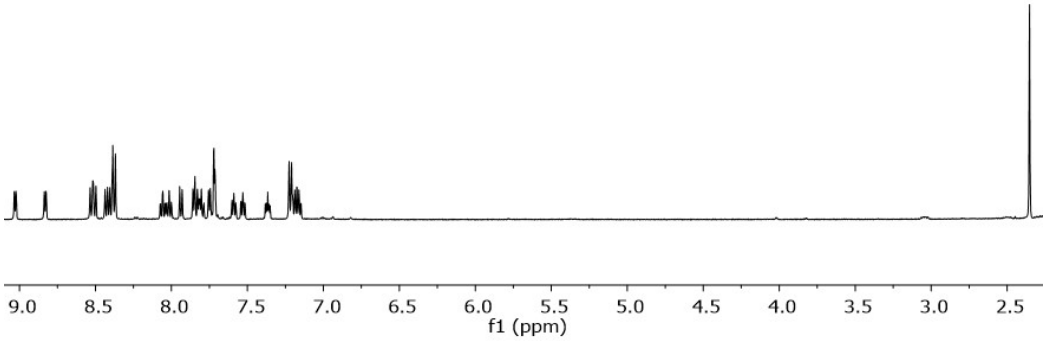

Figure 5.5 [1]H NMR spectrum of complex **2**

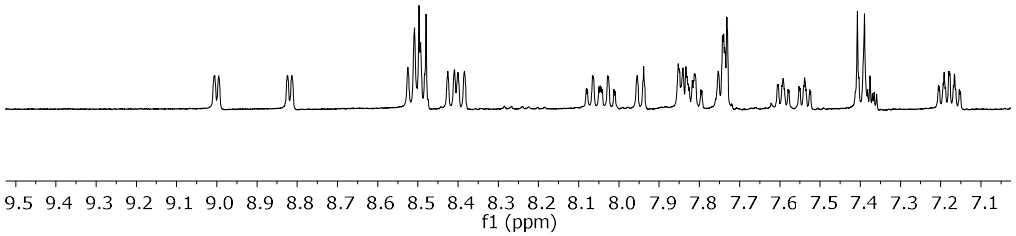

Figure 5.6 ^{1}H NMR spectrum of complex **4**

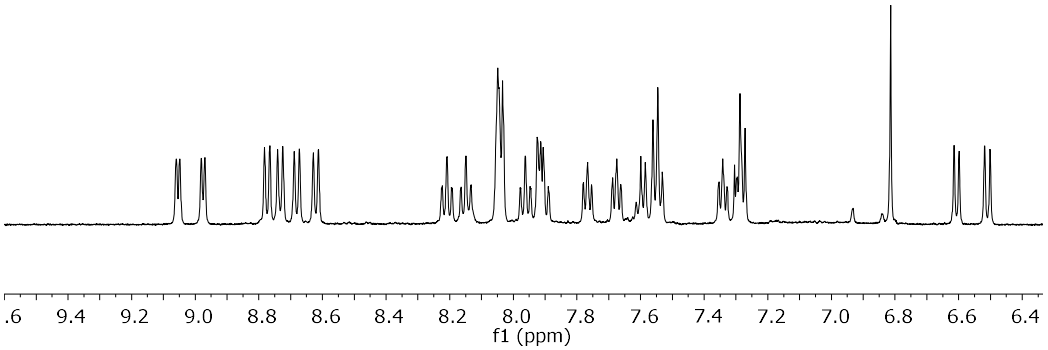

Figure 5.7 ^{1}H NMR spectrum of complex **5**

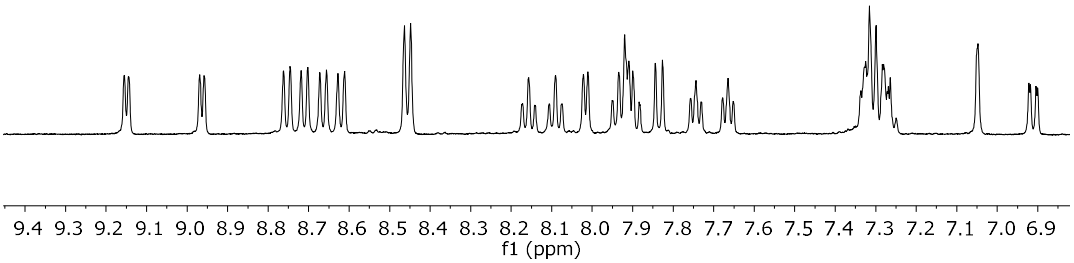

Figure 5.8 ^{1}H NMR spectrum of complex **6**

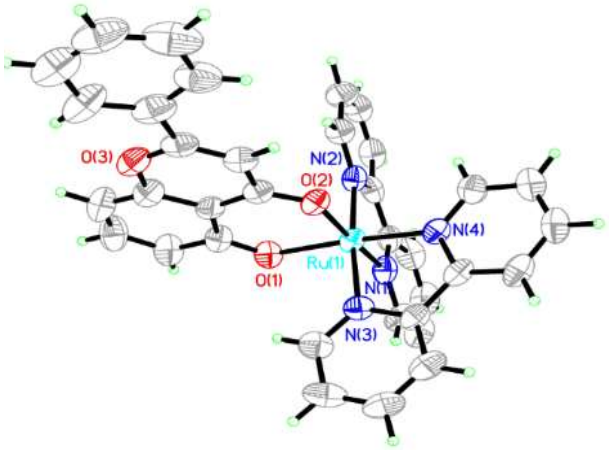

Figure 5.9 Crystal structure of the [$Ru^{II}(bpy)_2$(5-hydroxyfla)] cation, complex **6**. Selected bond lengths (Å): Ru(1)-O(2) 2.053(4); Ru(1)-O(1) 2.068(4); C(4)-O(2) 1.259(8); C(5)-O(1) 1.291(8); C(2)-C(3) 1.337(10). Selected bond angles (deg): O(2)-Ru(1)-O(1) 89.73(17); C(4)-O(2)-Ru(1) 127.7(4); C(5)-O(1)-Ru(1) 126.1(4)

The single-crystal X-ray structure of the complex [$Ru^{II}(bpy)_2$(5-hydroxyfla)] [PF_6] (**6**) is shown in Figure 5.9 and Table 5.1 with selective bond distances and angles. In the structure of [$Ru^{II}(bpy)_2$(5-hydroxyfla)] (**6**) cation, metal center has a octahedral geometry involving two oxygens of flavonol (O (2): carbonyl and O (1) 3-hydroxyl), and four nitrogen atoms of bis-bipyridyl. The bond lengths of Ru -O(1) is 2.068(3) Å and Ru-O(2) is 2.053(3) Å, respectively, which are closer to each other compared to complex **3** (Ru-O(1) = 2.059 Å, Ru-O(2) = 2.098 Å) indicating electrons in the ligand of 5-flavonolate on the ruthenium complex are more delocalized than 3-flavonolate.[29] The C(4)-O(2) (corresponding to C=O, carbonyl group) and C(5)-O(1) (corresponding to C-O, 5-hydroxy) bond lengths are 1.259(8) Å and 1.291(8) Å, which is shorter than that in complex **3** (C=O 1.266 Å, C-O 1.360 Å respectively).[29] The bond length of C(2)=C(3) is 1.337(10) Å, much shorter than the carbon-carbon double bond length in complex **3** (C=C 1.402(6) Å) and close to double bond length in ethylene (1.339 Å), suggesting that the C(2) = C(3) bond in

complex **6** is not influenced by the coordination of metal ruthenium, which may explain C(2)=C(3) bond is not cleaved during photo-induced reaction with oxygen.[29,31]

Table 5.1 Crystal data and structure refinement for complex **6**

Empirical formula	C35 H25 F6 N4 O3 P Ru
Formula weight	795.63
Temperature (K)	150(2) K
Crystal system	Monoclinic
Space group	C 2/c
a (Å)	26.107(3) Å
b (Å)	16.170(2) Å
c (Å)	17.270(2) Å
α (°)	90
β (°)	118.868(3)
γ (°)	90
V ($Å^3$)	6384.5(13)
Z	8
D_{calcd} (g cm^{-3})	1.655
Absorption coefficient (mm^{-1})	0.621
$2\theta_{max}$ (°)	27.243
Reflections collected	69667
Independent reflections	7115 [R(int) = 0.0904]
Final R indices [I > 2sigma(I)]	R1 = 0.0798, wR2 = 0.1970
R indices (all data)	R1 = 0.1244, wR2 = 0.2193
Goodness-of-fit on F^2	1.045

Redox Properties of the Complexes

The redox properties of complexes **1- 6** were examined by cyclic voltammetry in CH_3CN at room temperature under N_2, shown in Figure 5.10 and Figure 5.11. The results are summarized in Table 5.2. All potentials are reported versus NHE. Electrochemically reversible oxidation couples are observed for all complexes, with ΔE_p equal to ca. 65 mV and i_{pa}/i_{pc} close to unity, which can be assigned to the $Ru^{II/III}$ couple. For each complex, $E_{1/2}$ was observed at 0.63 V for $[Ru^{II}(bpy)_2(3\text{-hydroxyfla}^{OCH3})]^+$ (**1**), 0.65 V for $[Ru^{II}(bpy)_2(3\text{-hydroxyfla}^{CH3})]^+$ (**2**), 0.67 V for $[Ru^{II}(bpy)_2(3\text{-hydroxyfla}^{H})]^+$ (**3**), 0.71 V for $[Ru^{II}(bpy)_2(3\text{-hydroxyfla}^{Cl})]^+$ (**4**), 0.66 V for $[Ru^{II}(bpy)_2(3,7\text{-dihydroxyfla})]^+$ (**5**) and 0.72 V for $[Ru^{II}(bpy)_2(5\text{-hydroxyfla})]^+$ (**6**). The difference in $E_{1/2}$ of complexes **1-6** ranges from 0.43 V to 0.52 V (over a range of 90 mV) and has an order of **1** < **2** < **5** < **3** < **4** < **6**. The plot of $E_{1/2}$ vs Hammett constant σ is linear, shown in Figure 5.12.[32] These results indicate that the redox potentials of the Ru^{II} ion are affected by the electronic nature of the substituent group of the ligands, namely, the electron-donating group could increase the electron density at the ruthenium (II) center.

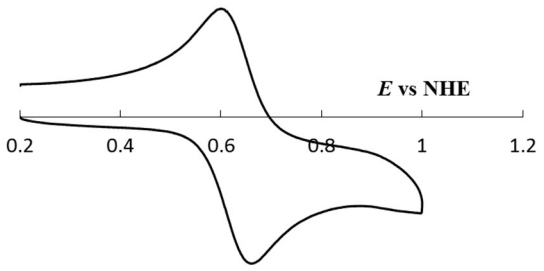

Figure 5.10 Cyclic voltammograms of oxidation of complex **1** in CH_3CN under N_2 at room temperature

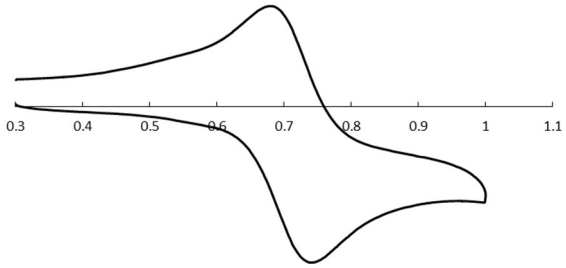

Figure 5.11 Cyclic voltammograms of oxidation of complex **2** in CH_3CN under N_2 at room temperature

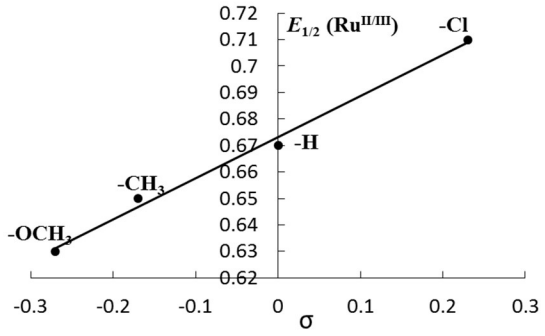

Figure 5.12 Plot of $E_{1/2}$ of the $Ru^{II/III}$ of complexes **1 - 4** vs Hammett constant σ

Table 5.2 Electrochemical data for complexes **1 - 6**[a]

Complex	$E_{1/2}$ (V)	ΔE_p (V)	i_{pa}/i_{pc}	σ^b
1	0.63	0.061	0.93	-0.27
2	0.65	0.070	0.88	-0.17
3	0.67	0.067	0.78	0.00
4	0.71	0.063	0.91	0.23
5	0.72	0.064	0.72	~
6	0.66	0.062	0.77	~

[a]All potentials measured using NHE reference electrode, Pt disc working electrode, and Pt wire counter electrode; scan rate of 100 mV/sec in CH_3CN, 0.1M $TBAPF_6$
[b]Hammett constants σ for each substituent (-OCH_3, -CH_3, -H, and -Cl) are from reference 32.

Photophysical and Photochemical Studies

The normalized absorption spectra of complex **1**, complex **6** and $[Ru^{II}(bpy)_3]^{2+}$ in CH_3CN are compared in Figure 5.13. The UV-vis absorption spectra of **1-5** have similar identifiable bands attributable to ligand flavonolate from 300 to 400 nm as well characteristic MLCT (metal ligand charge transfer) bands between 400 and 700 nm. The parent complex $[Ru^{II}(bpy)_3]^{2+}$ has an absorption band centered at ~ 450 nm corresponding to a MLCT transition that produces a redox-active photoexcited state. Complexes **1-5** show significantly shifted and broadened absorption spectrum inside the visible range, with MLCT ca. 520 nm. Complex **6** has two MLCT bands close to absorbances in both $[Ru^{II}(bpy)_3]^{2+}$ at 450 nm, and Ru-flavonolate at 520 nm.

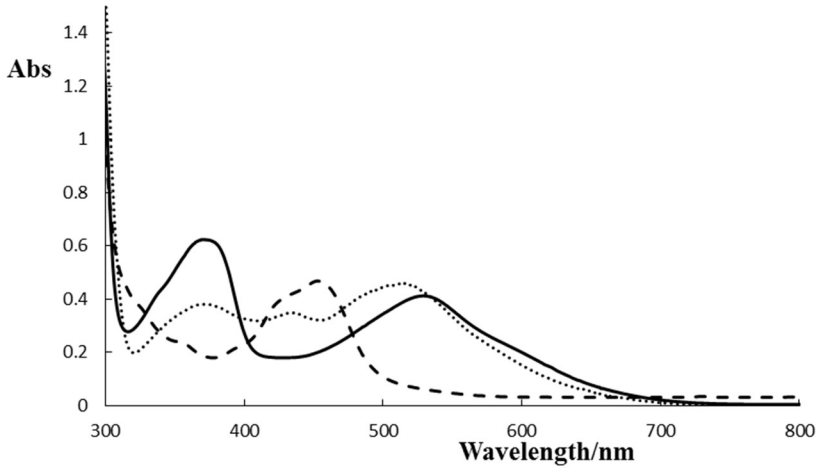

Figure 5.13 UV-vis absorbance of 65 μM complex **1** (solid line), 30 μM complex **5** (dotted line) and 30 μM $[Ru^{II}(bpy)_3]^{2+}$ (dashed line) in CH_3CN

Excitation of complexes **1-5** in CH_3CN solution at wavelengths > 430 nm generates no observable emissions, but excitation in the 410 nm obtains a fluorescence (λ_{em} = 460 nm) and a phosphorescence in the near IR region (λ_{em} = 960 nm) (Figure 5.14, Figure 5.15,

Figure 5.16 and Table 5.3), in contrast, complex **6** did not produce any emission upon irradiation at 410 nm.

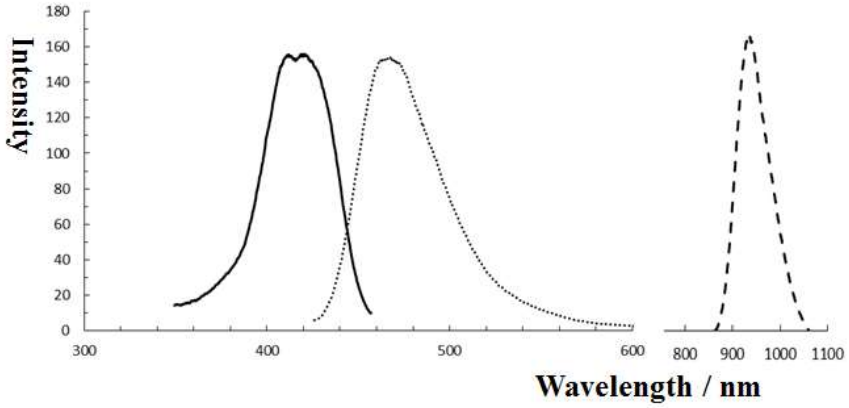

Figure 5.14 Normalized action and emission spectra of complex **1** in CH_3CN: excitation (black line); fluorescence emission (dotted line); NIR emission (dashed line)

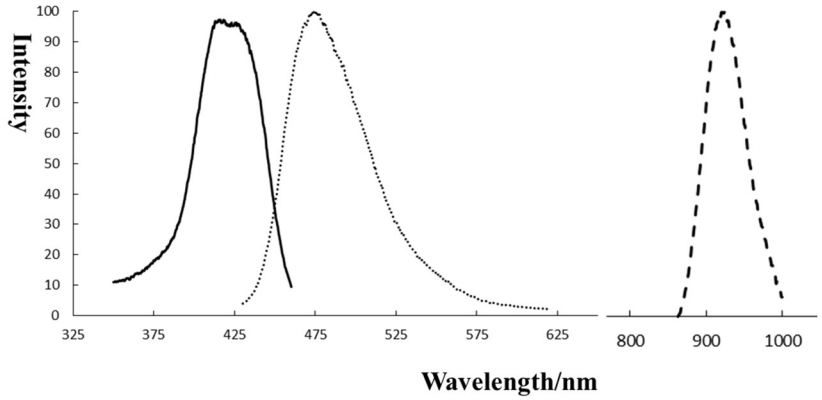

Figure 5.15 Normalized action and emission spectra of complex **2** in CH_3CN: excitation (black line); fluorescence emission (dotted line); NIR emission (dashed line)

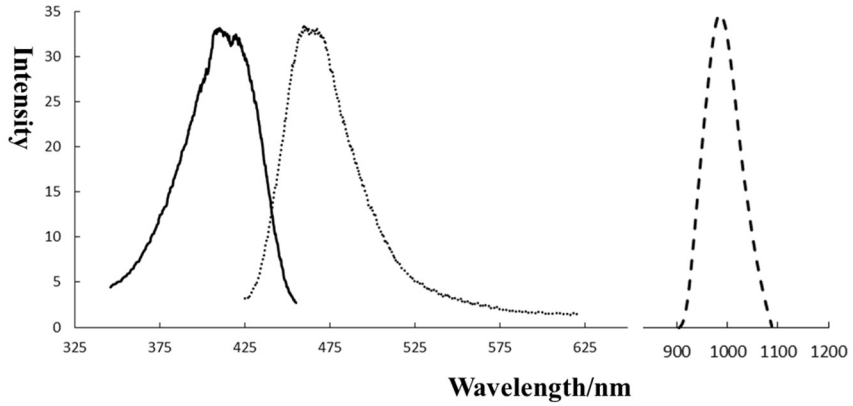

Figure 5.16 Normalized action and emission spectra of complex **5** in CH_3CN: excitation (black line); fluorescence emission (dotted line); NIR emission (dashed line)

Exposure of complexes **1-5** under in to anaerobic acetonitrile solution to room light in the presence 200-fold excess of $MV^{2+}Cl_2$ (methyl viologen dichloride) shows the characteristic blue coloring indicative of the formation of reduced $MV^{\cdot+}$, indicating the complexes photo-reductants, Figure 5.17.

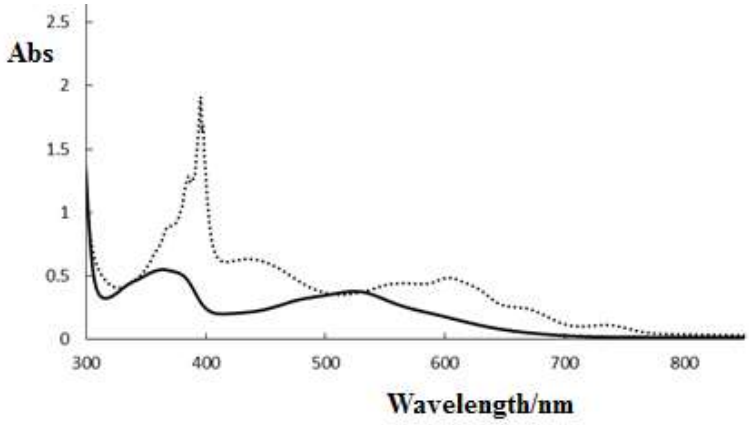

Figure 5.17 UV-Vis spectra of CH_3CN solution of 30 μM complex **1** with 60 μM MV^{2+} in Ar after 10 mins irradiation by visible light, in the dark (solid line); after irradiation (dotted line)

Table 5.3 Photochemical data of **1-6**

Complex	Abs λ_{max} (nm)	Ext. Coeff. ($M^{-1}cm^{-1}$)	Ex. λ_{max} (nm)	Em. λ_{max} (nm)	Lifetime under Ar (μs)
1	380	9678	419	472	
	529	6256		935	31.7
2	376	10572	415	464	
	527	6899		922	15.3
3	370	11228	410	460	
	526	7712		912	10.5
4	364	13780	410	467	
	523	8679		922	24.3
5	375	8768	416	461	
	513	4971		985	9.53

In collaboration with the Selke lab at California State University, we examined if these complexes act as sensitizers for the production of singlet oxygen, as is the case for the parent $[Ru^{II}(bpy)_3]^{2+}$ complex. Upon excitation by a Nd:YAG pulsed laser either in the visible (532 nm) or UV range (355 nm), emission in the near-infrared (NIR) is observed for all complexes, with that of complex **6** being considerably weaker than complexes **1**-**5**. However, the emission is not due to singlet oxygen, but rather originates from the complexes themselves. Both the emission intensity and emission lifetimes in acetonitrile do not vary appreciably between air-saturated solutions and solutions purged with argon, shown in Figure 5.18, Figure 5.19, Figure 5.20, Figure 5.21 and Table 5.4. Analogous experiments with singlet oxygen quenchers such as 9,10-dimethyl anthracene, and NaN_3, found the both the NIR emission intensities and lifetimes unaffected. Hence these complexes do not produce singlet oxygen, and $^1O_2$ cannot be a reactive intermediate in the ligand oxidation reactions described below.

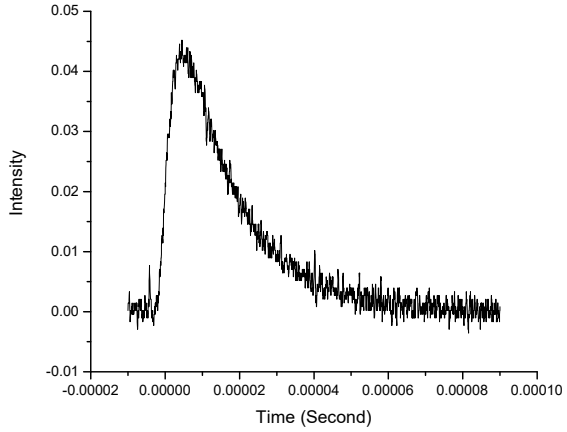

Figure 5.18 NIR emission decay traces of complex **2** under air by the excitation at 532 nm in CH_3CN

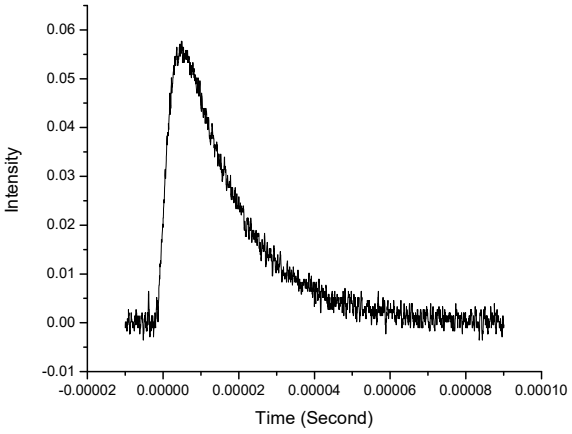

Figure 5.19 NIR emission decay traces of complex **2** under Argon by the excitation at 532 nm in CH_3CN

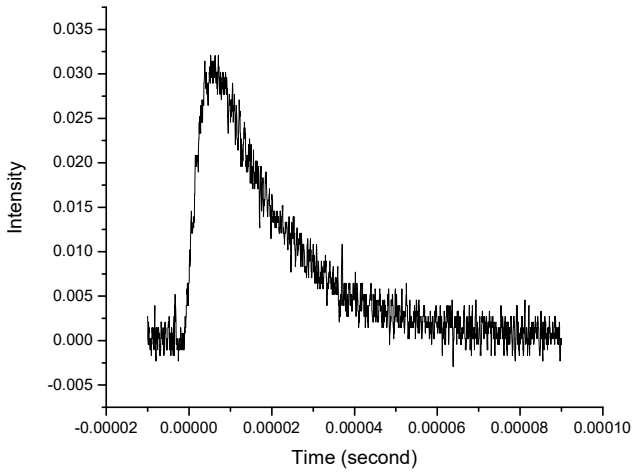

Figure 5.20 NIR emission decay traces of complex **5** under air by the excitation at 532 nm in CH_3CN

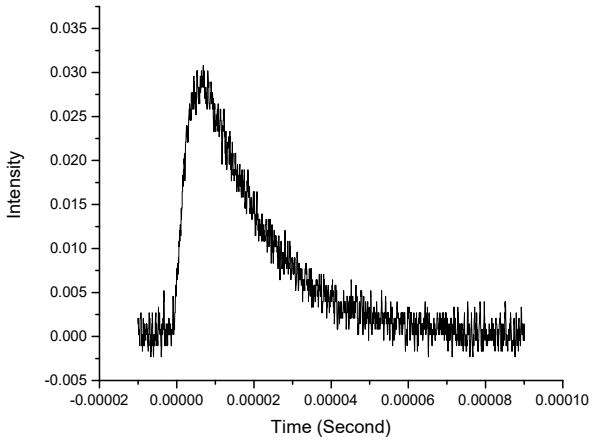

Figure 5.21 NIR emission decay traces of complex **5** under Argon by the excitation at 532 nm in CH_3CN

Table 5.4 Near infrared (NIR) emission lifetimes and relative intensities of complexes **1-6** under air and argon in acetonitrile, determined in the Selke lab

	Abs. at 532 nm	Lifetime under Air (μs) (NIR Intensity at t = 0)	Lifetime under Ar (μs) (NIR Intensity at t = 0)
Compound **1**	0.2895	15.9 (0.06810)	15.3 (0.07088)
Compound **2**	0.3072	15.3 (0.08809)	15.4 (0.06736)
Compound **3**	0.2800	16.8 (0.03855)	15.2 (0.04610)
Compound **4**	0.2989	17.6 (0.03928)	15.0 (0.04526)
Compound **5**	0.2960	18.6 (0.01316)	16.4 (0.01423)
Compound **6**	0.2971	17.9 (0.04575)	16.8 (0.04678)

Reaction Product Characterizations

The photo-induced reactions between complexes **1-5** and oxygen in CH_3CN give rise to oxygenated products, as demonstrated by ESI – MS data are shown in Table 5.5: $[Ru^{II}(bpy)_2bpg]^+$ (bpg = 2-benzoatopheylglyoxylate) (m/z (pos.): 713.14 for complex **1**; 697.11 for complex **2**; 683.09 for complex **3**; 717.05 for complex **4**; 699.09 for complex **5**. Under mild conditions, e.g., oxygen saturated solutions in an ice bath illuminated using 400 nm cut-on filter, conversions of the complexes are ca. 90%, estimated by NMR. However, under analogous conditions, no oxygenation product was observed for complex **6**. Therefore, a hydroxyl (-OH) in the 3 position is required for the oxygenation.

Subsequent illumination of the benzoatopheylglyoxylate complexes causes decomposition into the products typical of the enzymatic reactivity, as identified in ESI-MS of reaction mixtures. For example, photo-oxidation of complex **1** gives an the nascent product $[Ru^{II}(bpy)_2bpg]^+$ (bpg = 2-benzoatopheylglyoxylate) (m/z (pos.): 713.07; which

then decomposes to $[Ru^{II}(bpy)_2(O\text{-benzoylsalicyclate})]^+$ (m/z (pos.): 685.08 and $[Ru^{II}(bpy)_2(benzoate)]^+$ (m/z (pos.): 565.06, shown in Figure 5.22 and Figure 5.23.

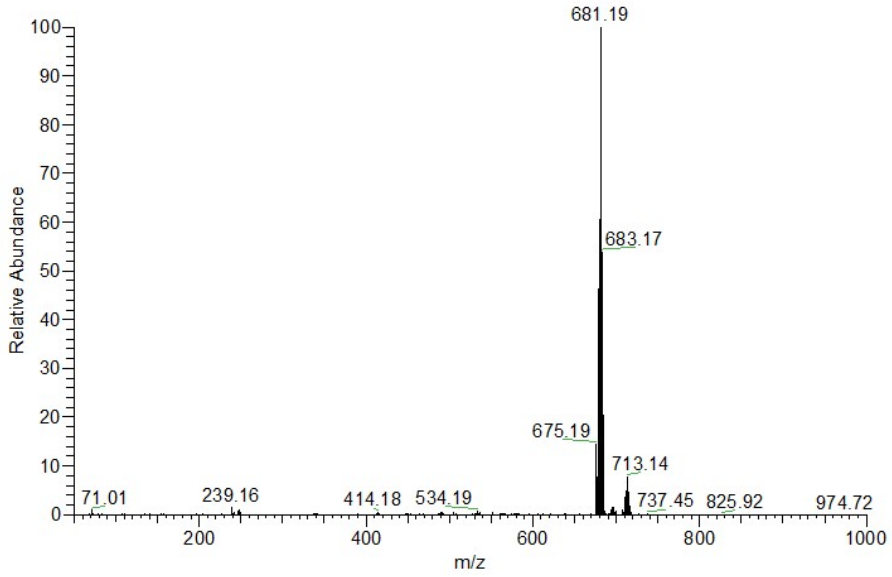

Figure 5.22 ESI-MS of complex **1** and oxygenated species

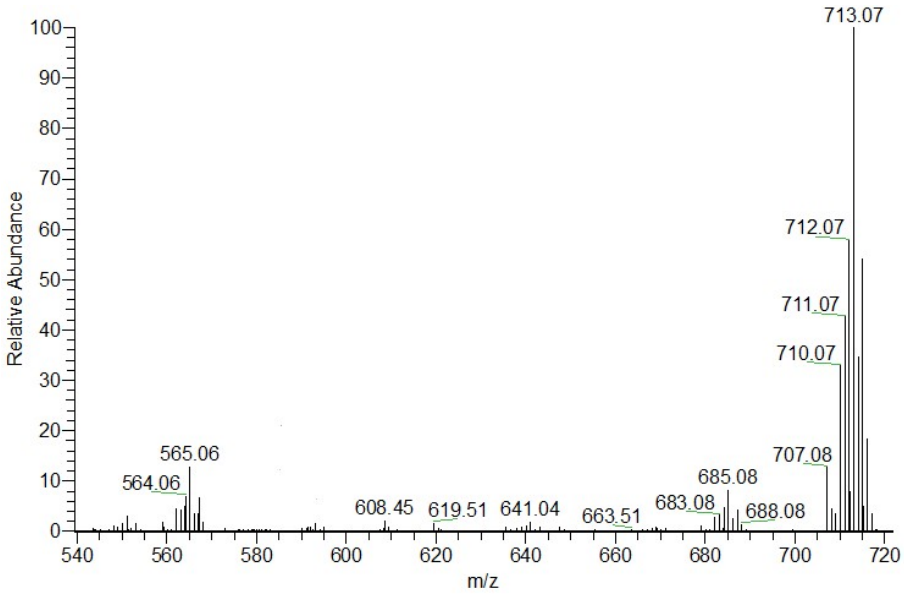

Figure 5.23 ESI-MS of reaction mixture after oxygenation of complex **1**

Table 5.5 ESI – MS (m/z (pos.)) results of the complexes **1-6** before and after photolysis under O_2, under condition described

	1	**2**	**3**	**4**	**5**	**6**
Before	681.19	665.12	651.10	685.06	667.10	651.10
After	713.14	697.11	683.09	717.05	699.09	651.10

Kinetic Measurements

The oxygenations of the complexes **1-5** were followed by monitoring the decrease of the band absorbance of the coordinated flavonolate at λ_{max} = 380 nm. The kinetic data and activation parameters of the complexes are listed in Table 5.6. The initial reaction rate of each complex exhibits a linear relationship with respect to the initial concentrations of both complexes **1-5** and oxygen, so the rate law was determined as $-d[Ru^{II}(bpy)_2fla^R]^+/dt = k[Ru^{II}(bpy)_2fla^R]^+[O_2]$. ($fla^R$ including 3-hydroxyfla^R and 3,7-dihydroxyfla). The second-order reaction rate constants k_2 were determined as 0.55-1.43 × 10^{-2} $M^{-1}s^{-1}$ at 30 ºC ($\Delta H^{\neq}$ = 26.32-35.21 kJ mol^{-1}, $\Delta S^{\neq}$ = -196.7 to -172.3 J mol^{-1} K^{-1}). Other reported metal flavonolate complexes exhibit lower reactivity and require higher temperature (0.82 × 10^{-2} $M^{-1}s^{-1}$ for $[Mn^{II}L(fla)]$ at 80 ºC; 2.07 × 10^{-2} $M^{-1}s^{-1}$ for $[Fe^{III}(salen)(fla)]$ at 100 ºC; 0.31 × 10^{-2} $M^{-1}s^{-1}$ for $[Zn^{II}(idpa)(fla)]$ at 100 ºC; 0.61 × 10^{-2} $M^{-1}s^{-1}$ for $[Cu^{II}(idpaH)(fla)]$ at 100 ºC).[16-19] Thus, complexes **1-5** show higher reactivity at lower temperature (30-55 ºC), attributed to the photo-reactivity. Although the structures of complexes **1-4** are similar, the oxygenation reactivity decreases in the order of **1 > 2 > 3 > 4** and the Hammett plot (log (k_2^R/k_2^H) vs σ) is linear (ρ = -0.65) (Figure 5.24a). Thus the bimolecular rate constants for oxygenation of complexes **1-4** correlates with the order of the $E_{1/2}$ of complexes, and the plot of k_2 vs $E_{1/2}$ (Ru^{III}/Ru^{II}) is linear (Figure 5.24b). These plots provide evidence that the reactivity of the

ruthenium bis-bipyridyl flavonolate complexes are strongly influenced by the electronic nature of the substituent group on the ligand.

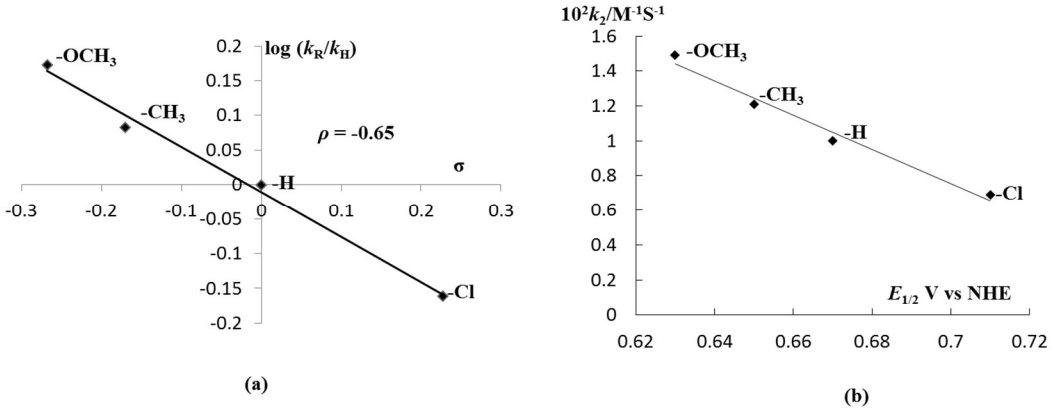

Figure 5.24 (a) 70 μM complex **1** reacts with saturated O_2 in CH_3CN at 30 ºC under room light; (b) Hammett plot of log (k^R/k^H) vs σ; (c) Correlation of rate constants vs $E_{1/2}$ of complexes

Table 5.6 Kinetic data (at 30 ºC) and activation parameters of the complexes

	10^2k_2 ($M^{-1}s^{-1}$)	$\Delta H^{\neq}$ (kJ mol^{-1})	$\Delta S^{\neq}$ (J mol^{-1} K^{-1})	$-T\Delta S^{\neq}$ (kJ mol^{-1})	$\Delta G^{\neq}$ (kJ mol^{-1})
5	0.55	35.21	-172.3	52.21	87.42
4	0.69	32.33	-179.4	53.46	86.69
3	1.00	26.32	-196.7	58.62	85.92
2	1.21	27.06	-192.7	57.42	85.44
1	1.43	28.40	-186.6	55.61	84.92

Reaction condition: 70 μM complexes **1-5** and saturated O_2 (according to literature:[30] 8.0 mM) in CH_3CN at 30 ºC under light.

Mechanistic Considerations

Photo-induced oxygenations are typically initiated by way of two fundamental pathways, energy or electron transfer. In the former, sensitization of singlet oxygen is effected, either by the substrate itself or a surrogate, and this high-energy species performs the oxygenation directly. In the latter case, a long-lived excited state of the substrate or surrogate undergoes an electron transfer reaction with dioxygen, forming superoxide, which subsequently engenders the oxygenation. Our initial results were misleading, in that we observed near IR emissions upon photolysis of the substrate complexes similar to those from singlet oxygen itself. But controls showed identical emissions in the absence of dioxygen, suggesting the complexes themselves emit in this region, which was subsequently confirmed using more specialized instrumentation.

A similar photo-induced electron transfer mechanism related to a non-oxygen dependent oxidation of a dithiomaltolato complex $[Ru(bpy)_2(ttma)]^+$, which requires an electron acceptor such as methyl-viologen to promote a ligand-based C-H oxidation. In this instance also, an unusual near IR emission was observed and proposed as ligand-based. In that case, singlet oxygen was both generated and consumed by the Ru complex, but shown to be uninvolved in the C-H activation. Simple electrochemical oxidation of the complex at high pH afforded the C-oxygenated products from addition of water; no similar reactivity was seen for the Ru-flavonolates.

Scheme 5.4 notes the structural similarity of the photoactive ligands, it may suggest that the near IR emission is due in part to the coordinated α-hydroxypyrone. Indeed, similar photochemical reactivity has been reported for flavonolate complexes of main group complexes as well as for a family of 3-hydroxyflavothionate complexes. It is distinctly

possible that all of these reported photo-reactivities occur through long-lived near IR emissive states.

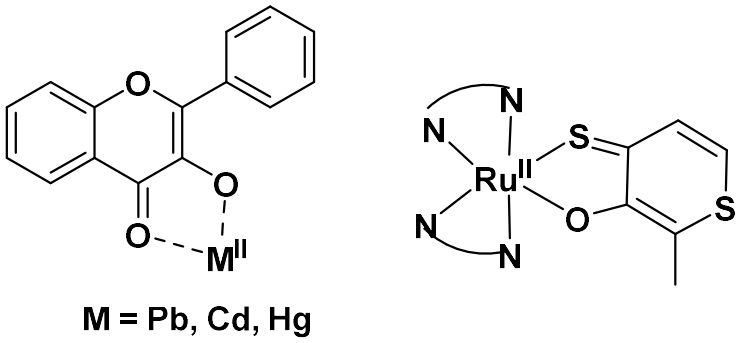

Scheme 5.4 Photoreactive α-hydroxypyrone metal complexes

A second unusual aspect of the Ru-flavonolate reactivity is that the central ring is cleaved via a 1,2-dioxetane intermediate as evidenced by a chemiluminescence unique to such species; a 1,3-endoperoxide pathway is widely proposed for native flavonolate dioxygenase and most model systems, shown in Scheme 5.5. Subsequent decomposition of the product Ru-bound benzoatophenylglyoxylate does generate the release of CO and other expected products of the native enzymatic reactivity. Complex **6**, which lacks the α-hydroxypyrone moiety, does not react with oxygen when irritated by light, and it is also not a substrate for QDO.[33]

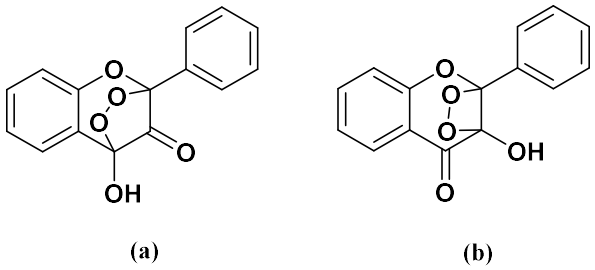

Scheme 5.5 (a) endoperoxide (b) 1,2-dioxetane

Photochemical studies indicate that complexes **1-5** can absorb visible light to generate a long lived redox-active state. A simple thermodynamic cycle quantitatively shows the redox potentials of the excited ruthenium flavonolate complex, Scheme 5.6.[34] The short-wavelength edge at 860 nm of the near IR emission for complex **1**, shown in Figure 5.14, was used to calculate the energy between the lowest triplet state and ground state.[33] As is seen in Scheme 5.6, the long-lived excited state of complex **1** should be thermodynamically capable of reducing both MV^{2+} ($E^{0'}$ = -0.44 V vs NHE) and O_2 ($E^{0'}$ = -0.33 V vs NHE).

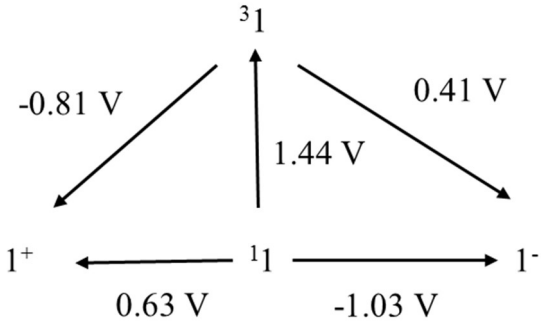

Scheme 5.6 Thermodynamic cycles based on triplet reactivity

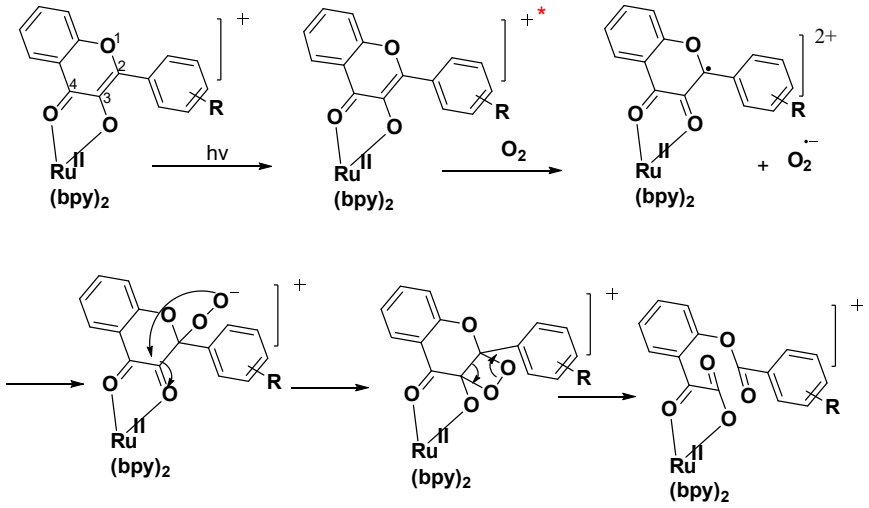

Scheme 5.7 Proposed mechanism for photo-induced oxygenation of ruthenium bis-bipyridyl flavonolate complexes

On the basis of these results, we propose the following mechanism, shown in Scheme 5.7. First, the flavonolate complexes absorbs light to generate a redox-active state which can reduce oxygen to generate $O_2^{\cdot -}$ (superoxide). Next, a fast radical-radical coupling reaction occurs between fla· radical and $O_2^{\cdot -}$. Then, an intramolecular nucleophilic attack of peroxy on C3 forms the 1,2-dioxetane intermediate. The formation of a 1,2-dixoetane intermediate is confirmed by the chemiluminescence during its decomposition, shown in Figure 5.25, which was also observed in the oxygenation of $[Cu^{II}(L)(Fla)_2]$ (Fla = 3-hydroxyflavone; L = 1,10-phenanthroline).[17c] The resulting product $[Ru^{II}(bpy)_2bpg^R]^+$ has been previously characterized.[29] A similar product 2-benzoatophenylglyoxylate was also found in the reaction of free flavonol and superoxide anion by Speier's group.[35,36]

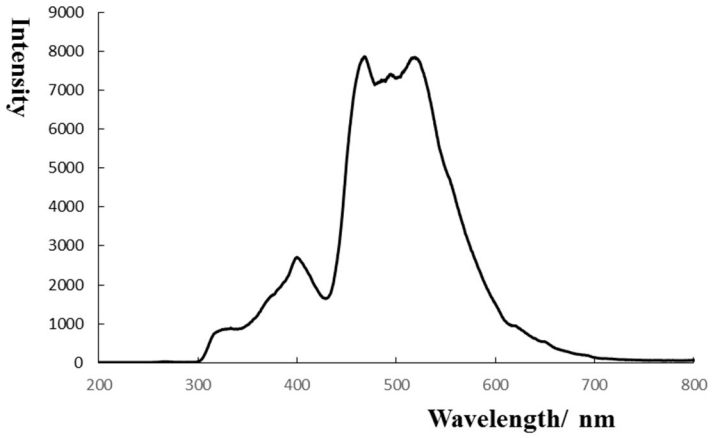

Figure 5.25 Chemiluminescence spectrum of the emitted light during the oxygenation of complex **1** in CH_3CN

Conclusions

In summary, a series of ruthenium bis-bipyridyl flavonolate complexes were synthesized to investigate the mechanism of oxidative cleavage of flavonol during photolysis. Their structures, spectroscopic features, redox properties and reactivity with oxygen were studied in detail. Complexes **1-5** show high reactivity with oxygen compared to other metal flavonolate complexes upon photo-excitation due to a long lived redox-active state which can reduce O_2 to form $O_2^{\cdot -}$. The oxidative ring-cleavage oxygenation of Ru-bound flavonolate complexes takes place through a 1,2-dioxetane intermediate, resulting in the formation of the product $[Ru^{II}(bpy)_2bpg]^+$ (bpg = 2-benzoatophenylglyoxylate), as verified by the characteristic chemiluminescence.

References

1. Pietta, P. G. *J. Nat. Prod.* **2000**, *63*, 1035-1042.

2. Rice-Evans, C. A.; Miller, N.; Paganga, G. *Free Radical Biol. Med.* **1996**, *20*, 933-956.

3. Cotelle, N.; Bernier, J. L.; Catteau, J. P.; Pommery, J.; Wallet, J. C.; Gaydou, E. M. *Free Radical Biol. Med.* **1996**, *20*, 35-43.

4. Guohua, C.; Emin, S.; Ronald, L. *Free Radical Biol. Med.* **1997**, *22*, 749-760.
5. Van Hoof, L.; Van den Berghe, D. A.; Hatfield, G. M.; Vlietinck, A. J. *Planta Med.* **1984**, *50*, 513-517.

6. Brasseur, T. *J. Pharm. Belg.* **1989**, *44*, 235-241.

7. Wei, B. L.; Lu, C. M.; Tsao, L. T.; Wang, J. P.; Lin, C. N. *Planta Med.* **2001**, *67*, 745-747.

8. Fischer, M.; Mills, G. D.; Slaga, T. J*Carcinogenesis* **1982**, *3*, 1243-1245.

9. Huang, M.; Ferraro, T. In *Phenolic Compounds in Food and their Effect on Health II*, Huang, M. T., Ho, C. T., Lee, C. Y., Eds.; ACS Symposium Series; American Chemical Society: Washington, DC, **1992**; Chapter 2, p 507.

10. Huang, M. T.; Wood, A. W.; Newmark, H. L.; Sayer, J. M.; Yagi, H.; Jerina, D. M.; Conney, A. H. *Carcinogenesis* **1983**, *4*, 1631-1637.

11. Musialik, M.; Kuzmicz, R.; Litwinienko, G. *J. Org. Chem.*, **2009**, *74*, 2699-2709.

12. Wollenweber, E. *Flavonoids: Advances in Research*; Harborne, J. B.; Mabry, T. J., Eds.; Chapman&Hall: London, UK, **1982**.

13. Fusetti, F.; Schröter, K. H.; Steiner, R. A.; van Noort, P. I.; Pijning, T.; Rozeboom, H. J.; Kalk, K. H.; Egmond, M. R.; Dijkstra, B. W. *Structure* **2002**, *10*, 259−268.

14. (a) Gopal, B.; Madan, L. L.; Betz, S. F.; Kossiakoff, A. A. *Biochemistry* **2005**, *44*, 193−201. (b) Schaab, M. R.; Barney, B. M.; Francisco, W. A. *Biochemistry* **2006**, *45*, 1009−1016.

15. (a) Laura, B.; Shirley, A. F.; Victoria, J. J.; Stephen, B. *FEBS Lett.* **2004**, *557*, 45−48. (b) Barney, B. M.; Schaab, M. R.; LoBrutto, R.; Francisco, W. A. *Protein Expr. Purif.* **2004**, *35*, 131−141.

16. (a) Kaizer, J.; Barath, G.; Pap, J. S.; Speier, G. *Chem. Commun.* **2007**, 5235−5237. (b) Matuz, A.; Giorgi, M.; Speier, G.; Kaizer, *J. Polyhedron* **2013**, *63*, 41−49. (c) Balogh-Hergovich, É.; Kaizer, J.; Speier, G.; Fulop, V.; Parkanyi, L. *Inorg. Chem.* **1999**, *38*, 3787-3795.

17. (a) Grubel, K.; Rudzka, K.; Arif, A. M.; Klotz, K. L.; Halfen, J. A.; Berreau, L. M. *Inorg. Chem.* **2010**, *49*, 82−96. (b) Grubel, K.; Laughlin, B. J.; Maltais, T. R.; Smith, R. C.; Arif, A. M.; Berreau, L. M. *Chem. Commun.* **2011**, *47*, 10431−10433.

18. (a) Barhacs, L.; Kaizer, J.; Speier, G. *J. Mol. Catal. A.* **2001**, 172, 117−125. (b) Kaizer, J.; Pap, J.; Speier, G.; Párkányi, L. *Eur. J. Inorg. Chem.* **2004**, 2253−2259. (c) Balogh-Hergovich, É.; Kaizer, J.; Pap, J.; Speier, G.; Huttner, G.; Zsolnai, L. *Eur. J. Inorg. Chem.* **2002**, 2287−2295.

19. (a) Sun, Y. J.; Huang, Q. Q.; Zhang, J. J. *Inorg. Chem.*, **2014**, *53*, 2932-2942. (b) Sun, Y. J.; Huang, Q. Q.; Tano, T.; Itoh, S. *Inorg. Chem.*, **2013**, *52*, 10936-10948.

20. Saraf, S. L.; Fish, T. J.; Bennighoff, A. D.; Buelt, A. A.; Smith, R. C.; Berreau, L. M. *Organometallics*, **2014**, *33*, 6341-6351.

21. Bruner, B.; Walker, M. B.; Zhang, D.; Selke, M.; Ghimire, M. M. M.; Omary, M. A.; Klausmeyer, K.; Farmer, P J. *Dalton Trans.* **2014***, 43,*11548-11557.

22. Durham, B.; Wilson, S. R.; Hodgson, D. J.; Meyer, T. J. *J. Am. Chem. Soc.* **1980**, *102*, 600-607.

23. Collin, J. P.; Jouvenot, D.; Koizumi, M.; Sauvage, J. P. *Inorg. Chem.* **2005**, *44*, 4693-4698.

24. Bjerrum, M. J.; Casimiro, D. R.; Chang, I. J.; Di Bilio, A. J.; Gray, H. B.; Hill, M. G.; Langen, R.; Mines, G. A.; Skov, L. K.; Winkler, J. P. *J. Bioenerg. Biomembr.* **1995**, *27*, 295-302.

25. Hurst, J. K. *Coord. Chem. Rev.* **2005**, *249*, 313-328.

26. Ghosh, P. K.; Brunschwig, B. S.; Chou, M.; Creutz, C.; Sutin, N. *J. Am. Chem. Soc*. **1984**, *106*, 4772-4783.

27. Lebeau, E. L.; Adeyemi, S. A.; Meyer, T. J. *Inorg. Chem.* **1998**, *37*, 6476-6484.

28. Backlund M.; Ziller, J.; Farmer, P. J. *Inorg. Chem.* **2008**, *47*, 2864–2870.

29. Han, X. Z.; Klausmeyer, K. K.; Farmer, P. J. Inorg. Chem. **2016**, *55*, 7320 – 7322.

30. Achord, J. M.; Hussey, C. L. *Anal. Chem.* **1980**, *52*, 601-602.

31. Craig, N. C.; Groner, P.; McKean, D. C. *J. Phys. Chem. A* **2006**, *110*, 7461-7469.

32. McDaniel, D. H.; Brown, H. C. *J. Org. Chem.* **1958**, *23*, 420-427.

33. Han, X. Z.; Kumar, M. R.; Farmer, P. J. *The Chemistry and Biology of Nitroxyl (HNO)* Elsevier, *Amsterdam, Netherlands*, **2016**, *Chp. 15*, 287-304.

34. McDaniel, D. H.; Brown, H. C. *J. Org. Chem.* **1958**, *23*, 420-427.

35. El-Sukkary, M.; Speier, G. *J.C.S. Chem. Comm.* **1981**, *15*,745.

36. Singh, K. N.; Kumar, R. *Indian J. Chem.* **2006**, *46B*. 1554-1557.

REFERENCES

1. Pietta, P. G. *J. Nat. Prod.* **2000**, *63*, 1035-1042.

2. Rice-Evans, C. A.; Miller, N.; Paganga, G. *Free Radical Biol. Med.* **1996**, *20*, 933-956.

3. Cotelle, N.; Bernier, J. L.; Catteau, J. P.; Pommery, J.; Wallet, J. C.; Gaydou, E. M. *Free Radical Biol. Med.* **1996**, *20*, 35-43.

4. Guohua, C.; Emin, S.; Ronald, L. *Free Radical Biol. Med.* **1997**, *22*, 749-760.

5. Van Hoof, L.; Van den Berghe, D. A.; Hatfield, G. M.; Vlietinck, A. J. *Planta Med.* **1984**, *50*, 513-517.

6. Brasseur, T. *J. Pharm. Belg.* **1989**, *44*, 235-241.

7. Wei, B. L.; Lu, C. M.; Tsao, L. T.; Wang, J. P.; Lin, C. N. *Planta Med.* **2001**, *67*, 745-747.

8. Fischer, M.; Mills, G. D.; Slaga, T. J. *Carcinogenesis* **1982**, *3*, 1243-1245.

9. Huang, M.; Ferraro, T. In *Phenolic Compounds in Food and their Effect on Health II*, Huang, M. T., Ho, C. T., Lee, C. Y., Eds.; ACS Symposium Series; American Chemical Society: Washington, DC, **1992**; Chapter 2, p 507.

10. Huang, M. T.; Wood, A. W.; Newmark, H. L.; Sayer, J. M.; Yagi, H.; Jerina, D. M.; Conney, A. H. *Carcinogenesis* **1983**, *4*, 1631-1637.

11. Musialik, M.; Kuzmicz, R.; Litwinienko, G. *J. Org. Chem.*, **2009**, *74*, 2699-2709.

12. Wollenweber, E. *Flavonoids: Advances in Research*; Harborne, J. B.; Mabry, T. J., Eds.; Chapman&Hall: London, UK, **1982**.

13. Demaster, E. G.; Redfern, B.; Nagasawa, H. T. *Biochem. Pharmacol.* **1998**, *55*, 2007-2015.

14. Kumar, R. M.; Zapata, A.; Ramirez, A.; Bowen, S.; Francisco, W.; Farmer, J. P. *Proc. Natl. Acad. Sci.* **2011**, *108*, 18926-18931.

15. Kumar, M. R. Farmer, P. J. *Biochemistry*, **2009**, *48*, 5018–5025.

16. Fukuto, J. M. *Chem. Res. Toxicol.* **2005**, *18*, 790–801.

17. Fukuto, J. M.; Switzer, C. H.; Miranda, K. M.; Wink, D. A. Annu. Rev. Pharmacol. Toxicol. **2005**, *45*, 335–355.

18. Shafirovich, V.; Lymar, S. V. *J. Am. Chem. Soc.* **2003**, *125*, 6547–6552.

19. Lymar, S. V.; Shafirovich, V.; Poskrebyshev, G. A. *Inorg. Chem.* **2005**, *44*, 5212–5221.

20. Hughes, M. N.; Cammack, R. *Methods Enzymol.* **1999**, *301*, 279–287.

21. King, S. B.; Nagasawa, T. *Methods Enzymol.* **1999**, *301*, 211–220.

22. Momiyama, N.; Yamamoto, H. *Chem. Commun.* **2005**, 3514.

23. Lewis, J.W.; Meyer, P. L.; Ormerod, J. A. *J. Chem. Soc., Perkin Trans.* **1972**, *20*, 2521-2524.

24. Sasaki, T.; Ishibashi, Y.; Ohno, M. *Chem. Lett.*, **1983**, *12*, 863-866.

25. Sasaki, T.; Mori, K.; Ohno, M. *Synthesis*, **1985**, *3*, 280-282.

26. Momiyama, N.; Yamamoto, H. *Org. Lett.*, **2002**, *4*, 3579-3582.

27. Kawasaki, M.; Li, P.; Yamamoto, H. *Angew. Chem. Int. Ed.*, **2008**, *47*, 3795-3797.

28. Momiyama, N.; Yamamoto, H. *J. Am. Chem. Soc.*, **2005**, *127*, 1080.

29. Oka, T.; Simpson, F. J. *Biochem. Biophys. Res. Commun.* **1971**, *43*, 1.

30. Hund, H. K.; Breuer, J.; Lingens, F.; Hüttermann, J.; Kappl, R.; Fetzner, S. *Eur. J. Biochem.* **1999**, *263*, 871.

31. Fusetti, F.; Schroter, K. H.; Steiner, R. A.; van Noort, P. I.; Oijning, T.; Rozeboom, H. J.; Kalk, K. H.; Egmond, M. R.; Dijkstra, B. W. *Structure* **2002**, *10*, 259.

32. Bowater, L.; Fairhurst, S. A.; Just, V. J.; Bornemann, S. *FEBS Lett.* **2004**, *557*, 45.

33. Gopal, G.; Madan, L. L.; Betz, S.F.; Kossiakoff, A. A. *Biochemistry* **2005**, *44*, 193.

34. Merkens, H.; Kappl, R.; Jakob, R.P.; Schmid, F.X.; Fetzner, S. *Biochemistry* **2008**, *47*, 12185.

35. Merkens, H.; Fetzner, S. *FEMS Microbiol. Lett.* **2008**, *287*, 100.

36. Kooter, I. M.; Steiner, R. A.; Dijkstra, B. W.; van Noort, P. I.; Egmond, M. R.; Huber, M. *Eur. J. Biochem.* **2002**, *269*, 2971–2979.

37. 50. R.A. Steiner, R. A.; Kooter, I. M.; Dijkstra, B. W. *Biochemistry* **2002**, *41*, 7955–7962.

38. Allpress, C. J.; Berreau, L. M. *Coord. Chem. Rev.* **2013**, *257*, 3005-3029.

39. (a) Kaizer, J.; Barath, G.; Pap, J. S.; Speier, G. *Chem. Commun.* **2007**, 5235−5237. (b) Matuz, A.; Giorgi, M.; Speier, G.; Kaizer, *J. Polyhedron* **2013**, *63*, 41−49. (c) Balogh-Hergovich, É.; Kaizer, J.; Speier, G.; Fulop, V.; Parkanyi, L. *Inorg. Chem.* **1999**, *38*, 3787-3795.

40. (a) Grubel, K.; Rudzka, K.; Arif, A. M.; Klotz, K. L.; Halfen, J. A.; Berreau, L. M. *Inorg. Chem.* **2010**, *49*, 82−96. (b) Grubel, K.; Laughlin, B. J.; Maltais, T. R.; Smith, R. C.; Arif, A. M.; Berreau, L. M. *Chem. Commun.* **2011**, *47*, 10431−10433.

41. (a) Barhacs, L.; Kaizer, J.; Speier, G. *J. Mol. Catal. A.* **2001**, 172, 117−125. (b) Kaizer, J.; Pap, J.; Speier, G.; Párkányi, L. *Eur. J. Inorg. Chem.* **2004**, 2253−2259. (c) Balogh-Hergovich, É.; Kaizer, J.; Pap, J.; Speier, G.; Huttner, G.; Zsolnai, L. *Eur. J. Inorg. Chem.* **2002**, 2287−2295.

42. (a) Sun, Y. J.; Huang, Q. Q.; Zhang, J. J. *Inorg. Chem.*, **2014**, *53*, 2932-2942. (b) Sun, Y. J.; Huang, Q. Q.; Tano, T.; Itoh, S. *Inorg. Chem.*, **2013**, *52*, 10936-10948.

43. Saraf, S. L.; Fish, T. J.; Bennighoff, A. D.; Buelt, A. A.; Smith, R. C.; Berreau, L. M. *Organometallics*, **2014**, *33*, 6341-6351.

44. Bruner, B.; Walker, M. B.; Zhang, D.; Selke, M.; Ghimire, M. M. M.; Omary, M. A.; Klausmeyer, K.; Farmer, P J. *Dalton Trans.* **2014***, 43,*11548-11557.

45. Backlund M.; Ziller, J.; Farmer, P. J. *Inorg. Chem.*, **2008**, *47*, 2864–2870.

46. Paolocci, N.; Saavedra, W. F.; Miranda, K. M.; Martignani, C., Isoda, T.; Hare, J. M.; Espey, M. G.; Fukuto, J. M.; Feelisch, M.; Wink, D. A.; Kass, D. A. "Nitroxyl anion exerts redox-sensitive positive cardiac inotropy *in vivo* by calcitonin gene-related peptide signaling." *Proc. Natl. Acad. Sci.*, **2001**, *98*, 10463-10468.

47. Paolocci, N.; Katori, T.; Champion, H. C.; St John, M. E.; Miranda, K. M.,; Fukuto, J. M.; Wink, D. A.; Kass, D. A. "Positive inotropic and lusitropic effects of HNO/NO^- in failing hearts: Independence from β-adrenergic signaling." *Proc. Natl. Acad. Sci.*, **2003**, *100*, 5537-5542.

48. Paolocci, N.; Jackson, M. I.; Lopez, B. E.; Miranda, K.; Tocchetti, C. G.; Wink, D. A.; Hobbs, A. J.; Fukuto, J. M. "The pharmacology of nitroxyl (HNO) and its therapeutic potential: not just the Janus face of NO." *Pharmacol. Ther.*, **2007**, *113*, 442- 458.

49. Dai, T.; Tian, Y.; Tocchetti, C. G.; Katori, T.; Murphy, A. M.; Kass, D. A.; Paolocci, N.; Gao, W. D. "Nitroxyl increases force development in rat cardiac muscle." *J. Physiol.,* **2007**, *580*,951-960.

50. Kappaka V.; Thomposon, D. C.; Chen, Y.; Vasiliou, V. "Aldehyde dehydrogenase inhibitors: a comprehensive review of the pharmacology, mechanism of action, substrate specificity, and clinical application." *Pharma. Rev.*, **2012**, *64*,520-539.

51. DeMaster, E. G.; Redfern, B.; Nagasawa, H. T. "Mechanisms of inhibition of aldehyde dehydrogenase by nitroxyl, the active metabolite of the alcohol deterrent agent cyanamide." *Biochem. Pharmacol.*, **1998**, *55*, 2007-2015.

52. Irvine, J. C.; Ritchie, R. H.; Favaloro, J. L.; Andrews, K. L.; Widdop, R. E.; Kemp-Harper, B. K. "Nitroxyl(HNO): the Cinderella of the nitric oxide story." *Trends Pharmacol. Sci.*, **2008**, *29*, 601-608.

53. Irvine, J. C.; Cao, N.; Gossain, S.; Alexander, A.; Love, J. E.; Qin, C.; Horowitz, J. D.; Kemp-Harper, B. K.; Ritchie, R. H. "HNO/cGMP-dependent antihypertrophic actions of isopropylamine-NONOate in neonatal rat cardiomyocytes: potential therapeutic advantages of HNO over NO." *Am. J. Physiol. Heart Circ Physiol.*, **2013**, *305*, H365-H377.

54. Chin, K. Y.; Qin, C.; Kemp-Harper, B. K.; Woodman, O. L.; Ritchie, R. H. "The concomitant coronary vasodilator and positive inotropic actions of the nitroxyl donor Angeli's salt in the intact rat heart: contribution of soluble guanylyl cyclase-dependent and -independent mechanisms." *Br. J. Pharmacol.*, **2014**, *7*, 1722-1734.

55. Miller, T.M.; Cherney, M.E.; Franco, N.; Farmer, P.J.; King, S.B.; Hobbs, A.J.; Miranda, K.; Burstyn, J.N.; Fukuto, J.M. "The effects of nitroxyl (HNO) on soluble guanylate cyclase activity: Interactions at ferrous heme and cysteine thiols." *J. Biol. Chem.* **2009**, *284*, 21788-21796.

56. Irvine, J. C.; Favaloro, J. L.; Kemp-Harper, B. K. "NO^- activates soluble guanylate cyclase and K_v channels to vasodilate resistance arteries." *Hypertension,* **2003,** *41,* 1301-1307.

57. Liochev, S. I.; Fridovich, I. "Nitroxyl (NO^-): a substrate for superoxide dismutase." *Archives of Biochemistry and Biophysics*, **2002**, *402*, 166-171.

58. Zeller, A.; Wenzl, M.; Beretta, M.; Stessel, H.; Russwurm, M.; Koesling, D.; Mayer, B. "Mechanism underlying activation of soluble guanylate cyclase by the nitroxyl donor angeli's salt." *Mol. Pharmacol.*, **2009**, *76*, 1115-1122.

59. (1) Kumar, R. M.; Pervisky, D.; Chem, L.; Poulos, T.; Kundu, S.; Hargrove, M. S.; Rivera, E. J.; Diaz, A.; Colon, J. L.; Farmer, J. P. "Nitrosyl hydride (HNO) as an O_2 analogue: long-lived HNO-adducts of ferrous globins." *Biochemistry,* **2009**, *48*, 5018-5025. (2) Reisz, J. A.; Bechtold, E.; King, S. B. "Oxidative heme protein-mediated nitroxyl (HNO) generation." *Dalton Trans.*, **2010**, *39*, 5203-5212.

60. Bugg, T. "Dioxygenase enzymes: catalytic mechanisms and model chemistry." *Tetrahedron*, **2003**, 59, 7075 – 7101.

61. Bugg, T.; Ramaswamy, S. "Non-heme iron-dependent dioxygenases: unraveling catalytic mechanisms for complex enzymatic oxidations." *Curr. Opin. Chem. Biol.*, **2008**, *12*, 134-140.

62. Schaab, M. R.; Barney, B. M.; Francisco, W. A. "Kinetic and spectroscopic studies on the quecetin 2,3-dioxygenase from *Bacillus subtilis*." *Biochemistry*, **2006**, *45*, 1009-1016.

63. Fusetti, F.; Schroter, K. H.; Steiner, R. A.; Noort, P.; Pijing, T.; Rozeboom, H. J.; Kalk, K. H.; Egmond, M. R.; Dijkstra, B. W. "Crystal structure of the copper-containing quercetin 2,3-dioxygenase from *Aspergillus japonicus*." *Structure*, **2002**, *10*, 259-268.

64. Gopal, B.; Madan, L. L.; Betz, S. F.; Kossiakoff, A. A. "The crystal structure of a quercetin 2,3-dioxygenase from *Bacillus subtilis* suggests modulation of enzyme activity by a change in the metal ion at the active site." *Biochemistry*, **2005**, *44*, 193-201.

65. Sun, Y. J.; Huang, Q. Q.; Zhang, J. J. "Series of structural and functional models for the ES (enzyme-substrate) complex of the Co(II)-containing quercetin 2,3-dioxygenase." *Inorg. Chem.*, **2014**, *53*, 2932-2942.

66. Kumar, R. M.; Zapata, A.; Ramirez, A.; Bowen, S.; Francisco, W.; Farmer, J. P. "Nitrosyl hydride (HNO) replaces dioxygen in nitroxygenase activity of manganese quercetin dioxygenase". *Proc. Natl. Acad. Sci*., **2011**, *108*, 18926-18931.

67. Shafirovich, V.; Lymar, S. V. "Nitroxyl and its anion in aqueous solutions: Spin states, protic equilibria, and reactivities toward oxygen and nitric oxide." *Proc. Natl. Acad. Sci*., **2002**, *99*, 7340-7345.

68. Lunte, C.; Sanli, S. "Determination of eleven flavonoids in chamomile and linden extracts by capillary electrophoresis." *Anal. Methods*, **2014**, *6*, 3858-3864.

69. Musialik, M.; Kuzmicz, R.; Litwinienko, G. "Acidity of hydroxyl groups: An overlooked influence on antiradical properties of flavonoids." *J. Org. Chem.,* **2009**, *74*, 2699-2709.

70. Yang B.; Kotani A.; Arai, K.; Kusu, F. "Estimation of the antioxidant activities of flavonoids from their oxidation potentials." *Anal. Sci.*, **2001**, *17*, 599-604.

71. a) *REACT for Windows, Version 1.2*; Manka, M. J., Ed.; Alchemy Software, Wesley: Chapel, FL, 2001; b) Braun, W.; Herron, J. T.; Kahaner, D.K. "Acuchem: A computer program for modeling complex chemical reaction systems." *Int. J. Chem. Kinet.*, **1988**, *20*, 51-62.

72. Costas, M.; Mehn, M. P.; Jensen, M. P.; Que, L. "Dioxygen activation at mononuclear nonheme iron active sites: enzymes, models, and intermediates." *Chem. Rev.*, **2004**, *104*, 939-986.

73. Kaizer, J.; Speier, G. "Radical-initiated oxygenation of flavonols by dioxygen." *J. Mo.l Catal. A: Chem.,* **2001**, *171*, 33-36.

74. Balogh-Hergovich, E.; Speier, G. "Kinetics and mechanism of the base-catalyzed oxygenation of flavonol in DMSO-H_2O solution." *J. Org. Chem.*, **2001**, *66*, 7974-7978.

75. Nishinaga, A.; Tojo, T.; Tomita, H.; Matsuura, T. "Base-catalyzed oxygenolysis of 3-hydroxyflavones." *J. Chem. Soc. Perkin Trans.*, **1979**, *10*, 2511-25.
76. Dragsted, L.; Strube M.; Larsen, J. *Pharmacology & Toxicology.* **1993**, *72*, 116-135.

77. Bors, W.; Heller, W.; Stettmaier K. *Handbook of Antioxidants.* **1996**, 409-466.

78. Shahidi F. and Wanasundara P. *Critical Reviews in Food Science and Nutrition.* **1992**, *32*, 67-103.

79. a) Schaab, M. R.; Barney, B. M.; Francisco, W. A. *Biochemistry*, **2006**, *45*, 1009-1016. b) Fusetti, F.; Schroter, K. H.; Steiner, R. A.; Noort, P.; Pijing, T.; Rozeboom, H. J.; Kalk, K. H.; Egmond, M. R.; Dijkstra, B. W. *Structure*, **2002**, *10*, 259-268. c) Gopal, B.; Madan, L. L.; Betz, S. F.; Kossiakoff, A. A. *Biochemistry*, **2005**, *44*, 193-201.

80. a) Hergovich, E. B. and Speier G. *J. Org. Chem.* **2001**, *66*, 7974-7978. b) Czaun, M.; Speier, G. *Tetrahedron Lett*. **2002**, *43*, 5961-5963. c) Czaun, M.; Speier, G.; Kaizer, J.; Farkas, E. *Tetrahedron* **2013**, *69*, 6666-6672.

81. a) Pap, J. S.; Kaizer, J.; Speier, G. *Coord. Chem. Rev*., **2010**, *254*, 781-793. b) Balogh-Hergovich, E.; Speier, G.; Argay, G. *J. Chem. Soc. Chem. Commn.*, **1991**, 551-552. c) Matuz, A.; Giorgi, M.; Speier, G.; Kaizer, J. *Polyhedron*, **2013**, *63*, 41-49. d) Lippai, I.; Speier, G. *J. Mol. Cata. A:*, **1998**, *130*, 139-148. e) Balogh-Hergovich, E.; Kaizer, J.; Speier G.; Hutter, G.; Jacobi, A. *Inorg. Chem.*, **2000**, *39*, 4224-4229. f) Balogh-Hergovich, E.; Kaizer, J.; Sperier, G.; Fulop, V.; Parkanyi, L. *Inorg. Chem.* **1999**, *38*, 3787-3795.

82. a) Grubel, K.; Rudzka, K.; Arif, A. M.; Klotz, K. L.; Halfen, J. A.; Berreau, L. M. *Inorg. Chem*., **2010**, *49*, 82-96. b) Berreau, L. M.; Borowski, T.; Grubel, K.; Allpress, C. J.; Wikstrom, J. P.; Germain, M. E.; Rybak-Akimova, E. V.; Tierney, D. L. *Inorg. Chem.*, **2011**, *50*, 1047-1057. c) Szajna-Fuller, E.; Rudzka, K.; Arif, A. M.; Berreau, L. M. *Inorg. Chem*., **2007**, *46*, 5499-5507. d) Grubel, K.; Fuller, A. L.; Chambers, B. M.; Arif, A. M.; Berreau, L. M. *Inorg. Chem*., **2010**, *49*, 1071-1081.

83. a) Nishinaga, A.; Tojo, T.; Matsuura, T. *J. Chem. Soc., Chem. Commun.* **1974**, 896-897. b) Nishinaga, A,; Numada, N.; Maruyama, K. *Tetrahedron Lett.* **1989**, *30*, 2257-2258. C) Nishinaga, A.; Kuwashige, T.; Tsutsui, T.; Mashino, T.; Maruyama, K. *J. Chem. Soc., Dalton Tran.* **1994**, 805-810.

84. Kumar, M.; Zapata, A.; Ramirez, A.; Bowen, S.; Francisco, W.; Farmer, P. *Proc. Natl. Acad. Sci*. **2011,** *108*, 18926-18931.

85. Demaster, E. G.; Redfern, B.; Nagasawa, H. T. *Biochem. Pharmacol.* **1998**, *55*, 2007-2015.

86. Momiyama, N.; Yamamoto, H. *Chem. Commun.* **2005**, 3514.

87. Lewis, J.W.; Meyer, P. L.; Ormerod, J. A. *J. Chem. Soc., Perkin Trans.* **1972**, *20*, 2521-2524.

88. Sasaki, T.; Ishibashi, Y.; Ohno, M. *Chem. Lett.*, **1983**, *12*, 863-866.

89. Sasaki, T.; Mori, K.; Ohno, M. *Synthesis*, **1985**, *3*, 280-282.

90. Momiyama, N.; Yamamoto, H. *Org. Lett.*, **2002**, *4*, 3579-3582.

91. Kawasaki, M.; Li, P.; Yamamoto, H. *Angew. Chem. Int. Ed.*, **2008**, *47*, 3795-3797.

92. Momiyama, N.; Yamamoto, H. *J. Am. Chem. Soc.*, **2005**, *127*, 1080.

93. Lunte, C.; Sanli, S. *Anal. Methods*, **2014**, *6*, 3858-3864.

94. (a) Shafirovich, V.; Lymar. S. *J. Am. Chem. Soc.* **2003**, *125*, 6547-6552. (b) Lymar, S. V.; Shafirovich, V.; Poskrebyshew, G. A. *Inorg. Chem.* **2005**, *44*, 5212-5221.

95. *REACT for Windows, Version 1.2*; Manka, M. J., Ed.; Alchemy Software, Wesley: Chapel, FL, 2001; as described in Braun, W.; Herron, J. T.; Kahaner, D.K. *Int. J. Chem. Kinet.* **1988**, *20*, 51-62.

96. Schaab, M. R.; Barney, B. M.; Francisco, W. A. *Biochemistry*, **2006**, *45*, 1009-1016.

97. Shafirovich V. and Lymar S. V. *Proc. Natl. Acad. Sci*. **2002,** *99*, 7340-7345.

98. Yang B.; Kotani A.; Arai, K.; Kusu, F. *Anal. Sci.* **2001**, *17*, 599-604.

99. Yang B.; Arai K.; Kusu F. *Anal. Sci.* **2001**, *17*, 987-989.

100. Lind, J.; Merenyi, G. *J. Phys. Chem. A* **2006**, *110*, 192-197.

101. Wood, P.M. *Biochem. J.* **1988** *253*, 287–289.

102. Han X. Z.; Parker, V. D. and Zhu, X. Q. *J. Org. Chem.* **2012**, *77*, 6520-6529.

103. (a) Page, M.; Williams, A. Organic and Bio-organic Mechanism; Longman: Harlow, UK, 1997; Chapter 3, pp. 52-79. (b) Williams, A. *Acc. Chem. Res.* **1984**, *17*, 425–430. (c) Williams, A. *Acc. Chem. Res*. **1989**, *22*, 387–392. (d) Williams, A. *Adv. Phys. Org. Chem*. **1991**, *27*, 1.(e) Williams, A. *J. Am. Chem. Soc.* **1985**, *107*, 6335–6339.

104. a) Buongiorno, D.; Straganz, G. D. *Coord. Chem. Rev*. **2013**, *257*, 541-563. b) Costas, M.; Mehn, M. P.; Jensen, M. P.; Que, L. Jr. *Chem. Rev.* **2004**, *104*, 939-986.c) Kovaleva, E. G.; Lipscomb, J. D. *Nat. Chem. Biol.* **2008**, *4*, 186 –193.

105. a) Fusetti, F.; Schröter, K. H.; Steiner, R. A.; van Noort, P. I.; Pijning, T.; Rozeboom, H. J.; Kalk, K. H.; Egmond, M. R.; Dijkstra, B. W. *Structure* **2002**, *10*, 259−268. b) Bugg, T.; Ramaswamy, S. *Curr. Opin. Chem. Biol.*, **2008**, *12*, 134-140. (c) Kumar, M.; Zapata, A.; Ramirez, A.; Bowen, S.; Francisco, W.; Farmer, P. *Proc. Natl. Acad. Sci.* **2011**, *108*, 18926-18931. (d) Han, X. Z.; Kumar, M. R.; Farmer, P. J. *Tetrahedron Lett*. **2016**, *57*, 399-402.

106. a) Matuz, A.; Giorgi, M.; Speier, G.; Kaizer, J. *Polyhedron* **2013**, *63*, 41-49. b) Gopal, B.; Madan, L. L.; Betz, S. F.; Kossiakoff, A. A. *Biochemistry* **2005**, *44*, 193-201. c) Schaab, M. R.; Barney, B. M.; Francisco, W. A. *Biochemistry* **2006**, *45*, 1009–1016.

107. a) Hergovich, E. B. and Speier G. *J. Org. Chem.* **2001**, *66*, 7974-7978. b) Czaun, M.; Speier, G. *Tetrahedron Lett.* **2002**, *43*, 5961-5963. c) Czaun, M.; Speier, G.; Kaizer, J.; Farkas, E. *Tetrahedron* **2013**, *69*, 6666-6672.

108. a) Sisa, M.; Bonnet, S.L.; Ferreira, D.; Van der Weshuizen, J.H. *Molecules*, **2010**, *15*, 5196-5245. b) Balogh-Hergovich, É.; Kaizer, J.; Pap, J.; Speier, G.; Huttner, G.; Zsolnai, L. *Eur. J. Inorg. Chem.* **2002**, 2287−2295.

109. Barhacs, L.; Kaizer, J.; Speier, G. *J. Mol. Catal. A.* **2001**, *172*, 117−125.

110. a) Matuz, A.; Giorgi, M.; Speier, G.; Kaizer, *J. Polyhedron* **2013**, *63*, 41−49. b) Balogh-Hergovich, É.; Kaizer, J.; Speier, G.; Fulop, V.; Parkanyi, L. *Inorg. Chem.* **1999**, *38*, 3787-3795. c) Kaizer, J.; Pap, J.; Speier, G.; Párkányi, L. *Eur. J. Inorg. Chem.* **2004**, 2253−2259.

111. a) Grubel, K.; Rudzka, K.; Arif, A. M.; Klotz, K. L.; Halfen, J. A.; Berreau, L. M. *Inorg. Chem.* **2010**, *49*, 82−96. b) Grubel, K.; Laughlin, B. J.; Maltais, T. R.; Smith, R. C.; Arif, A. M.; Berreau, L. M. *Chem. Commun.* **2011**, *47*, 10431−10433.

112. a) Sun, Y. J.; Huang, Q. Q.; Zhang, J. J. *Inorg. Chem.*, **2014**, *53*, 2932-2942. b) Sun, Y. J.; Huang, Q. Q.; Tano, T.; Itoh, S. *Inorg. Chem.*, **2013**, *52*, 10936-10948.

113. Saraf, S. L.; Fish, T. J.; Bennighoff, A. D.; Buelt, A. A.; Smith, R. C.; Berreau, L. M. *Organometallics*, **2014**, *33*, 6341-6351.

114. a) Backlund M.; Ziller, J.; Farmer, P. J. *Inorg. Chem.*, **2008**, *47*, 2864–2870. b) Bruner, B.; Walker, M. B.; Zhang, D.; Selke, M.; Ghimire, M. M. M.; Omary, M. A.; Klausmeyer, K.; Farmer, P J. *Dalton Trans.* **2014***, 43,*11548-11557.

115. a) Szeman, N.; Ziller, J. W.;Farmer, P. J. *Inorg. Chem.* **2004**, *43*, 8301-8309. b) Szeman, N.; Backlund, M.; Farmer, P. J. *Inorg. Chim. Acta* **2009**, *362*, 4013-4016.

116. Etter, M. C.; Urbanczyk-Lipkowska, Z.; Baer, S.; Barbara, P. F. *J. Mol. Struct.* **1986**, *144*, 155−167.

117. (a) Marfak, A.; Trouillas, P; Allais, D. p.; Champavier, Y.; Calliste, C. A.; Duroux, J. L. *J. Agric. Food Chem.* **2002**, *50*, 4827-4833. (b) El-Sukkary, M.; Speier, G. *J.C.S. Chem. Comm.* **1981**, *15*,745. (c) Singh, K. N.; Kumar, R. *Indian J. Chem.* **2006**, *46B*. 1554-1557.

118. R. Hiatt, Organic Peroxides, (Ed.: D. Swern), Wiley Intersciene, New York, 1971, 2511-1516.

119. Pietta, P. G. *J. Nat. Prod*. **2000**, *63*, 1035-1042.

120. Rice-Evans, C. A.; Miller, N.; Paganga, G. *Free Radical Biol. Med*. **1996**, *20*, 933-956.

121. Cotelle, N.; Bernier, J. L.; Catteau, J. P.; Pommery, J.; Wallet, J. C.; Gaydou, E. M. *Free Radical Biol. Med*. **1996**, *20*, 35-43.

122. Guohua, C.; Emin, S.; Ronald, L. *Free Radical Biol. Med*. **1997**, *22*, 749-760.

123. Van Hoof, L.; Van den Berghe, D. A.; Hatfield, G. M.; Vlietinck, A. J. *Planta Med*. **1984**, *50*, 513-517.

124. Brasseur, T. *J. Pharm. Belg*. **1989**, *44*, 235-241.

125. Wei, B. L.; Lu, C. M.; Tsao, L. T.; Wang, J. P.; Lin, C. N. *Planta Med*. **2001**, *67*, 745-747.

126. Fischer, M.; Mills, G. D.; Slaga, T. J*Carcinogenesis* **1982**, *3*, 1243-1245.

127. Huang, M.; Ferraro, T. In *Phenolic Compounds in Food and their Effect on Health II*, Huang, M. T., Ho, C. T., Lee, C. Y., Eds.; ACS Symposium Series; American Chemical Society: Washington, DC, **1992**; Chapter 2, p 507.

128. Huang, M. T.; Wood, A. W.; Newmark, H. L.; Sayer, J. M.; Yagi, H.; Jerina, D. M.; Conney, A. H. *Carcinogenesis* **1983**, *4*, 1631-1637.

129. Musialik, M.; Kuzmicz, R.; Litwinienko, G. *J. Org. Chem.*, **2009**, *74*, 2699-2709.

130. Wollenweber, E. *Flavonoids: Advances in Research*; Harborne, J. B.; Mabry, T. J., Eds.; Chapman&Hall: London, UK, **1982**.

131. Fusetti, F.; Schröter, K. H.; Steiner, R. A.; van Noort, P. I.; Pijning, T.; Rozeboom, H. J.; Kalk, K. H.; Egmond, M. R.; Dijkstra, B. W. *Structure* **2002**, *10*, 259−268.

132. (a) Gopal, B.; Madan, L. L.; Betz, S. F.; Kossiakoff, A. A. *Biochemistry* **2005**, *44*, 193−201. (b) Schaab, M. R.; Barney, B. M.; Francisco, W. A. *Biochemistry* **2006**, *45*, 1009−1016.

133. (a) Laura, B.; Shirley, A. F.; Victoria, J. J.; Stephen, B. *FEBS Lett.* **2004**, *557*, 45−48. (b) Barney, B. M.; Schaab, M. R.; LoBrutto, R.; Francisco, W. A. *Protein Expr. Purif.* **2004**, *35*, 131−141.

134. (a) Kaizer, J.; Barath, G.; Pap, J. S.; Speier, G. *Chem. Commun.* **2007**, 5235−5237. (b) Matuz, A.; Giorgi, M.; Speier, G.; Kaizer, *J. Polyhedron* **2013**, *63*, 41−49. (c) Balogh-Hergovich, É.; Kaizer, J.; Speier, G.; Fulop, V.; Parkanyi, L. *Inorg. Chem.* **1999**, *38*, 3787-3795.

135. (a) Grubel, K.; Rudzka, K.; Arif, A. M.; Klotz, K. L.; Halfen, J. A.; Berreau, L. M. *Inorg. Chem.* **2010**, *49*, 82−96. (b) Grubel, K.; Laughlin, B. J.; Maltais, T. R.; Smith, R. C.; Arif, A. M.; Berreau, L. M. *Chem. Commun.* **2011**, *47*, 10431−10433.

136. (a) Barhacs, L.; Kaizer, J.; Speier, G. *J. Mol. Catal. A.* **2001**, 172, 117−125. (b) Kaizer, J.; Pap, J.; Speier, G.; Párkányi, L. *Eur. J. Inorg. Chem.* **2004**, 2253−2259. (c) Balogh-Hergovich, É.; Kaizer, J.; Pap, J.; Speier, G.; Huttner, G.; Zsolnai, L. *Eur. J. Inorg. Chem.* **2002**, 2287−2295.

137. (a) Sun, Y. J.; Huang, Q. Q.; Zhang, J. J. *Inorg. Chem.*, **2014**, *53*, 2932-2942. (b) Sun, Y. J.; Huang, Q. Q.; Tano, T.; Itoh, S. *Inorg. Chem.*, **2013**, *52*, 10936-10948.

138. Saraf, S. L.; Fish, T. J.; Bennighoff, A. D.; Buelt, A. A.; Smith, R. C.; Berreau, L. M. *Organometallics*, **2014**, *33*, 6341-6351.

139. Bruner, B.; Walker, M. B.; Zhang, D.; Selke, M.; Ghimire, M. M. M.; Omary, M. A.; Klausmeyer, K.; Farmer, P J. *Dalton Trans.* **2014***, 43,*11548-11557.

140. Durham, B.; Wilson, S. R.; Hodgson, D. J.; Meyer, T. J. *J. Am. Chem. Soc.* **1980**, *102*, 600-607.

141. Collin, J. P.; Jouvenot, D.; Koizumi, M.; Sauvage, J. P. *Inorg. Chem.* **2005**, *44*, 4693-4698.

142. Bjerrum, M. J.; Casimiro, D. R.; Chang, I. J.; Di Bilio, A. J.; Gray, H. B.; Hill, M. G.; Langen, R.; Mines, G. A.; Skov, L. K.; Winkler, J. P. *J. Bioenerg. Biomembr.* **1995**, *27*, 295-302.

143. Hurst, J. K. *Coord. Chem. Rev.* **2005**, *249*, 313-328.

144. Ghosh, P. K.; Brunschwig, B. S.; Chou, M.; Creutz, C.; Sutin, N. *J. Am. Chem. Soc*. **1984**, *106*, 4772-4783.

145. Lebeau, E. L.; Adeyemi, S. A.; Meyer, T. J. *Inorg. Chem.* **1998**, *37*, 6476-6484.

146. Backlund M.; Ziller, J.; Farmer, P. J. *Inorg. Chem.* **2008**, *47*, 2864–2870.

147. Han, X. Z.; Klausmeyer, K. K.; Farmer, P. J. Inorg. Chem. **2016**, *55*, 7320-7322.

148. Achord, J. M.; Hussey, C. L. *Anal. Chem.* **1980**, *52*, 601-602.

149. Craig, N. C.; Groner, P.; McKean, D. C. *J. Phys. Chem. A* **2006**, *110*, 7461-7469.

150. McDaniel, D. H.; Brown, H. C. *J. Org. Chem.* **1958**, *23*, 420-427.

151. Han, X. Z.; Kumar, M. R.; Farmer, P. J. *The Chemistry and Biology of Nitroxyl (HNO)* Elsevier, *Amsterdam, Netherlands*, **2016**, *Chp. 15*, 287-304.

152. McDaniel, D. H.; Brown, H. C. *J. Org. Chem.* **1958**, *23*, 420-427.

153. El-Sukkary, M.; Speier, G. *J.C.S. Chem. Comm.* **1981**, *15*,745.

154. Singh, K. N.; Kumar, R. *Indian J. Chem.* **2006**, *46B*. 1554-1557.